NTNU
Norwegian University of
Science and Technology

Probabilistic Damage Stability

Evaluating the Attained Subdivision Index by
Analysing the Effect of Changes in the
Arrangement and Intact Stability for an
Offshore Vessel

Stian Røyset Salen

Marine Technology
Submission date: June 2016
Supervisor: Svein Aanond Aanondsen, IMT
Co-supervisor: Bjørn Egil Asbjørnslett, IMT

Norwegian University of Science and Technology
Department of Marine Technology

Preface

This master's thesis represents the finalisation of my MSc degree in Marine Technology, Marine Systems Design from the Norwegian University of Science and Technology (NTNU). The thesis counts 30 credits, which corresponds to the work rate of four regular courses at NTNU. The study was carried out during the spring semester of 2016.

The work with the thesis started already during the fall semester of 2015, in the course TMR4560 Marine Systems Design, Specialization Project, where the author wrote a project thesis titled 'A Pre-Study on Probabilistic Damage Stability'. The theory part of this project is included in Chapter 2 of the master's thesis.

The thesis aims to give naval architects a better insight to how probabilistic damage stability, or more precisely the attained subdivision index, is influenced by certain changes in the arrangement and intact stability for offshore vessels. A 'wind farm service vessel' that is applicable to the SOLAS-2009 damage stability regulations, provided by Salt Ship Design, was used to conduct the study.

The author of the thesis, Stian Røyset Salen, would first of all like to thank Johannes Eldøy in Salt Ship Design for providing access to a NAPA-license throughout the semester. Having access to this market-leading stability software, certainly lifted the quality of the study. Furthermore, Ole Martin Djupvik in Salt Ship Design should be thanked for his endless support during the semester. Without his help, the author would have struggled much more in the process of learning how NAPA works. Additionally, Jørgen Hammersland and Frode Marton Meling at Salt Ship Design deserve a thanks, for being helpful upon request from the author. At last, the author is grateful for the guidance from the thesis' primary and secondary supervisors from NTNU, respectively Svein Aanond Aanondsen and Bjørn Egil Asbjørnslett.

Trondheim, 17/6/2016

Stian Røyset Salen

Abstract

The motivational basis and underlying goal of this master's thesis is to provide more knowledge to the 'experience data bank' for ship designers with respect to probabilistic damage stability (PDS). More precisely, the thesis aims to give more insight to how certain changes in the arrangement and intact stability affect the PDS or A-index for a specific offshore vessel.

The author has co-operated with Salt Ship Design in order to achieve the abovementioned goal; a NAPA-license and GA drawings to a 'wind farm service vessel (WFSV)' were provided. In agreement with Salt Ship Design, the following two objectives have been investigated:

1. What is the effect on the A-index of changing the size of the wing ballast tanks located above the void 'U-tanks' at the mid-section of the WFSV, by changing the height of the horizontal surface ('U-deck') separating these two tanks?
2. What is the effect on the A-index of changing the intact stability of the ship, i.e. the ship's initial GM values for the three subdivision draughts d_S, d_P and d_L?

The background for the abovementioned goal and research questions, is the introduction of the PDS regulations by IMO in 2009. Ship designers were then forced to use the probabilistic approach instead of the deterministic approach (DDS), for certain vessel types when calculating damage stability. PDS offers more freedom than DDS in the design of the ship's internal watertight arrangement. However, since PDS calculations usually are conducted at late design stages due to the widely used top-down design approach, it may be challenging to utilise this flexibility due to time pressure. Thus, ship designers often rely on experience, since there is little time for research and optimisation. The author would therefore like to contribute with more knowledge to the ship designers' 'experience data bank'. Furthermore, the results for objective 1 and 2, respectively, are presented in the below figures:

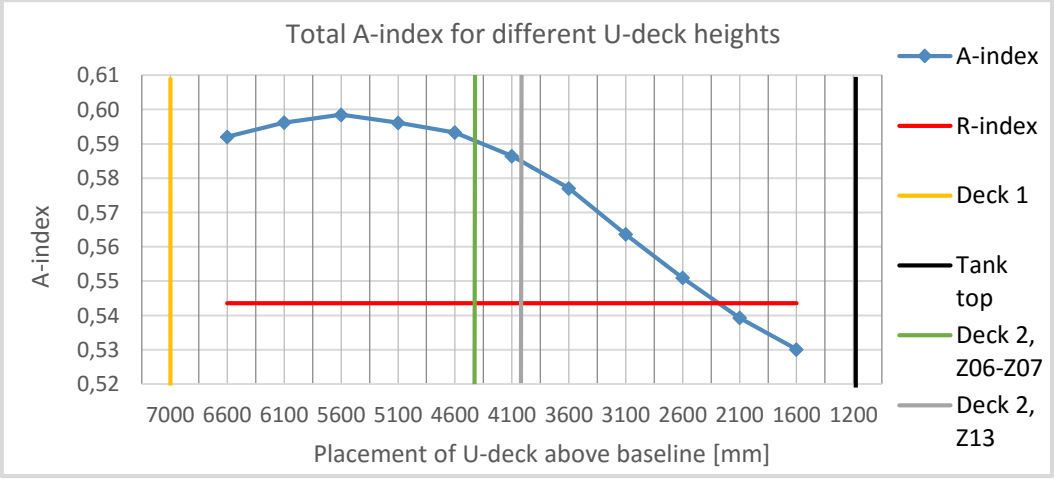

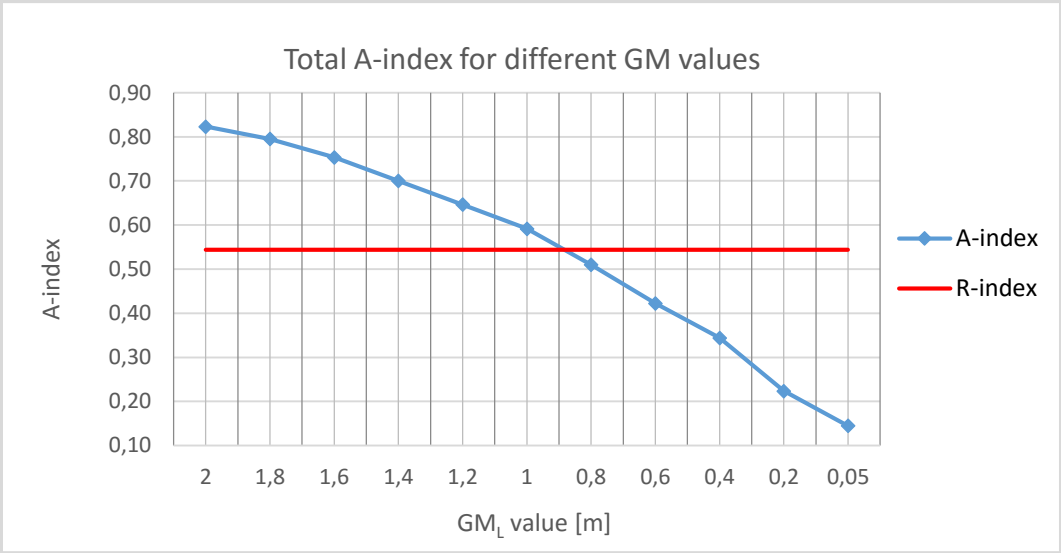

From the results presented above, it can be concluded that the A-index in objective 1 generally decreases when U-deck is lowered beneath the maximum value on the curve, which corresponds to 5.6 m. From the analysis and discussion conducted in this study, it can furthermore be concluded that the factors contributing to the change are s_i and v_i. The p_i-factor does not contribute, since there are no changes in the arrangement in longitudinal or transverse direction. Both the s_i- and v_i-factor generally decreases when the U-deck height is decreased below 5.6 m. For the s_i-factor, this is most likely due to increasing heeling moments, in case of damage, for larger sized wing ballast tanks; the s_i-factor is reduced due to larger heel angles. In addition, larger wing ballast tanks leads to smaller U-tanks, thus the stabilising effect of the U-tanks is reduced as well.

The results for objective 2 show that the A-index is generally better for larger initial GM values. The analysis and discussion related to objective 2, additionally conclude that the A-index is mainly dependent on the heeling moment in case of damage. The heeling moment will give the ship a new floating position, i.e. the ship obtains an equilibrium heel angle larger than zero degrees. This heel angle reduces the s_i-factor, which in turn reduces the A-index. The p_i- and v_i-factor will not contribute to the changes in A-index for objective 2, because there are no changes in the arrangement.

The abovementioned results and conclusions are the key findings in this thesis. Whether the results are generic or not, is questionable; for offshore vessels with approximately the same arrangement as the WFSV, the results from this thesis could be useful.

Sammendrag

Inspirasjonen bak, samt det underliggende målet, med denne masteroppgaven er å kunne bidra til en kunnskapsøking blant skipsdesignere generelt, i forhold til probabilistisk skadestabilitet (PDS). Mer spesifikt så satser oppgaven på å gi bedre innsikt i hvordan visse endringer i arrangementet og intaktstabiliteten for et spesifikt skip påvirker PDS eller A-indeksen.

Forfatteren har samarbeidet med Salt Ship Design for å oppnå det overnevnte målet; en NAPA-lisens og GA-tegninger for et 'wind farm service vessel (WFSV)' ble gitt til forfatteren. I enighet med Salt Ship Design har de følgende problemstillingene blitt forsket på:

1. Hva er effekten på A-indeksen av å endre størrelsen på wing ballast tankene som er lokalisert rett over de såkalte 'U-tankene', ved å endre høyden på den horisontale flaten ('U-dekk') som skiller disse to tankene?
2. Hva er effekten på A-indeksen av å endre intaktstabiliteten til skipper, det vil si skipets initiale GM-verdier for de tre lastkondisjonene d_S, d_P and d_L?

Bakgrunnen for det overnevnte målet, samt problemstillingene over, er IMOs introduksjon av det nye PDS-regelverket i SOLAS-2009. Skipsdesignere ble da tvunget til å bruke den probabilistiske metoden fremfor den tradisjonelle, deterministiske metoden (DDS), for visse skipstyper. PDS tilbyr designere mer fleksibilitet sammenlignet med DDS. Likevel, siden PDS-beregninger vanligvis blir utført mot slutten av prosjekter, på grunn av den vidstrakte bruken av 'top-down' designmetoden, kan det være utfordrende å utnytte denne fleksibiliteten. På grunn av dette, stoler designere ofte på gammel kunnskap og erfaring, siden det som regel er lite tid til forskning og optimalisering. Forfatteren av denne oppgaven ønsker derfor å bidra med ytterligere kunnskap. Resultatene for problemstilling 1 og 2, respektivt, er videre presentert i figurene som følger:

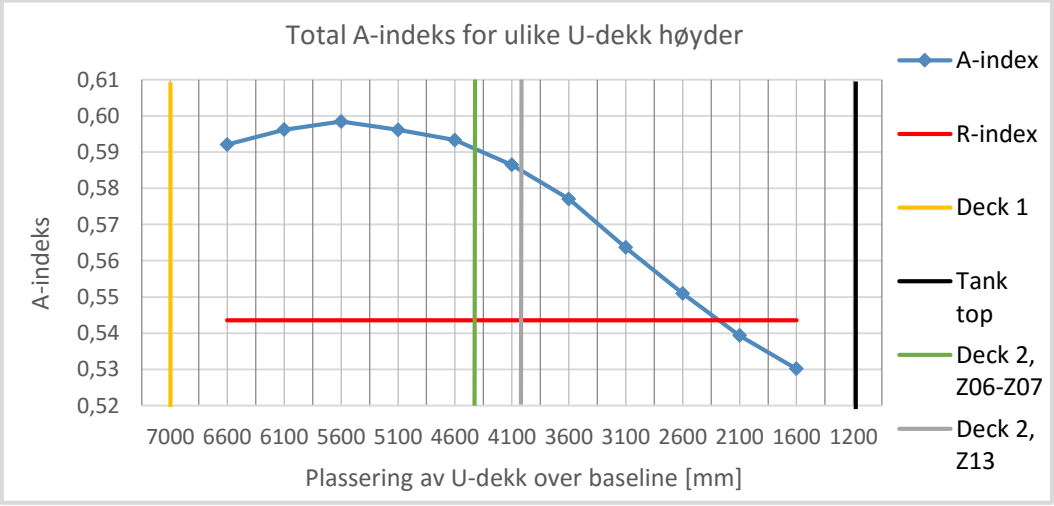

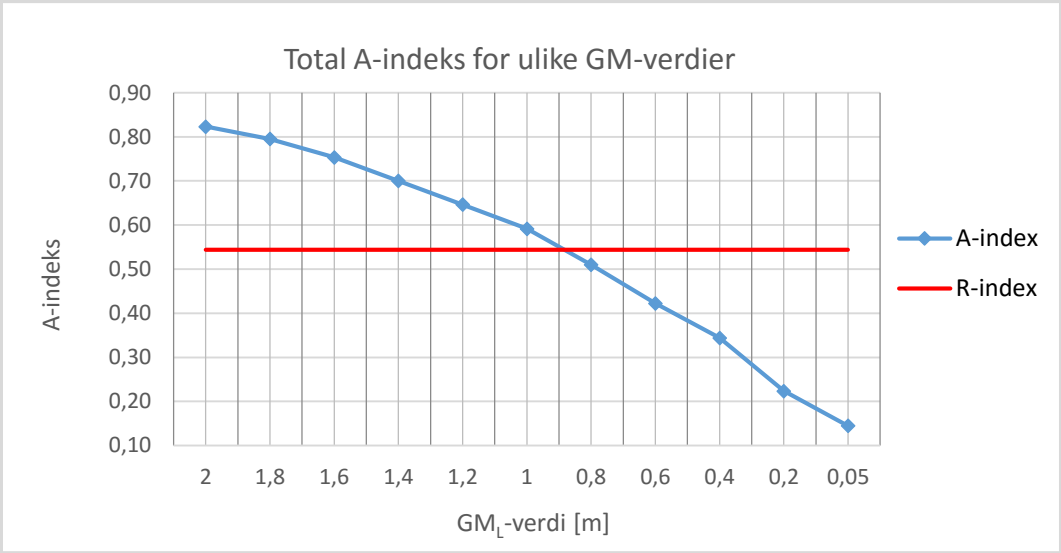

Basert på resultatene over, kan det konkluderes med at A-indeksen for problemstilling 1 generelt sett minsker når U-dekkshøyden reduseres under den maksimale verdien på kurven, som svarer til U-dekkshøyde 5.6 m. Fra analysene og diskusjonen som er gjort i denne studien, kan det videre konkluderes med at faktorene som bidrar til endringene er s_i og v_i. Den tredje faktoren, p_i, bidrar ikke, fordi det ikke gjøres noen endringer i langskips eller tverrskips retning. Både s_i- og v_i-faktoren reduseres når U-dekkshøyden senkes under 5.6 m. For s_i-faktoren er dette mest sannsynlig på grunn av en økning i krengemomentet, ved et skadetilfelle, fordi størrelsen på wing ballast tankene øker som en konsekvens av lavere U-dekkshøyde. I tillegg vil større wing ballast tanker medføre mindre U-tanker, som igjen fører til at U-tankene sin stabiliserende effekt reduseres.

Resultatene tilknyttet problemstilling 2, viser at A-indeksen generelt sett bedrer seg for større initiale GM-verdier. Analysene og diskusjonen relatert til problemstilling 2 videre konkluderer med at A-indeksen mer eller mindre bare er avhengig av krengemomentet i et skadetilfelle. Krengemomentet gir skipet en krengevinkel, som reduserer s_i-faktoren, som igjen reduserer A-indeksen. De to andre faktorene, p_i og v_i, bidrar ikke noes om helst til endringer i A-indeksen, fordi det ikke gjøres noen endringer i arrangementet i studien tilknyttet problemstilling 2.

Resultatene og konklusjonene presentert over, utgjør i korte trekk nøkkelfunnene i denne masteroppgaven. Om resultatene er generelle nok til å kunne dras nytte av ved design av andre typer fartøy, kan diskuteres. Forfatteren vil likevel si at offshorefartøy med tilnærmet likt arrangement som fartøyet brukt i denne studien, muligens kan dra nytte av resultatene.

Table of Contents

List of Figures

List of Tables

List of Equations

List of Symbols

A	Attained Subdivision Index (‘A-index’)
A	Projected lateral area above the waterline (Wind area)
A_C	Attained Subdivision Index for a particular loading condition
A_i	Attained Subdivision Index for a specific damage case at a particular loading condition
B	Beam of the ship at the deepest subdivision draught
B	Centre of buoyancy
b	Mean transverse distance between the shell (hull) and a longitudinal barrier
d	Draught in question
d_A	Contribution to A in the event of horizontal subdivision above the waterline
d_s	Deepest subdivision draught
d_P	Partial subdivision draught
d_L	Light service draught
Δ	Displacement of the ship
G	Centre of gravity
GZ_{max}	Max. GZ value; usually the peak of the GZ curve, but not always
$H_{j,n,m}$	‘*…the least height above the baseline, in metres, within the longitudinal range of x1(j)...x2(j+n-1) of the mth horizontal boundary which is assumed to limit the vertical extent of flooding for the damaged compartments under consideration…*’
$H_{j,n,m-1}$	*‘… the least height above the baseline, in metres, within the longitudinal range of x1(j)...x2(j+n-1) of the (m-1)th horizontal boundary which is assumed to limit the vertical extent of flooding for the damaged compartments under consideration…*’
j	The aftmost involved damage zone number, starting with number 1 at the stern
j	*‘…signifies the aft terminal of the damaged compartments under consideration…*’ (Related to the ‘v-factor’)
J	Non-dimensional damage length
J_{max}	Overall normalised maximum damage length = 10/33
J_k / J_{kn}	Knuckle point in the damage statistics distribution from the HARDER project
J_m	The maximum non-dimensional damage length for the particular ship in question
J_n	The normalised length of a compartment or group of compartments

k	No. particular longitudinal bulkhead functioning as a barrier for transverse penetration
K	Intersection point between the line that goes through GM and the keel
L_S	Subdivision length; the 'ship length' used in the 'PDS regulations'
l_{max}	Maximum absolute damage length = 60 m
L*	Length where normalised distribution ends = 260 m
m	Metre(s)
m	Represents each horizontal boundary counted upwards from the waterline under consideration
M	Metacentric height
M_{heel}	Maximum assumed heeling moment
$M_{passenger}$	Moment caused by movement of passengers
M_{wind}	Moment caused by wind
$M_{survivalcraft}$	Moment caused by davit-launching of survival crafts
N_1	Number of persons for whom lifeboats are provided
N_2	Number of persons in excess of N_1, including officers and crew
N	$N_1 + 2N_2$
n	The number of adjacent damage zones involved in the damage
N_P	The maximum number of passengers permitted to be on board in the service condition, corresponding to the deepest subdivision draught
p_i	Probability that a specific damage condition occurs
p_k	Cumulative probability at J_{kn} = 11/12
p(x1,x2)	Accounts for the probability of the considered longitudinal damage extent
r(x1,x2,b)	A factor accounting for the transverse damage extent
Range	Distance between θ_e and θ_v
R	Required Subdivision Index
R_0	The R value calculated for cargo ships with a length above 100 m
s_i	Factor accounting for the probability of survival after damage to the ship
$S_{intermediate, i}$	The probability of surviving all intermediate flooding stages until the equilibrium stage
$S_{final, i}$	The probability of surviving in the final equilibrium stage of flooding
$S_{mom, i}$	The probability of surviving heeling moments
S_{min}	The least 's-factor'
θ_e	Equilibrium angle

θ_v	Angle of vanishing stability
θ_{min}	Minimum heel angle = 7 degrees for passenger ships; 25 degrees for cargo ships
θ_{max}	Maximum heel angle = 15 degrees for passenger ships; 30 degrees for cargo ships
v_i	Probability that a watertight deck above the waterline remains intact after damage
x1	Distance from the aft terminal of the ship to the aft end of the zone in question
x2	Distance from the aft terminal of the ship to the forward end of the zone in question
Z	Distance from the centre of A to T/2, where T is the draught of the ship

List of Acronyms

A-index	Attained Subdivision Index A
Ch.	Chapter
DDS	Deterministic damage stability
FSE	Free surface effect
GA	General Arrangement
HARDER	Harmonization of Rules and Design Rationale
ICCL	International Convention on Load Lines
IMO	International Maritime Organization
LCB	Longitudinal centre of buoyancy
LCF	Longitudinal centre of flotation
LCG	Longitudinal centre of gravity
LOA	Length over all
LSA	Life-saving appliances
LPP	Length between perpendiculars
MCA	Maritime and Coastguard Agency
MSC	Maritime Safety Committee
PDF	Portable Document Format
PDS	Probabilistic damage stability
pdf	Probability distribution function
PhD	Doctor of Philosophy
Reg.	Regulation
SPS	Special Purpose Ship
SOLAS	Safety of Life at Sea
WFSV	Wind Farm Service Vessel

1. Introduction

In an ideal world, Naval Architects would optimise ship designs in order to achieve the best possible solutions in terms of: ship performance, environmental footprint, safety and costs for instance. To find an optimal balance between all design parameters is unrealistic as time and resources are limited in all projects. In ship design today, the top-down design approach is widely used; main dimensions are determined first whereas more detailed design such as the watertight subdivision appears later in the process. The watertight subdivision is restricted by damage stability regulations, and the required calculations are time-consuming. Due to the time pressure that usually occurs at the end of projects, it is thus advantageous to limit the number of design iterations. Relying on previous experience is challenging when ship designs are constantly developed. In consequence, predicting the outcome of the damage stability calculations is not straightforward. Thus, to know the effects of certain changes in the internal watertight arrangement of a ship at early design stages, would surely be beneficial in order to reduce the number of iterations at late design stages.

1.1 Historical Background and Motivation

There are two applicable damage stability calculation methods for ships: deterministic damage stability (DDS) and probabilistic damage stability (PDS). The appropriate method depends on the ship in question. The probabilistic approach, which is based on damage statistics in terms of the size and location of the damage on previously rammed ships, is considered to be more rationale than the deterministic approach.

The development of PDS regulations started in the late 60s, and a few years later Resolution A.265 (VIII) of SOLAS-74 entered into force. This was only an alternative to the deterministic procedure for dry cargo ships and passenger ships, which still was a part of SOLAS. Today's prevailing PDS regulations can be found in SOLAS Chapter II-1, Part B-1, and stems from a project called 'Harmonization of Rules and Design Rationale' (HARDER)'. The HARDER project started to collect large amounts of collision and grounding data in 2001, with the aim of harmonizing the damage stability regulations for all ship types. All existing approaches to PDS calculations were re-evaluated and new formulations were proposed to the existing regulations. The final proposals were adopted in 2005 by the Maritime Safety Committee (MSC), an underlying committee of IMO, and the new regulations entered into force in 2009. These are relevant for dry cargo ships with a length above 80 meters and passenger ships built after

January 1st, 2009. With the new PDS regulations in place, IMO actually proclaimed that DDS has no future (Papanikolaou & Eliopoulou, 2008; Vassalos, 2014).

Due to the 'Code of Safety for Special Purpose Ships, 2008' (SPS Code), which was adopted in 2008 by IMO Resolution MSC.266(84), Special Purpose Ships (SPSs) are also covered by the PDS regulations. If a ship has SPS notation[1], it is in general considered a passenger ship in accordance with the damage stability regulations in SOLAS Chapter II-1, Part B-1. Platform supply vessels (PSVs) are for instance not covered by the SPS Code, which means that PSVs are excluded from the PDS regulations. IMO Resolution MSC.235(82) should then be applied, which follows a deterministic approach. An increasing number of other offshore service vessel (OSV) types, however, are classified with SPS notation; more OSVs than before are now involved in operations that requires more on-board special personnel. Wind farm service vessels could be an example of this.

There are certain design advantages with the probabilistic approach. One advantage with the deterministic approach is the simple calculation procedure that makes it possible to quickly estimate the survivability of ships. The complexity of the PDS regulations indicates that the probabilistic approach is more accurate and realistic. Additionally, the PDS regulations offer flexibility in the design of watertight arrangements which the DDS regulations cannot offer. With the DDS regulations, the location of bulkheads is defined by pre-determined damage extents. That is not the case with the PDS regulations; bulkheads can be placed anywhere. The 'million-dollar question' then arises: how can the ship designer take advantage of the flexibility in design that the PDS regulations offer? (Djupvik, Aanondsen, & Asbjørnslett, 2015; Hjort & Olufsen, 2014).

One obvious obstacle related to the abovementioned flexibility is the top-down design approach. Top down design ironically makes the probabilistic approach less flexible than it potentially could be and is unlikely to be switched out with a bottom-up approach. Thus, time pressure will continue to be a limiting factor for PDS calculations at the end of projects. It is therefore interesting to know as much as possible, on beforehand of projects, about effects that certain design changes have on the results of PDS calculations. This problem is the motivational basis for the master's thesis.

[1] *'...a special purpose ship is a ship of not less than 500 gross tonnage which carries more than 12 special personnel, i.e. persons who are specially needed for the particular operational duties of the ship and are carried in addition to those persons required for the normal navigation, engineering and maintenance of the ship or engaged to provide services for the persons carried on board.'* (IMO, 2008b)

1.2 Previous Work

There is a limited amount of existing research related to the objectives of the master's thesis, i.e. how changes in the arrangement and initial stability of an offshore vessel impacts the attained subdivision index (A-index). Most research on probabilistic damage stability focus on optimisation methods that can be used to maximise the A-index for passenger vessels or Ro-Ro vessels. This research will not be elaborated further in this thesis as it is considered less relevant for the topic of the thesis. For further reading on the subject it is referred to the PhD thesis by Erik Sonne Ravn from 2003 and a study presented in the Journal of Shipping and Ocean Engineering 2 in 2012 by Puisa, Tsakalakis and Vassalos (Puisa, Tsakalakis, & Vassalos, 2012; Ravn, February 2003).

The master's thesis written by Ole Martin Djupvik in 2015 at the Department of Marine Technology at NTNU (Djupvik et al., 2015), seems to be the research with strongest relevance to this master's thesis. Mr. Djupvik looked at two different arrangement configurations for four different sizes of an offshore vessel. He investigated how the placement of a specific longitudinal bulkhead (LBH) typically located in the mid-ship section of offshore vessels affects the A-index. It was also investigated whether or not this effect changes proportionally with the size of the vessel, in order to see whether a generic model for optimal placement of the LBH could be developed for offshore vessels in general. Such a model could not be developed, unfortunately. However, Mr. Djupvik discovered for example that the A-index decreases when damages to the wing ballast tanks becomes critical to the survivability of the vessel (Djupvik et al., 2015).

1.3 Objectives and Scope of Work

The use of so-called U-tanks in the mid-section of offshore vessels is a well-known method to attain a higher A-index in the PDS calculations (Djupvik et al., 2015). The void space in Figure 1 illustrates a U-tank. It is also common to have wing ballast tanks above these U-tanks, in order to adjust the draught and improve the ship's stability when the cargo is discharged (Djupvik, 2015). In Salt Ship Design, it has been up to discussion whether the height of the 'deck', i.e. horizontal surface, separating these two tanks has a significant impact on the A-index or not. The first objective of this thesis is therefore to investigate how the A-index is affected by the height of this 'deck', which hereafter is referred to as the 'U-deck'.

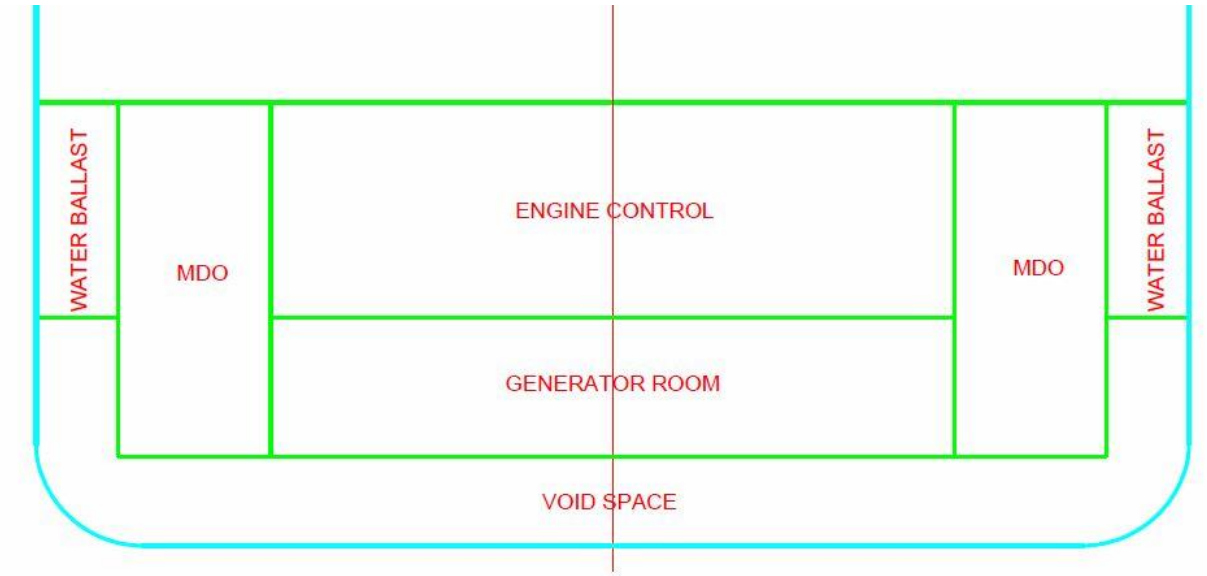

Figure 1. A cross-section of the 'Wind Farm Service Vessel' illustrating a void U-tank and wing ballast tanks.

A second problem that has been discussed, is how large impact the initial GM (or KG) value has on the A-index. If a lower GM value than first assumed is sufficient in terms of damage stability, and in terms of the intact stability criterion, this may allow removal of certain water ballast tanks for instance. To summarize, the two objectives of the master's thesis are:

1. Investigate the effect on the A-index of changing the height of the horizontal surface ('U-deck') separating the void U-tanks and wing ballast tanks at the mid-section of a 'Wind Farm Service Vessel (WFSV)' designed by Salt Ship Design.
2. Investigate the effect on the A-index of changing the intact stability of the ship, i.e. the ship's initial GM values for the three subdivision draughts d_S, d_P and d_L.

The overall goal and, thus, the common thread for these two objectives is to analyse the effect of changes on the A-index of the WFSV.

Briefly described, the scope of work related to the abovementioned objectives is:

- Carry out a literature study on intact stability, DDS and PDS – the theory that the individual study in this thesis is built upon.
- Learn how the stability software NAPA works.
- Use NAPA to model the watertight arrangement of the ship used in the individual study.
- Use NAPA to calculate PDS for the ship in question, for objective 1 and 2 of the thesis.
- Post-process the results with Microsoft Excel or another software, in order to plot the results and present them in a tidy manner.
- Analyse the results in-depth, i.e. study all 'PDS factors' that may have influenced the results, to achieve a thorough understanding.
- Discuss the analysed results with respect to the objectives.
- Finally, draw conclusions and suggest further work.

1.4 Limitations

One ship is investigated with respect to the development of the A-index. Preferably, the study should have been conducted for several offshore vessels that may apply to the SPS Code, to obtain as generic results and conclusions as possible.

The scope of the study is furthermore limited to four variables: the height of the deck separating the void U-tanks and wing ballast tanks, and the three GM values corresponding to the subdivision draughts that are accounted for in the PDS regulations.

1.5 Thesis Structure

This master's thesis follows the 'IMRAD - Introduction, Methods, Results and Discussion' style, with some alterations. For instance, a theory chapter regarding ship stability theory is included in chapter 2, between the introduction in chapter 1 and the methods of the individual study in chapter 0. This is considered beneficial, because some readers will benefit of having PDS theory easily accessible when reading the thesis. Chapter 5 includes both analysis and discussion of the results presented in chapter 4. A detailed content description for each chapter is given below.

Chapter 2: Ship Stability Theory

This chapter presents theory on intact stability, DDS and PDS. One could say that the PDS part of chapter 2 is a re-presentation of SOLAS-2009, but it better explains how the theory should be interpreted. By studying this chapter, the reader should get a basic understanding of stability and damage stability theory on ships, which will benefit the reader when studying the rest of the thesis.

Chapter 3: Individual Study on Probabilistic Damage Stability

Chapter 0 describes how the individual study in this thesis was conducted, including some more information regarding the two objectives of the thesis. The chapter also provides information about the ship used in the study, and furthermore explains the approaches used to model the ship and carry out PDS calculations in NAPA. Descriptions of some analysis tools in NAPA are also given.

Chapter 4: Results of Individual Study

This chapter presents the post-processed results from the PDS calculations in NAPA. Some comments and evaluation of the results are also included in chapter 4.

Chapter 5: Analysis and Discussion

In Chapter 5, the results from chapter 4 are analysed in-depth, in order to fully understand the development of the ship’s damage stability. In addition to the results' analyses a discussion on the quality and interpretation of results is given.

Chapter 6: Conclusion

Finally, conclusions regarding objective 1 and 2 of the thesis are drawn based on the analysed results in chapter 5. Additionally, suggestions to further work related to the study conducted in this master’s thesis are provided.

Chapter 7: Bibliography

All references that are referred to in the thesis are listed in Chapter 7.

2. Ship Stability Theory[2]

A ship's ability to stay afloat relies on the stability of the ship. Ship stability may in simple terms be defined as a ship's ability to return to its upright position, i.e. an angle of heel equal to 0°, after external forces have acted on the ship and, consequently, created a heeling moment. External forces are often induced by environmental phenomena such as waves and wind, but other sources may be shifting cargo, contact with obstacles in the sea or collision with other ships. Generally, ship stability can be divided into two categories: intact stability and damage stability (Magnussen, Amdahl, & Fuglerud, 2014).

2.1 Introduction to Intact Stability

Intact stability evaluates the stability of a ship in an undamaged condition, both in transverse and longitudinal direction. It is assumed that the reader has basic knowledge regarding intact stability, and it is not within the scope of the master's thesis to go into full detail on the topic. Some fundamentals that are considered important to have fresh in mind will be touched upon.

2.1.1 Transverse Stability

When the forces acting upwards through the centre of buoyancy (B) equals the forces acting downwards through centre of gravity (G) in Figure 2, the ship floats. By analysing the relative positions of B and G a stability assessment of the ship can be made. B changes when the ship rolls, but remains at the centre of the overall underwater volume. G can be considered a fixed point relative to the ship as long as the cargo does not shift (Patterson & Ridley, 2014).

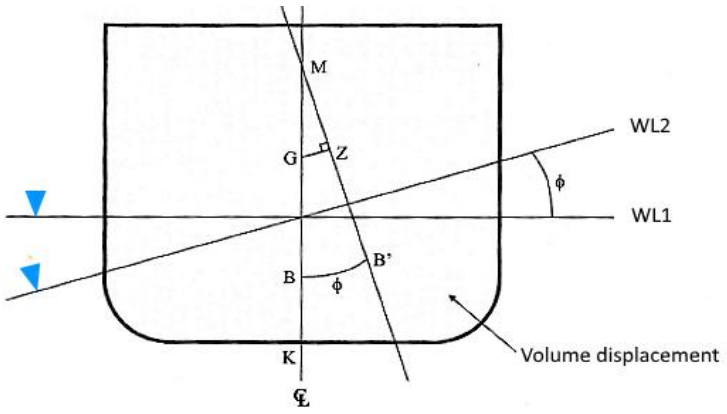

Figure 2. Transverse stability measurements for small angles. The figure is adapted from Magnussen et al. (2014).

[2] This chapter is taken from the author's project thesis written in TMR4560 Marine Systems Design, Specialization Project, fall 2015. Some changes, including re-writing, re-arrangement of text and formatting, have been done.

Although the ship floats, it is not necessarily stable. A ship is considered stable when the distance GM has a positive value. GM = KB + BM – KG. This method of using the metacentric height (M) as a measure of stability is called initial stability, and is only valid for small angles, i.e. up to 10 to 15 degrees of heel. That is because M is not considered stationary for larger angles (Patterson & Ridley, 2014).

Instead a method called large angle stability is used. This method also utilizes B and G, but now the heeling moment, or listing moment, caused by the misalignment of the forces acting through these points are in focus. This moment is controlled by the transverse distance between G and B, namely GZ, which is defined as the ship's righting lever, or righting arm. The product of GZ and the ship's displacement, Δ, then defines the righting moment, or torque of the ship. When the heeling moment equals the righting moment the ship enters a steady state of equilibrium, and the angle of heel will stabilize at a specific value (Patterson & Ridley, 2014).

When experiencing a heeling moment, GZ is said to be positive if the ship tries to return upright. If the GZ value is negative, the ship will capsize. As the GZ value varies with the heeling angle, it is usually presented as a graph with the heeling angle on the horizontal axis and the GZ value on the vertical axis. This graph is known as the GZ curve, and is illustrated in Figure 3 (Patterson & Ridley, 2014).

Figure 3. An example of a GZ curve. The figure is inspired by Djupvik et al. (2015).

θ_e is the angle of heel where the GZ value changes from negative to positive, and is known as the equilibrium angle. θ_v is known as the angle of vanishing stability, and is the point where the GZ value changes from positive to negative. Furthermore, the peak of the curve is known as GZ_{max}, and the range from θ_e to θ_v is naturally known as the range of stability, or just range. For any vessel, it is possible to create a curve of righting moments. This will look identical to the GZ curve, as the righting moment equals GZ multiplied with a constant. The area under this curve up to a certain angle is equal to the energy needed to roll the vessel to that angle. The area under the GZ curve up to a certain angle is thus proportional to the energy needed to roll the vessel to that angle. In other words, the larger area under the curve, the more energy is needed to roll the vessel (Patterson & Ridley, 2014).

IMO's 'International Code On Intact Stability, 2008' (2008 IS Code), include requirements both concerning the metacentric height criteria and minimum values for areas under the GZ curve. The 2008 IS Code requires that the area under the GZ curve have minimum values between specific angles, and that the peak of the GZ curve is in a certain region of the graph (IMO, 2008a).

2.1.2 Longitudinal Stability

In the same way as when the ship rolls, B will move to the new centre of underwater volume when the pitch of the ship changes, as shown in Figure 4. The longitudinal metacentre, M_L, is then the intersection of the line of action through the 'new B' and the line which was originally drawn vertically through the 'old B'. The longitudinal metacentric height, GM_L, is determined in the same manner as for transverse direction: $GM_L = KB + BM_L - KG$.

As Figure 4 illustrates, the GM_L value is typically very large compared to the transverse metacentric height, GM_T. This indicates that ships are usually very stable fore and aft, and that is the reason why ships tend to capsize transversely rather than stern over bow or bow over stern. For designers, an important effect of the large GM_L is the small contribution of the free surface effects (FSEs) in a longitudinal sense. In consequence, it is common to only use the lightship or a worst case loaded value when calculating the stability, and GM_L is assumed constant (Patterson & Ridley, 2014).

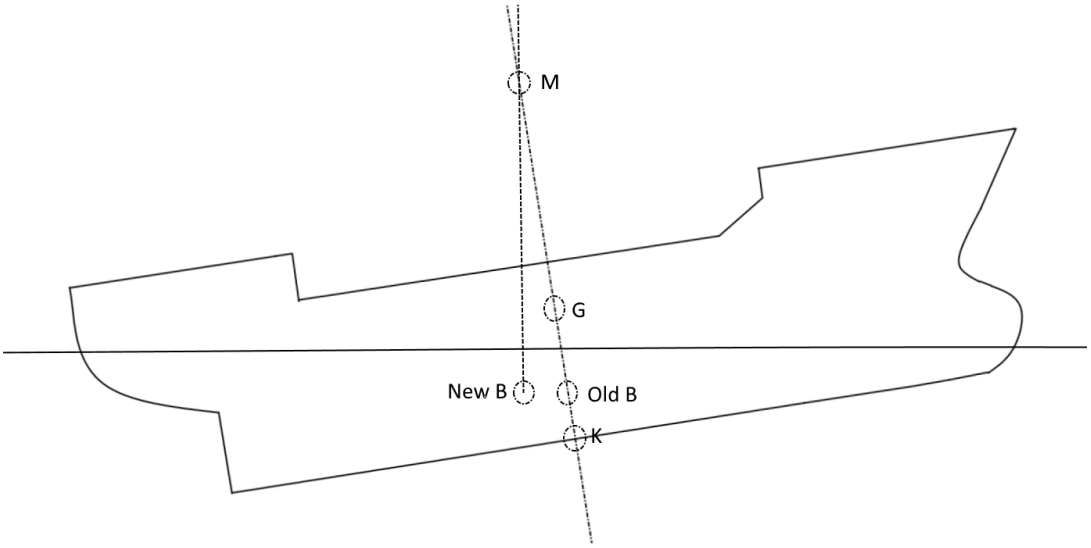

Figure 4. A ship that is trimmed by the stern (positive trim). The figure is inspired by Patterson and Ridley (2014).

Furthermore, a ship is said to be trimmed if the draughts measured at the after perpendicular and the forward perpendicular are different. The trim is controlled by the relative positions of the longitudinal centres of buoyancy and gravity, abbreviated LCB and LCG respectively. However, the trim is only said to be a part of the problem regarding longitudinal stability. The draughts at both ends of the ship, which varies with the trim, and the draught at the longitudinal centre of flotation (LCF) is of equal importance. At the LCF, the draught is independent of the trim, as it is the rotation point in trim. The draught at this point is known as the true mean draught, D_{TMD} or D_{LCF}, and is the value listed in the hydrostatic tables used in stability calculations (Patterson & Ridley, 2014).

2.2 Introduction to Damage Stability

Damage stability is naturally related to the stability characteristics of a damaged ship. In SOLAS, a damage is defined as *'the three dimensional extent of the breach in the ship'* (IMO, 2008c). After damage, one or more compartments of the ship may be filled with water, depending on the damage location, the three dimensional damage extent and the watertight subdivision of the ship. A compartment is defined by SOLAS as *'an onboard space within watertight boundaries'*, where space is defined as *'a combination of rooms'*. A room is a part of the ship limited by bulkheads and decks, with a specific permeability (IMO, 2008c). A compartment is said to be exposed to bilging or flooding when it is filled with water, and the water can move freely in and out of the compartment (Patterson & Ridley, 2014).

2.2.1 The Lost Buoyancy Method

There are several ways to evaluate the trim and stability of a ship after flooding, but the most common method adopted by IMO is known as 'lost volume' or 'lost buoyancy'. The effect of flooding is then determined in several steps (Patterson & Ridley, 2014):

1. Parallel sinkage (Initial sinkage)
2. New position of B
3. New BM and BM_L
4. New GM and GM_L
5. Resulting heel and trim

Steps 2 to 5 will not be explained, but some elaboration on step 1 is considered relevant within the scope of the master's thesis. First of all, when one or more compartments are flooded, the ship will get a higher draught. This initial sinkage is known as parallel sinkage. Dependent on the position of the compartments, the ship will also heel or trim. This is because the compartments in question, before flooding, contributes to the overall underwater volume of the ship. Thus they provide some of the ship's total buoyancy force supporting the vessel. After flooding, these compartments no longer provide this buoyancy, the total buoyancy force is consequently reduced and the ship becomes less stable (Patterson & Ridley, 2014).

As the ship moves vertically downwards due to flooding, the total underwater volume will gradually increase. The remaining buoyant volume is produced by the compartments that are still intact. At some point, the force of buoyancy has increased enough to be back in equilibrium with the gravity force, and the sinking stops. The overall underwater volume lost through flooding is now equal to the underwater volume (buoyant volume) gained through sinkage. The parallel sinkage can be determined from this principle (Patterson & Ridley, 2014).

The theory above assumes that the flooded compartments are completely filled with water. In reality this may not be the case. In the machinery rooms for instance, there are engines and other components that cannot flood. Let us say that these components take up 60% of the machinery room, then this is modelled using a factor of 0.6. This is known as the compartment permeability factor. The permeability has an effect on both the volume flooded and the waterplane area lost. This is taken into account by adjusting the parallel sinkage formula (Patterson & Ridley, 2014).

2.2.2 Damage Stability Regulations

Similar to intact stability, there are international regulations that ships must comply with regarding damage stability. The regulations are quite complex and do not guarantee safety, but they are meant to help the designers create safe ships. As explained previously, ships are designed to be safe both concerning initial and large angle stability, and also to some extent when the ship is damaged. The regulations introduced in Table 1 are developed in order to increase the probability of survival in case of ship damage. However, this probability can only be minimised; never set to zero. It is not possible to design an unsinkable passenger ship that is still feasible to invest in. The master's thesis will not go into detail on the regulations in the below table, except for 'regulation E' which includes PDS, but a short introduction to each of them is provided in this sub-section (Patterson & Ridley, 2014).

Table 1. Current damage stability regulations. The table is adapted from Patterson and Ridley (2014).

Current damage stability regulations		
A	Passenger vessels pre-2009	Deterministic
B	The Stockholm Agreement	Probabilistic
C	Safe return to port regulations	Deterministic
D	Damaged stability requirements - 'Type A/B' vessels (pre-2009)	Deterministic
E	SOLAS damaged stability rules post-2009	Probabilistic

'Regulation A' is described in MSN 1698M (MCA, 1998). A key element in this regulation is the margin line, which is related to the freeboard requirements. The margin line is defined as a datum line that goes all the way around the ship, 76 mm below the freeboard deck. A ship is considered lost if this line touches the water. According to the regulation, and depending on the ship type, ships must be designed so that this does not happen if one, two or three compartments are flooded. To ensure this, parallel sinkage must be minimised in the case of flooding. That is achieved by designing the compartments small enough and by using double bottom or wing tanks, or both. Regarding damage stability, the requirements are purely deterministic, i.e. the damage extent is predetermined. In addition, the regulation is conservative in the sense that it always assumes the worst-case scenario. This deterministic method is suitable when modelling a range of scenarios, but the problem is that realistic scenarios are hard to predict. That is the reason deterministic methods are slowly being replaced with probabilistic methods (Patterson & Ridley, 2014).

The Stockholm Agreement described in MSC/Circ. 574, which is applicable to large Ro-Ro passenger ships, is following a probabilistic approach. The agreement defines an additional standard that neighbouring port states may apply to Ro-Ro passenger ships. These requirements are not a part of the SOLAS Convention, as it in fact describes a maximum standard. The standard assesses the probability of a ship surviving a damage causing water ingress. The damage probability varies according to the location on the ship. The probability of compartment flooding and the probability of surviving the compartment flooding are also taken into account in the overall survival probability. The regulation requires the calculation of A and A_{max}, respectively representing a subdivision index and a maximum value of survivability of the ship. In addition, depending on the freeboard, a hypothetical effect of 0.5 m or less of water on the vehicle deck closest to the waterline is included. (Hjort & Olufsen, 2014; Patterson & Ridley, 2014).

The safe return to port regulations were approved by IMO in 2006, and is applicable to certain passenger ships with a length of 120 m and above. This set of regulations states that the safest lifeboat is the ship itself; a ship should be able to survive a damage and return safely to port, even in the event of flooding of any one single watertight compartment. In the case of more than one flooded compartment, the ship should be designed to be evacuated safely within three hours after the damage occurs (Patterson & Ridley, 2014).

Before 2009, the set of regulations in row D in Table 1, was mandatory to all type of ships. Two ship types are defined: A (carrying liquid cargo in bulk) and B (all other ships). The regulations are deterministic in the sense that the amount of damage on the ship is predetermined; the damage is assumed to be over the entire depth of the vessel in vertical extent and whichever is lesser of B/5 and 11.5 m in transverse extent. In longitudinal direction the damage is limited to a single compartment between transverse bulkheads, given that any longitudinal bulkheads are outside of the transverse damage extent. However, this is different for so-called B-60 and B-100 ships. B-60s are required to survive flooding of any compartments with a permeability of 95%. B-100s must survive flooding of any two adjacent compartments. Both of the two latter requirements are not required for machinery spaces if the ship is lesser than 150 m in length (Patterson & Ridley, 2014).

For any type of ship with a keel-laying date before January 1st 2009, the minimum requirements shown in Figure 5 are required (Patterson & Ridley, 2014).

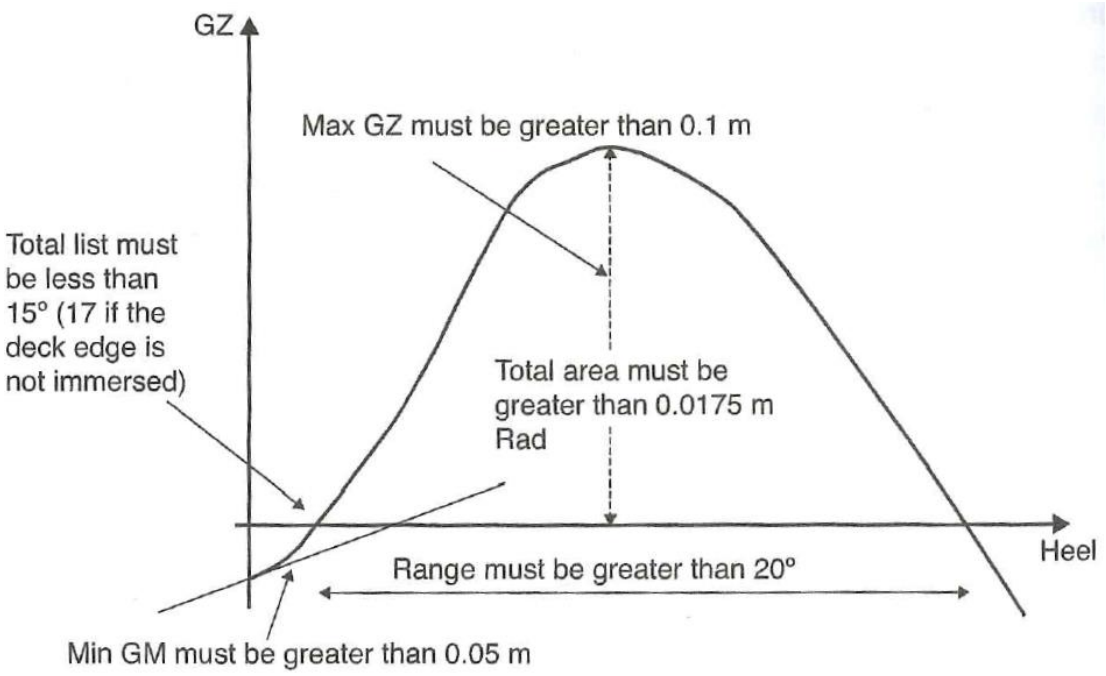

Figure 5. Damage stability requirements for all ships pre-2009. The figure is obtained from Patterson and Ridley (2014).

In 2009, IMO introduced new regulations for dry cargo and passenger ships, which are based on a mix of deterministic and probabilistic approaches. This set of regulations is referred to as the 'PDS regulations' in the master's thesis, and will be explained in Section 2.4. The deterministic damage stability regulations will be referred to as the 'DDS regulations' hereafter, and is briefly presented in Section 2.3. To sum up Section 2.2 and introduce the PDS regulations at the same time: the main factors that affect the three-dimensional damage extent of a ship with a given watertight subdivision, are listed below (IMO, 2008c):

- The zones or group of adjacent zones that are flooded ('zones' is defined later)
- Loading condition; draught, trim and intact GM at the time of damage
- Permeability of flooded compartments at the time of damage
- Sea state at the time of damage
- Factors such as possible heeling moments due to unsymmetrical weights

2.3 Deterministic Damage Stability

A deterministic approach is a perfectly predictable approach. That is, the approach follows a completely known rule, e.g. a fixed procedure, so that a given input will always give the same output. The states of a system described by a deterministic approach may be numbers specifying physical characteristics of the system, for instance observables such as length or mass. For damage stability of ships, the DDS regulations are said to follow a deterministic approach because the ship must survive a predetermined amount of damage (Kirchsteiger, 1999; Patterson & Ridley, 2014).

Deterministic damage stability is all about ensuring that a ship is 'safe enough'. It has been the dominating method for a long time, and the DDS regulations are still in use today due to various reasons. First of all, the PDS regulations do not cover all ship types. Secondly, despite the DDS regulations' well-known conservatism, it has a long track-record, and the society tends to trust well-proven methods. A, C and D in Table 1 in Sub-section 2.2.2 are following a deterministic approach. As mentioned, these three regulations apply to different types of passenger ships. In addition to the SOLAS-74 standard, which regulates ordinary passenger ships, Table 2 provides an overview of other IMO instruments that contain DDS provisions (Hjort & Olufsen, 2014).

Table 2. IMO instruments containing DDS provisions, besides of SOLAS-74.
The table is adapted from Hjort and Olufsen (2014).

Regulatory framework	Application area
ICCL-66	Cargo ships and tankers with reduced freeboard
MARPOL-73/78	Tankers carrying cargo oil
IBC Code	Ships carrying dangerous chemicals in bulk
IGC Code	Ships carrying liquefied gases in bulk
HSC Code	High speed crafts

2.3.1 Calculation Method

The outcome of DDS calculations, i.e. whether the ship is 'safe enough' or not, mainly depends on the ship size; the length, beam and depth of the ship in question. Together these three parameters determine the damage extent of the ship, as explained in Sub-section 2.3.2. In general, the parameters used in the calculations are the same for different ship types, but the impact of the parameters differ. This impact depends on factors such as ship type, ship size, cargo type and number of passengers.

Furthermore, the ship in question is required to survive certain damage scenarios, given by the predetermined damage extent. The goal is of course to identify the most critical damage scenarios. This is done by investigating all possible damage conditions within the boundaries of the damage extent. All damage scenarios must comply with the requirements as defined in SOLAS. Some of these requirements are presented in Sub-section 2.3.3. If the results from the calculations are not up to standard, the ship will not be approved by the flag state or the classification societies (Djupvik et al., 2015; Patterson & Ridley, 2014).

2.3.2 Damage Extent

The damage extent comprises the longitudinal-, transverse- and vertical extent of the damage. The longitudinal damage extent is determined by the length of the ship, L, as calculated by Equation 1 (Patterson & Ridley, 2014).

$$\text{Longitudinal damage extent} = \min(3 + 0.03 \cdot L\,, 11)\ [m] \tag{1}$$

The definition of the ship length goes all the way back to the International Convention on Load Lines, 1966 (ICCL-66), which states: *'"Length" means 96% of the total length on a waterline at 85% of the least moulded depth measured from the top of the keel, or the length from the fore-side of the stem to the axis of the rudder stock on that waterline, if that be greater. Where the stem contour is concave above the waterline at 85% of the least moulded depth, both the forward terminal of the total length and the fore–side of the stem respectively shall be taken at the vertical projection to that waterline of the aftermost point of the stem contour (above that waterline). In ships designed with a rake of keel the waterline on which this length is measured shall be parallel to the designed waterline.'(IMO, 1966).* This definition is still in use today, and is illustrated in Figure 6 (Djupvik et al., 2015).

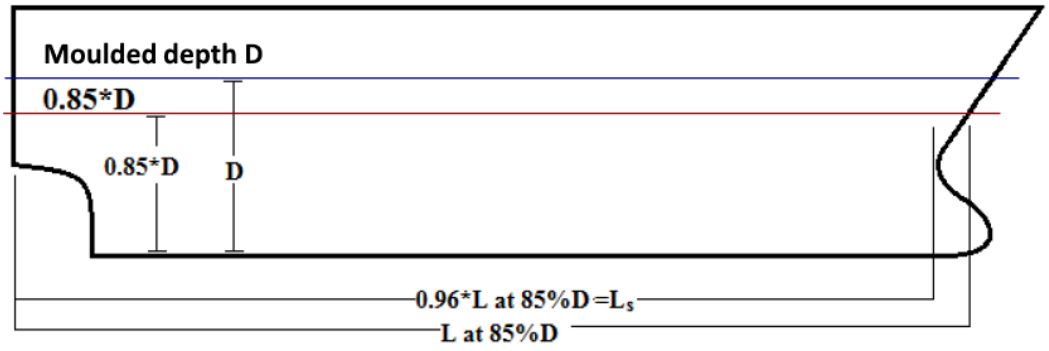

Figure 6. Ship length as stated in ICCL-66. The figure is adapted from Djupvik et al. (2015).

The transverse damage extent is determined by Equation 2, where B is the beam of the ship. B is measured at the deepest subdivision draught (load line), from the ship side 90° onto the centre line (Hjort & Olufsen, 2014; Patterson & Ridley, 2014).

$$\text{Transverse damage extent} = \text{Min}\left(\frac{B}{5}, 11.5\right)\ [m] \quad (2)$$

The vertical damage extent has no limitations, and is taken as the entire depth of the ship. Furthermore, a worst-case loading scenario shall always be assumed. The permeability is set to e.g. 95% for accommodation and 85% for machinery spaces. If a lesser damage causes a worse condition, then the worst case shall be used (Patterson & Ridley, 2014).

2.3.3 Requirements

After the ship has reached equilibrium position in a damage scenario where one or more compartments are exposed to flooding, and the lost buoyancy method is used to calculate the damaged trim and stability, the following requirements must be met (Patterson & Ridley, 2014):

1. GM > 0.05 m
2. Heel angle ≤ 7° for one compartment flooding, or 12° for two or more adjacent compartments.
3. Specific minimum requirements related to the area under the GZ curve (see Figure 5).
4. Range of stability ≥ 15°. This requirement may be reduced from 15° to 10° if the area under the GZ curve increases by a certain ratio.
5. Peak GZ value = $Max(\frac{Heeling\ moment}{\Delta} + 0.04, 0.10)\ [m]$, where the heeling moment is generated by:
    1. All passengers crowding to deck areas on one side of the ship where the muster stations are located, with a passenger weight of 75 kg and a density of 4 passengers to a square metre.
    2. Davit launching of all fully loaded survival crafts on one side of the ship.
    3. Wind pressure = 120 N/m^2 on one side of the ship.

- For any type of passenger vessel, the margin line must not be submerged in the final equilibrium position.

2.4 Probabilistic Damage Stability

Basically, what is a probabilistic approach? First of all, a probabilistic approach involves some degree of uncertainty. Thus, 'random variables' are required to develop prediction models, which for example can be used to describe the behaviour of a system. There is no universal definition of 'randomness', but in the context of damage stability it means that accidents and the damage extent of accidents are unpredictable. In order to map the unpredictable, the only available analytical tool is probability theory. Past knowledge, e.g. damage statistics, can be used to predict random factors that influence the final consequence of damage to a ship's hull. Such random factors may be the mass and the velocity of the ramming ship. The influence of these random factors is different for ships with different characteristics; for instance, differences in the range of permeability and service draught (IMO, 2008c; Kirchsteiger, 1999).

The PDS regulations that entered into force on the 1st of January 2009 as a part of SOLAS Chapter II-1, Part B-1 Stability, applies to dry cargo ships with a length of 80 m or above and all passenger ships with keel laying on or after this date. A passenger ship is per definition a ship carrying more than 12 passengers. In addition, because the 'Code of Safety for Special Purpose Ships, 2008' (SPS code) was adopted in 2008 by IMO Resolution MSC.266(84), Special Purpose Ships (SPSs) are also covered. Furthermore, all the ships applicable to the PDS regulations are required to have double bottom and automatic cross flooding arrangements that stabilize the ship within 10 minutes. On top of this, if the ship is carrying over 36 passengers, there are additional deterministic requirements. These will not be detailed here, as the scope of this section is to explain the probabilistic approach (IMO, 2006, 2008b).

Whether a ship is 'safe enough' according to the PDS regulations or not, is determined by Equation 3. In SOLAS Chapter II-1, Part B-1 Stability, Reg. 7, A is defined as the '*Attained Subdivision Index*' and R is defined as the '*Required Subdivision Index*'. Two different ships are considered equally safe if they have the same value of A. The calculation of A is based on the probability of damage, i.e. flooding of compartments, and the survivability of the ship after flooding. This and more are explained in detail throughout this section (IMO, 2006, 2008c; Patterson & Ridley, 2014).

$$A > R \tag{3}$$

2.4.1 Limitations

The current PDS regulations are based on damage statistics. More precisely, collision statistics. A 'collision' may be ship-to-ship or contact between a ship and an obstacle, e.g. an ice berg. For assessment of groundings there is no probabilistic approach available in the regulations, most likely due to lack of grounding statistics. However, a widely used technique for probabilistic approaches when relevant statistics are insufficient, is the Monte Carlo simulation. In other words, one could possibly use the damage statistics from the GOALDS project as a basis in combination with Monte Carlo simulation to develop an approach. The probability distributions from GOALDS can be found in IMO SLF 55/INF.7 (Hjort & Olufsen, 2014).

Furthermore, Table 3 provides a complete overview of which ship types that follow the PDS approach and which ship types that follow the DDS approach.

Table 3. An overview of damage stability conventions and codes for different ship types (Eklund & Lindroth, 2009; IMO, 2008b; Wärtsilä).

Code or convention	Ship type	Method
SOLAS-2009	All passenger ships: - Pure passenger ships - Ro-Ro ships - Cruise ships	Probabilistic
SPS Code / SOLAS-2009	- Special Purpose Ships	
SOLAS-2009	Dry cargo ships > 80 m in length: - RoRo cargo ships - Car carriers - General cargo ships - Bulk carriers with reduced freeboard and deck cargo (IACS Unified interpretation no. 65) - Cable laying ships	Probabilistic
1966 Load line convention	Dry cargo ships with reduced freeboard	Deterministic
1966 Load line convention / MARPOL 73/78 Annex 1	Oil tankers	Deterministic
International bulk chemical code	Chemical tankers	Deterministic
International liquefied gas carrier code	Liquefied gas carriers	Deterministic

2.4.2 Subdivision Length

Before explaining any further how the R- and A-indexes are calculated, it is useful to introduce a frequently used factor named subdivision length, which is denoted L_S in the PDS regulations. It is important to distinguish between this length factor and the one used in the DDS regulations. Figure 7 illustrates how the subdivision length is determined for three different scenarios. As the figure shows, the subdivision length depends on the buoyant hull and the reserve buoyancy of the ship, and whether these 'areas' are harmed or not. The buoyant hull comprises the enclosed volume of the ship below the waterline, which is denoted 'd_S' in the figure, while the reserve buoyancy is comprising the enclosed volume of the ship above the waterline. The black line is defined as the maximum vertical damage extent, and is always equal to d_s + 12.5 m measured from the baseline. The ship illustrated at the bottom of Figure 7 distinguishes between reserve buoyancy that is harmed and unharmed. The subdivision length is then measured from the stern to the foremost point of the harmed area at the stem (Hjort & Olufsen, 2014).

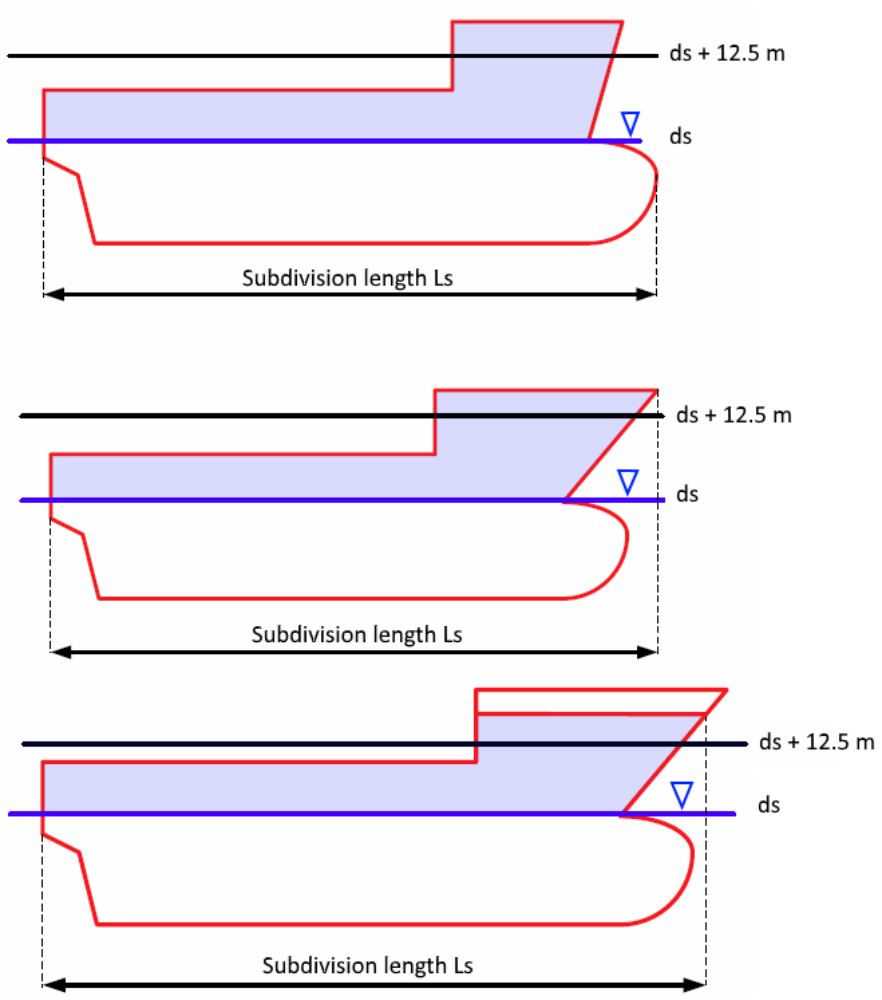

Figure 7. Examples of how the subdivision length is determined. The figure is adapted from Hjort and Olufsen (2014).

2.4.3 Required Subdivision Index R

Calculation Procedure

The calculation procedure for the Required Subdivision Index R (R-index) is dependent on the ship type. For passenger ships, the R-index is a function of ship length, number of persons on board and the lifeboat capacity, as shown by Equation 4. For cargo ships, the R-index is solely a function of the ship length. For cargo ships larger than 100 m in length and cargo ships between 80 m and 100 m in length, R-index is calculated by Equation 5 and 6 respectively. Explanations to the parameters used in the below equations are gathered in Table 4.

$$R = 1 - \frac{5000}{L_s + 2.5N + 15225} \tag{4}$$

$$R = 1 - \frac{128}{L_S + 152} \tag{5}$$

$$R = 1 - \left[\frac{1}{1 + \frac{L_S}{100} \cdot \frac{R_0}{1 - R_0}}\right] \tag{6}$$

Table 4. Parameters used in the calculation of R-index (Hjort & Olufsen, 2014).

Explanations to the parameters used in the calculation of R-index	
N	$N_1 + 2N_2$
N_1	Number of persons for whom lifeboats are provided
N_2	Number of persons in excess of N_1, including officers and crew
L_S	Subdivision length
R_0	The value of R calculated by Equation 5

For SPSs, there are some other specific requirements. In general, the SPS is considered a passenger ship in accordance with SOLAS Chapter II-1, and special personnel are considered passengers. However, the requirements related to the R-index varies with the number of persons that the SPS is allowed to carry (IMO, 2008b):

1. the R value is taken as R if the SPS is certified to carry 240 persons or more;
2. the R value is taken as 0.8R if the SPS is certified to carry not more than 60 persons; and
3. the R value is determined by linear interpolation between the R values given in 1 and 2 above, if the SPS is carrying more than 60 but less than 240 persons.

Background

The R-index for passenger ships was established based on sample ship calculations from the HARDER project (Hjort & Olufsen, 2014). More information on the development of the R-index is difficult to obtain. Some insight is however provided by Gunnar Hjort, whom at the time of writing worked under the title Principal Approval Engineer at DNV GL's stability section (Hjort, 2015):

An important objective of the development of PDS regulations was to ensure that new and existing ships should have approximately the same level of safety with the PDS regulations. Bearing this in mind, an initial formula for the R-index for passenger ships was developed in a scientific manner, by carrying out multiple test runs using existing ships. The problem with this approach was that the value of the R-index declined with increasing values of ship length and number of passengers. This was totally unacceptable for the membership countries of IMO; it was argued that it would give an unbalanced picture of the safety level of large existing passenger ships. In consequence, a 'political correct' compromise was agreed upon and a new, but not necessarily scientific 'correct' formula for the R-index was developed (Hjort, 2015).

The explanation of the declining value of R with the initial formula for passenger ships is not clear, but some thoughts are summarized here:

- With the old, deterministic rules the safety standard of the ship depended on the degree of watertight subdivision of the ship, i.e. the number of watertight bulkheads fitted. The damage extent represented the distance between watertight bulkheads, which was maximum 11 m. Thus, for the larger ships that were defined as 'two compartment ships' by means of damage stability, the damage extent was 22 m. In comparison, the maximum damage extent in the PDS regulations is 60 m. In other words, the relative damage extent was very low for the large ships and, thus, one may expect a declining R-index (Hjort, 2015).

- The deterministic ‘B/5 rule’, of which the watertight arrangements for existing ships at the time usually were optimised against, might also have had an impact on the unexpected declining R-index value; In the development of the probabilistic rules, the statistics from the HARDER project showed that the maximum transverse damage extent should be B/2, not B/5.

For cargo ships, the R-index formula was based on a probabilistic approach from the beginning, so there has been no major changes affecting the results. This in turn gives quite equal results for new and old cargo ships. However, it was commonly accepted that some designs would deviate due to the new foundation of statistical data, for instance from the HARDER project. It should also be noted that the old rules concerning dry cargo ships in reality was a compromise built on the ‘any rules are better than no rules’ mentality. In the development of the R-index, or the PDS regulations in general, they had to deal with these rules. As mentioned before, politics has always played an important role in the development of IMO regulations, and formulas may be developed based on political compromises. As a result, it can be difficult to understand the formulas completely (Hjort, 2015).

2.4.4 Attained Subdivision Index A

The final or total A-index is expressing the probability of surviving a collision that causes damage to the ship’s hull, accounting for all of the three loading conditions listed in Table 5. The A-index for each loading condition c, denoted A_c, is calculated by Equation 7. Here, N is the number of damages that is to be considered, while i represents each damage or group of damages that is considered. The p_i-, v_i- and s_i-factors will be thoroughly explained throughout Section 2.4, but they are also briefly introduced in Table 5. As shown in Equation 8, the final A-index is determined by summarizing and weighing the results from the three loading conditions. The weighting accounts for the corresponding percentual time in operation. The loading conditions are defined by their trim, GM value and the mean draught d, as shown in Figure 8 (Djupvik et al., 2015; IMO, 2006).

$$A_c = \sum_{i=1}^{N} p_i s_i v_i \; > \begin{cases} 0.9R, & for\ passenger\ ships \\ 0.5R, & for\ cargo\ ships \end{cases} \tag{7}$$

$$A = 0.4A_S + 0.4A_P + 0.2A_L > R \tag{8}$$

Table 5. Loading conditions and the p_i-, v_i- and s_i-factors (Lützen, 2001; Patterson & Ridley, 2014).

Important notations and factors for the PDS regulations	
$c = d_S$	Deepest subdivision draught (on an even keel)
$c = d_P$	Partial subdivision draught (on an even keel)
$c = d_L$	Light service draught; ballast condition for dry cargo ships or arrival condition for passenger ships, with corresponding trim (not more than 1% of the length)
p_i	Accounts for the probability of flooding of a compartment or a group of compartments, disregarding any horizontal subdivision
s_i	Accounts for the probability of survival after the flooding of a compartment or a group of compartments, including the effect of horizontal subdivision (the v_i-factor);
v_i	The probability that the space above a horizontal subdivision is not flooded

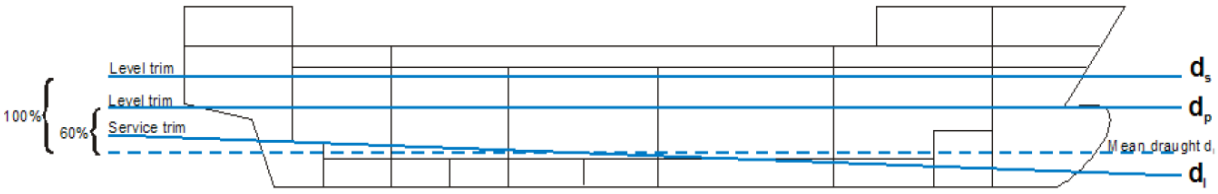

Figure 8. Illustration of the loading conditions, mean draught and trim levels. The illustration is obtained from IMO (2008c).

2.4.5 Zone Division

In order to prepare the calculation of A, the ship under consideration must be divided into a fixed discrete number of zones, in longitudinal, transverse and vertical direction. A longitudinal zone, or just 'zone', is defined as '*a longitudinal interval of the ship within the subdivision length'* (IMO, 2008c). It is up to the designer how the zone division is done; the only rule for subdivision is that the subdivision length L_S defines the extremes for the hull in longitudinal direction, as shown in Figure 9.

In order to maximise safety, the goal should be to obtain as large A-index as possible. Thus, it is important to be strategic when doing the subdivision, since each zone and all combinations of adjacent zones contribute to the A-index. More zones do in general give a larger A-index. The number of zones should however be limited to some extent, in order to keep the computation time at an acceptable level. One strategy may be to divide the zones according to the watertight subdivision of the ship, which is said to give profitable results. Furthermore,

Figure 9 illustrates a seven-zone division of a ship with the corresponding possible single- and multi-zone damages. The bottom line triangles indicate single-zone damages, while the parallelograms indicate multi-zone damages (Djupvik et al., 2015; IMO, 2008c; Lützen, 2001).

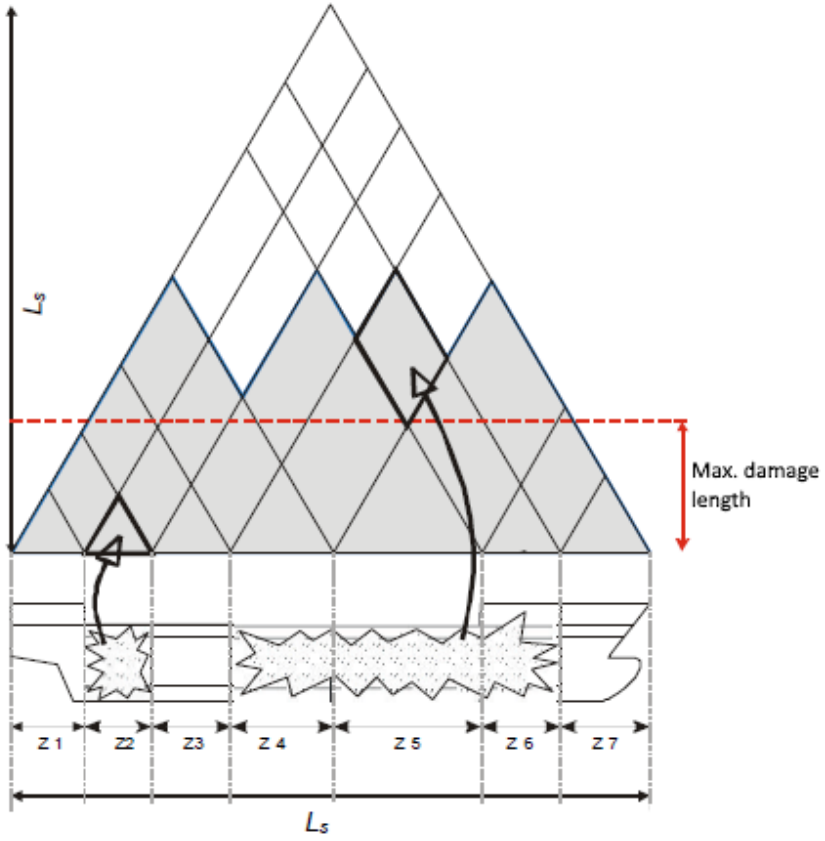

Figure 9. Possible single- and multi zone damages for a ship with 7 zones. The illustration is adapted from DELFTship ; the original source is IMO (2008c).

2.4.6 The Factor p_i

The p_i-factor is only dependent on the watertight arrangements and the zone division of the ship under consideration. This factor accounts for the probability of a specific damage to the ship, without considering any horizontal subdivision. The vertical damage extent is accounted for in the v_i-factor, which is elaborated in Sub-section 2.4.8. For single-zone damages, the formula for calculating p_i is given by Equation 9. Additionally, it is important to note that $\sum p_i$ is equal to 1 for the entire subdivision length. Explanations to the notations used in Equation 9 is provided in

Table 6. The formulas for multi-zone damages are not given in this sub-section, due to their complexity, but they can be found in Appendix A (IMO, 2006).

$$p_i = p(x1_j, x2_j) \cdot [r(x1_j, x2_j, b_k) - r(x1_j, x2_j, b_{k-1})] \quad (9)$$

Table 6. Factors and notations used in the formula for the p_i-factor (IMO, 2006).

Explanations to factors and notations related to the p_i-factor	
j	The aftmost damage zone number involved in the accident, starting with number 1 at the stern.
k	The number of a particular longitudinal bulkhead functioning as a barrier for transverse penetration, counted from the shell towards the centre line (k = 0 for the shell).
x1	Distance from the aft end (terminal) of the ship to the aft end of the zone in question.
x2	Distance from the aft end (terminal) of the ship to the forward end of the zone in question.
b	Mean transverse distance in metres measured from the shell to the longitudinal barrier in question. This distance is measured at the deepest subdivision load line, and should never be taken as greater than B/2. If the shell and the longitudinal barrier in question are not parallel to each other, then b is determined with an assumed line, as defined by IMO Resolution MSC.281(85) – "Explanatory Notes to the SOLAS Ch. II-1…Part B-1, Reg. 7-1.1.2".
p(x1,x2)	Accounts for the probability of the considered longitudinal damage extent.
r(x1,x2,b)	A probability factor accounting for the transverse damage extent.

Background and Calculation of $p(x1_j,x2_j)$

The calculation of $p(x1_j,x2_j)$ is carried out differently for three specific damage conditions, by using a number of formulas provided in SOLAS Chapter II-1, Part B-1, Reg. 7-1. Some non-dimensional lengths, which are key input to these formulas, are given in Table 7.

Table 7. Non-dimensional damage lengths used to calculate $p(x1_j,x2_j)$ (IMO, 2006).

Explanations to non-dimensional damage lengths used to calculate $p(x1_j,x2_j)$	
J_{max} = 10/33	Overall normalised maximum damage length
J_{kn} = 5/33	Knuckle point in the distribution ($L_s \leq 198$ m)
p_k = 11/12	Cumulative probability at J_{kn}
l_{max} = 60 m	Maximum absolute damage length
L* = 260 m	Length where normalised distribution ends

The above values are derived from statistics collected by the HARDER project. The left part of Figure 10 shows how damage lengths from the HARDER project is plotted as a function of the ship length, while the plot to the right shows the distribution density for non-dimensional damage length. This distribution density may be denoted pdf, and in accordance with Table 7 the non-dimensional damage length on the horizontal axis is denoted J. The red thick line in the plot represents the distribution as applied in the PDS regulations, while the blue dotted line was used in the old regulations for dry cargo ships. As can be seen, these two lines correspond quite well to each other (Hjort & Olufsen, 2014).

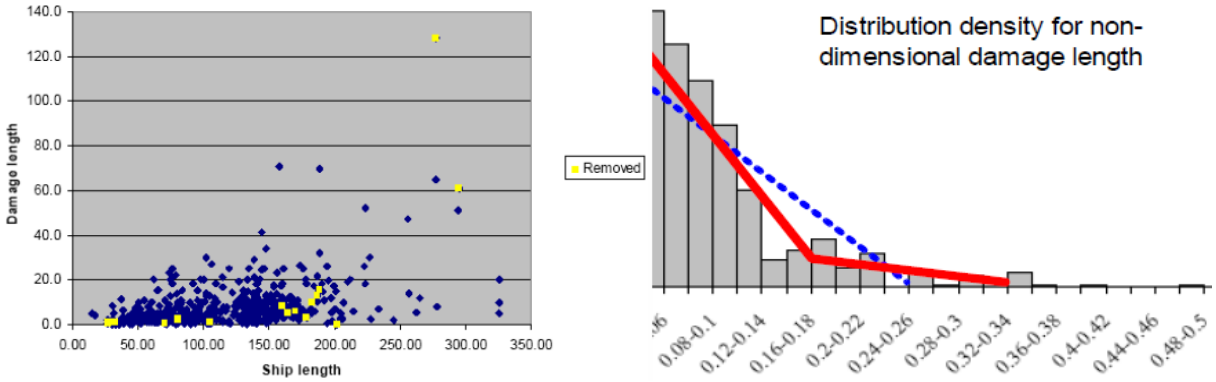

Figure 10. Distributions created based on statistics from the HARDER project (Hjort & Olufsen, 2014)

The red line above is a bi-linear function developed by Marie Lützen, as presented in her PhD thesis from 2001. All parameters used in this function are non-dimensional, because this was easy to implement in the probabilistic regulations prevailing at that time. The bi-linear function b(x) is written as Equation 10, and the integration of this function from zero to the maximum non-dimensional damage length $\bar{x}_{max}$ must be equal to one. J_k is the knuckle point in the above distribution. Thus, the factors b_{11} and b_{21} are the slopes of the red line before and after the knuckle point, respectively. The factors b_{12} and b_{22} must then be the starting points of the distributions, for $\bar{x} \leq J_k$ and $\bar{x} > J_k$ respectively (Djupvik et al., 2015; Lützen, 2001).

$$b(\bar{x}) = \begin{cases} b_{11} \cdot \bar{x} + b_{12}, & for\ \bar{x} \leq J_k \\ b_{21} \cdot \bar{x} + b_{22}, & for\ \bar{x} > J_k \end{cases} \tag{10}$$

Additionally, considering the diagram to the left in Figure 10, Lützen discovered that the non-dimensional damage location should be taken as a uniform distribution, equal to 1, along the length of the rammed ship. In other words, there was no clear correlation between ship length, damage length and damage location (Lützen, 2001).

The formulas used to determine $p(x1_j,x2_j)$ vary with the subdivision length L_S. Worth noticing is that the formula for the b_{12} coefficient is not the same for all L_S values; it depends on whether L_S is smaller, equal to or larger than L*. The formulas used to calculate b_{11}, b_{21} and b_{22} are given by Equation 11, 12 and 13 respectively, and they are the same independent of L_S (IMO, 2006).

Equation 14 and 15 represent the non-dimensional damage length J and the normalised length of a compartment or group of compartments J_n, respectively. Their values depend on L_S, which means that the values of b_{11}, b_{12} and b_{22} also depend on L_S. In Equation 15, J_m is the maximum non-dimensional damage length for the particular ship. The probability density at J = 0, denoted b_0, is given by Equation 16. All other relevant parameters were defined in Table 7 (Djupvik et al., 2015; IMO, 2006).

$$b_{11} = 4\frac{1-p_k}{(J_m - J_k)J_k} - 2\frac{p_k}{J_k^2} \tag{11}$$

$$b_{21} = -2\frac{1-p_k}{(J_m - J_k)^2} \tag{12}$$

$$b_{22} = -b_{21}J_m \tag{13}$$

$$J = \frac{(x2 - x1)}{L_S} \tag{14}$$

$$J_n = min\{J, J_m\} \tag{15}$$

$$b_0 = b_{J=0} = 2\left(\frac{p_k}{J_{kn}} - \frac{1-p_k}{J_{max} - J_{kn}}\right) \tag{16}$$

When $L_S \leq L^*$ (260 m):

$$J_m = min\left\{J_{max}, \frac{l_{max}}{L_S}\right\} \tag{17}$$

$$J_k = \frac{J_m}{2} + \frac{1 - \sqrt{1 + (1 - 2p_k)b_0 J_m + \frac{1}{4}b_0^2 J_m^2}}{b_0} \tag{18}$$

$$b_{12} = b_0 \tag{19}$$

When $L_S > L^*$ (260 m):

$$J_m^* = min\left(J_{max}, \frac{l_{max}}{L^*}\right) \tag{20}$$

$$J_k^* = \frac{J_m^*}{2} + \frac{1 - \sqrt{1 + (1 - 2p_k)b_0 J_m^* + \frac{1}{4}b_0^2 J_m^{*2}}}{b_0} \tag{21}$$

$$J_m = \frac{J_m^* \cdot L^*}{L_S} \tag{22}$$

$$J_k = \frac{J_k^* \cdot L^*}{L_S} \tag{23}$$

$$b_{12} = 2\left(\frac{p_k}{J_k} - \frac{1 - p_k}{J_m - J_k}\right) \tag{24}$$

An interesting observation related to Equation 17 and 18, is the fact that these give constant values equal for all ships with a subdivision length of 198 m or less. Ships with a subdivision length between 198 and 260 m thus have different values for J_m and J_k, where the value of J_k is decreasing towards L_S = 260 m. Further on, when considering $L_S > L^*$, the factors J_m^* and J_k^* are introduced. This is due to the damage statistics of the HARDER project: as shown in Figure 10, the relative amount of registered damages is very low for ships with a subdivision length of

260 m or above. Therefore, the distribution function was cut at $L^* = 260$ m, and consequently it was necessary to introduce new formulas for calculating J_m and J_k; respectively J_m^* and J_k^*. Furthermore, in order to calculate b_{12} it is necessary to convert J_m^* and J_k^* into J_m and J_k, respectively, which is done by using Equation 22 and 23 (Djupvik et al., 2015; IMO, 2006).

As mentioned, the damage under consideration must be categorised as one of the three specific conditions as defined below, and calculated accordingly. Because the derivations of p(x1,x2) for the different damage conditions are quite extensive, they are not included here, but can be found in Lützen's PhD thesis (2001).

1. *"Where neither limits of the compartment or group of compartments under consideration coincides with the aft or forward terminals"* (IMO, 2006), as illustrated in Figure 11:

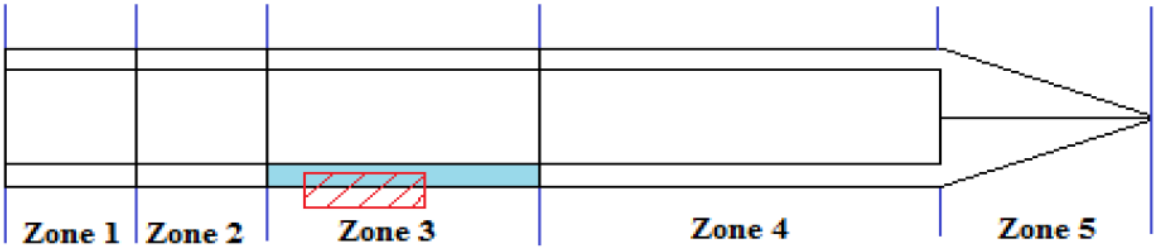

Figure 11. 'Damage category 1' seen from above (Djupvik et al., 2015).

When $J \leq J_k$:

$$p(x1,x2) = p_1 = \frac{1}{6} J^2(b_{11}J + 3b_{12}) \tag{25}$$

When $J > J_k$:

$$\begin{aligned} p(x1,x2) = p_2 \\ &= -\frac{1}{3}b_{11}J_k^3 + \frac{1}{2}(b_{11}J - b_{12})J_k^2 + b_{12}JJ_k - \frac{1}{3}b_{21}(J_n^3 - J_k^3) \\ &+ \frac{1}{2}(b_{21}J - b_{22})(J_n^2 - J_k^2) + b_{22}J(J_n - J_k) \end{aligned} \tag{26}$$

2. *" Where the aft limit of the compartment or group of compartments under consideration coincides with the aft terminal or the forward limit of the compartment or group of compartments under consideration coincides with the forward terminal"* (IMO, 2006). Such an example is illustrated in Figure 12:

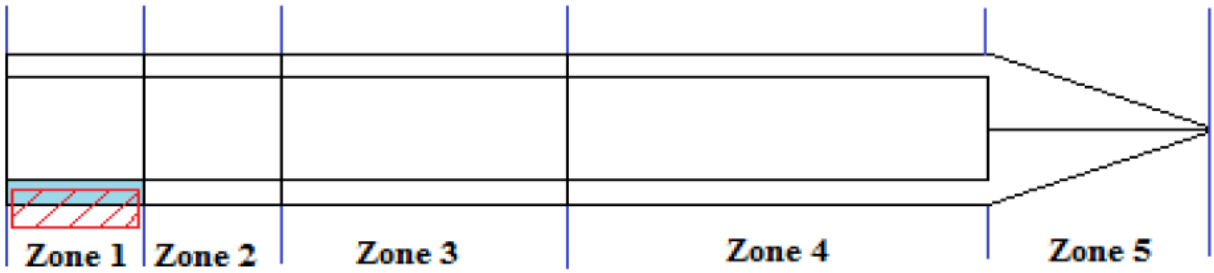

Figure 12. 'Damage category 2' seen from above (Djupvik et al., 2015).

When $J \leq J_k$:

$$p(x1, x2) = \frac{1}{2}(p_1 + J) \tag{27}$$

When $J > J_k$:

$$p(x1, x2) = \frac{1}{2}(p_2 + J) \tag{28}$$

3. *"Where the compartment or groups of compartments considered extends over the entire subdivision length (L_S)* (IMO, 2006), as illustrated in Figure 13.

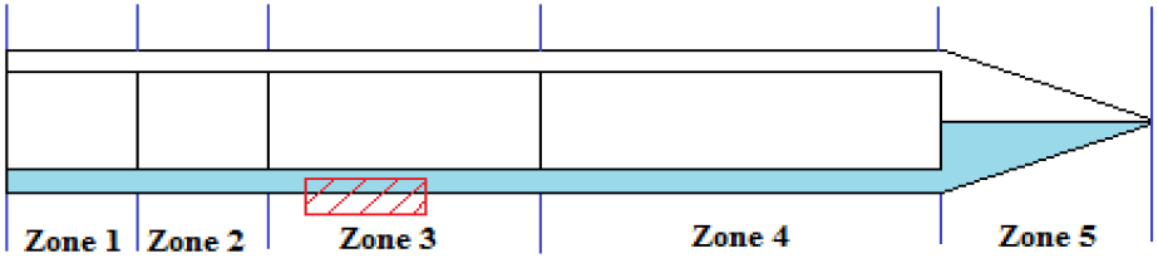

Figure 13. 'Damage category 3' seen from above (Djupvik et al., 2015).

$$p(x1, x2) = 1 \tag{29}$$

Background and Calculation of r($x1_j$,$x2_j$,b)

The r(x1,x2,b)-factor accounts for the probability of penetration, i.e. transverse damage extent, being lesser than a given transverse breadth b. In the same way as for p(x1,x2), the calculation of r(x1,x2,b) is based on damage statistics from the HARDER project. A distribution density plot for non-dimensional penetration was made out of 398 damage penetrations, as shown in Figure 14. From this plot it was revealed that very few cases penetrated beyond B/2. The extreme penetrations were thus neglected for the purpose of the PDS regulations; the illustration to the right shows that the distribution density function is cut short at B/2. In comparison with the DDS regulations, which uses the 'B/5 rule', this is a significant difference. In other words, there is a substantial amount of damage cases where a ship optimised for B/5 penetration might struggle to survive, in case of deeper penetration. In addition to the new 'B/2 rule', the HARDER analysis also discovered a certain dependency between penetration and damage length up to a non-dimensional damage length of 0.033. This is also accounted for in the calculation of r(x1,x2,b) in the PDS regulations (Hjort & Olufsen, 2014; Lützen, 2001).

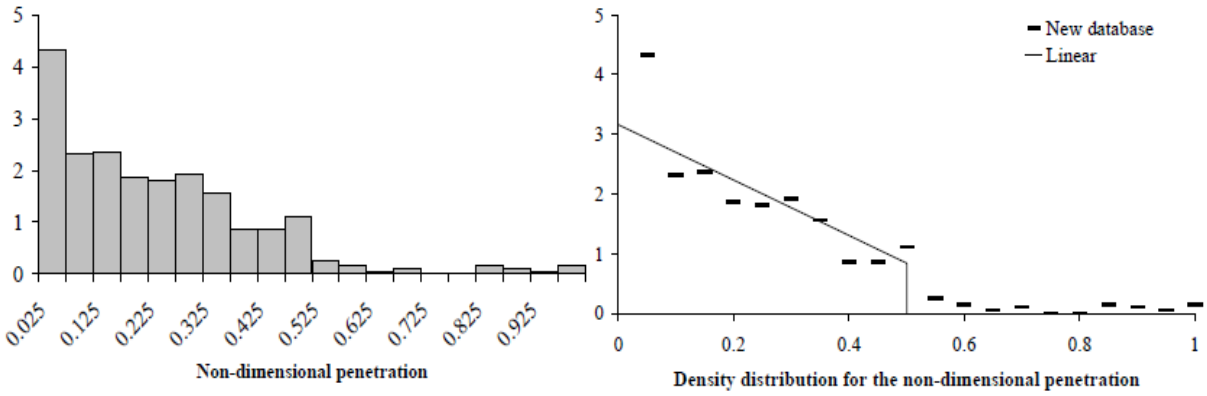

Figure 14. Distribution density (left) and distribution density function (right) for non-dimensional penetration. The figure is adapted from Lützen (2001).

The calculation of r(x1,x2,b), which is represented by the linear line drawn in Figure 14, is carried out by combining Equation 30, 31 and 32. In Equation 32, b is the penetration depth of the damage, as defined in Table 5 in Sub-section 2.4.4, and B is the maximum beam of the ship at the deepest subdivision draught (IMO, 2008c). As for p(x1,x2), the derivation of r(x1,x2,b) is not detailed here, but can be found in the PhD thesis by Lützen (2001).

$$r(x1, x2, b) = 1 - (1 - C) \cdot \left[1 - \frac{G}{p(x1, x2)}\right] \quad (30)$$

$$C = 12 \cdot J_b \cdot (-45 \cdot J_b + 4) \quad (31)$$

$$J_b = \frac{b}{15B} \quad (32)$$

The calculation of the G factor is dependent on the same damage conditions as for p(x1,x2):

1. *"Where neither limits of the compartment or group of compartments under consideration coincides with the aft or forward terminals"* (IMO, 2006). Here, J_0 is given by equation 34.

$$G = G_2 = -\frac{1}{3} b_{11} J_o^3 + \frac{1}{2}(b_{11} J - b_{12}) J_0^2 + b_{12} J J_0 \quad (33)$$

$$J_0 = \min(J, J_b) \quad (34)$$

2. *" Where the aft limit of the compartment or group of compartments under consideration coincides with the aft terminal or the forward limit of the compartment or group of compartments under consideration coincides with the forward terminal"* (IMO, 2006). Here, G_1 is given by 'damage condition 3', i.e. Equation 36.

$$G = \frac{1}{2}(G_2 + G_1 J) \quad (35)$$

3. *"Where the compartment or groups of compartments considered extends over the entire subdivision length (L_S)* (IMO, 2006):

$$G = G_1 = \frac{1}{2} b_{11} J_b^2 + b_{12} J_b \quad (36)$$

2.4.7 The Factor s_i

Calculation of the s_i Factor

The factor s_i is known as the survivability factor, because s_i accounts for the probability of survival when the ship is exposed to flooding of a compartment or group of compartments after a collision. This factor is quite complex to calculate, due to the large number of considerations in the regulation. There are a lot of factors involved in the calculation process; some of them are already defined in the master's thesis. However, for the convenience of this sub-section, all necessary factors are summarized in Table 8.

Table 8. Notations and parameters used in the calculation of s_i (IMO, 2006).

Parameters and notations related to the s_i-factor	
θ_e	Equilibrium heel angle in any stage of flooding
θ_v	The angle at any stage of flooding where the righting lever, GZ, becomes negative
θ_{min}	Minimum heel angle = 7 degrees for passenger ships; 25 degrees for cargo ships
θ_{max}	Maximum heel angle = 15 degrees for passenger ships; 30 degrees for cargo ships
Range	The range of positive GZ values = θ_v - θ_e
GZ_{max}	The maximum positive GZ value [metres] up to θ_v
$S_{intermediate, i}$	The probability of surviving all intermediate flooding stages until the equilibrium stage
$S_{final, i}$	The probability of surviving in the final equilibrium stage of flooding
$S_{mom, i}$	The probability of surviving heeling moments
M_{heel}	Maximum assumed heeling moment
Displacement	Intact displacement at the subdivision draught
N_p	The maximum number of passengers permitted to be on board in the service condition, corresponding to the deepest subdivision draught
B	Beam of the ship at the deepest subdivision draught
A	Projected lateral area above the waterline
Z	Distance from the centre of A to T/2, where T is the draught of the ship
P	Wind pressure: P = 120 N/m^2

The calculation of s_i is carried out using Equation 37. The index i represents the particular damage case for the considered loading condition (IMO, 2006).

$$s_i = min\left[s_{intermediate,i}, (s_{final,i} \cdot s_{mom,i})\right] \tag{37}$$

In the calculation of $s_{final,i}$, which is carried out using Equation 38, it is important to be aware that the maximum values for GZ_{max} and range are 0.12 m and 16 degrees respectively. This is because $s_{final,i}$ is a probability number, thus its value must be equal to or lesser than 1. This becomes clear when looking at the formula for K, which is represented by Equation 39. K is included as a factor to ensure that the heel angles for the different ship types are acceptable (Djupvik et al., 2015).

$$s_{final,i} = K \cdot \left[\frac{GZ_{max}}{0.12} \cdot \frac{Range}{16}\right]^{\frac{1}{4}} \tag{38}$$

$$K = \begin{cases} \sqrt{\dfrac{\theta_{max} - \theta_e}{\theta_{max} - \theta_{min}}}, & if\ \theta_{min} < \theta_e < \theta_{max} \\ 1, & if\ \theta_e \leq \theta_{min} \\ 0, & if\ \theta_e \geq \theta_{max} \end{cases} \tag{39}$$

Additionally, Equation 39 states that $s_{final,i}$ is equal to zero in two different scenarios: when a passenger ship heels more than 15 degrees (θ_{max}) or when a cargo ship heels more than 30 degrees (θ_{max}). In these two cases the survivability factor will not contribute to the A-index. This is obviously important for Naval Architects to pay attention to when designing the watertight arrangements (IMO, 2006).

Equation 40, which is used to calculate $s_{intermediate,i}$, is very similar to the formula for $s_{final,i}$. There are three important differences, however: the factor k is removed from the equation, $s_{intermediate,i}$ is taken as unity for cargo ships ($s_{intermediate,i}$ = 1) and the limits for GZ_{max} and range are now equal to or lesser than 0.05 m and 7 degrees respectively. In addition, if the intermediate heel angle exceeds 15 degrees, the value of $s_{intermediate,i}$ is equal to zero. It should also be noted that $s_{intermediate,i}$ must be taken as the least of the s_i-factors obtained from all flooding stages, including the final stage before equalization (IMO, 2006).

$$s_{intermediate,i} = \begin{cases} \left[\frac{GZ_{max}}{0.05} \cdot \frac{Range}{7}\right]^{\frac{1}{4}}, & if\ intermediate\ heel\ angle \leq 15° \\ 0, & if\ indermediate\ heel\ angle > 15° \end{cases} \quad (40)$$

At last, equation 41 is used to calculate the $s_{mom,i}$-factor. This factor accounts for the probability of surviving heeling moments created by wind, movement of passengers or the lowering of survival crafts, denoted $M_{passenger}$, M_{wind} and $M_{survivalcraft}$ respectively. Similar to $s_{intermediate,i}$, $s_{mom,i}$ is taken as unity for cargo ships.

$$s_{mom,i} = \frac{(GZ_{max} - 0.04) \cdot Displacement}{M_{heel} = max(M_{passenger}, M_{wind}, M_{survivalcraft})} \leq 1 \quad (41)$$

The heeling moments $M_{passenger}$ and M_{wind} are calculated by Equation 42 and 43, respectively. Explanations to the factors involved in these equations can be found in Table 8, except for the constant value 9.806, which is the gravitational acceleration constant with the unit m/s^2. As mentioned, $M_{passenger}$ is caused by the movement of passengers. In case of an emergency situation, the passengers will most likely crowd to one side of the ship where the mustering stations and lifeboats are located. As Equation 42 reveals, the PDS regulations consider the average weight of the passengers to be 75 kg or 0.075 tonnes, in similarity to the DDS regulations. Furthermore, as an alternative to Equation 42, the deterministic approach used to determine the 'heeling moment' as described in Sub-section 2.3.3 can be used (IMO, 2006).

$$M_{passenger} = (0.075 \cdot N_p) \cdot (0.45 \cdot B) \quad [tonnes \cdot m] \quad (42)$$

$$M_{wind} = \frac{(P \cdot A \cdot Z)}{9{,}806} \quad [tonnes \cdot m] \quad (43)$$

$M_{survivalcraft}$ is defined in SOLAS as *'the maximum assumed heeling moment due to the launching of all fully loaded davit-launched survival craft on one side of the ship'* (IMO, 2006). This heeling moment is not calculated by any one particular equation, but can be calculated following five specific assumptions given in SOLAS Ch. II-1, Part B-1, Reg. 7-2 (IMO, 2006).

Another important consideration, is how to determine the GZ_{max} value. This was briefly introduced in Sub-section 2.1.1, but there might occur situations where this regular approach no longer is appropriate. Such an example is the event of one or more submerged openings. This is illustrated in the graph to the right of Figure 15, where GZ_{max} is not located at the peak of the curve. In this case, the GZ_{max} value appears at θ_v and the GZ curve is cut at this point, because the righting lever per definition becomes negative when an opening of the ship is submerged. A common design strategy to avoid this problem is to place all openings at a certain distance above the bulkhead deck (Djupvik et al., 2015; IMO, 2008c).

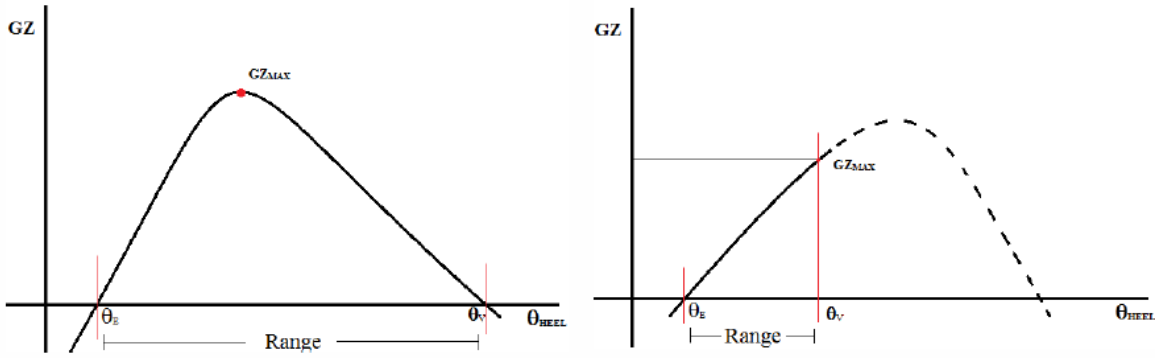

Figure 15. Illustration of a typical GZ curve (left) and a GZ curve for submerged opening (right). The illustration is obtained from Djupvik et al. (2015).

Background of the s_i Factor

A number of the criteria in the PDS regulations concerning the s_i factor appear as deterministic. Although, there are some elements that may be seen as probabilistic. For instance, the probability of successful evacuation will increase with a low static heel angle, if it is ensured that the evacuation routes not will be impeded by water. This is in fact nothing new, as the so-called 'margin line concept' of the DDS regulations implicitly cover issues related to watertight integrity, ship safety and the evacuation of passengers. However, an important difference between the PDS regulations and the DDS regulations regarding passenger ships, is thus the removal of the margin line requirements. The function of the margin line was to prohibit immersion of water on the bulkhead deck, and this was considered as being in conflict with the functionality of the probabilistic concept. However, it was realised that this change had to be compensated by some explicit requirements considering watertight integrity and evacuation of passengers. Examples here are design limitations related to watertight doors and launching devices for life-saving appliances (LSA), respectively. Another important compromise, was the introduction of 'penalties' on the A-index. These 'penalties' were given in the event of water

immersion of certain features, such as water on the bulkhead deck during evacuation, immersion of vertical emergency escape hatches, and progressive flooding through unprotected openings or damaged piping and ducts in the damage zone (Hjort & Olufsen, 2014).

Furthermore, the DDS and PDS regulations are quite similar in the sense that the GZ curve is used to estimate the ship's survivability. The difference becomes evident when looking at the criteria used. In the DDS regulations, the 'area criterion' is used; the area under the GZ curve must be greater than a certain value. The HARDER project revealed through model tests with systematic variation in sea-states that this criterion was of secondary importance to the survivability, as long as the range and GZ_{max} values were sufficiently high. Therefore, the 'area criterion' was dropped. It was also discovered that the 'angle of equilibrium criterion' was secondary to some extent, but an increasing risk of shifting cargo and loose objects on deck justified some limitations connected to heel angles. For passenger ships, the calculation of $s_{mom,i}$ was adopted from the wind, passenger and LSA heeling moment assumptions in the DDS regulations. In the case of cargo ships, $s_{mom,i}$ and $s_{intermediate,i}$ are always set to 1, as it was decided to maintain the practice from the DDS regulations; there should be no requirements related to the stability in the intermediate stages of flooding (Hjort & Olufsen, 2014).

2.4.8 The Factor v_i

Calculation of the v_i Factor

In the case of any horizontal watertight subdivisions above the waterline, the s_i value for the lower compartments or group of compartments must be multiplied by the 'reduction factor' v_i. This factor accounts for the probability that the spaces above the horizontal boundary under consideration remain intact after a ship collision. If these spaces are flooded due to a ship collision, the residual stability of the ship will be reduced. In consequence, the ship's buoyancy changes and the GZ curve is affected. The v_i factor is determined by Equation 44. The factors and notations involved in the equation are described in Table 9. In addition, an illustration exemplifying how the H measurements should be interpreted for a particular damage condition is provided in Figure 16 (IMO, 2006).

$$v_i = v\left(H_{j,n,m}, d\right) - v\left(H_{j,n,m-1}, d\right), \quad v_i \epsilon [0,1] \tag{44}$$

Table 9. Factors and notations involved in the calculation of the v_i factor (IMO, 2006).

Parameters and notations related to the v_i-factor	
$H_{j,n,m}$	'*…the least height above the baseline, in metres, within the longitudinal range of x1(j)...x2(j+n-1) of the mth horizontal boundary which is assumed to limit the vertical extent of flooding for the damaged compartments under consideration;'*
$H_{j,n,m-1}$	*'… the least height above the baseline, in metres, within the longitudinal range of x1(j)...x2(j+n-1) of the (m-1)th horizontal boundary which is assumed to limit the vertical extent of flooding for the damaged compartments under consideration;'*
j	*'signifies the aft terminal of the damaged compartments under consideration;'*
n	*'the number of adjacent damage zones involved in the damage;'*
m	' *represents each horizontal boundary counted upwards from the waterline under consideration;'*
d	*'is the draught in question as defined in regulation 2…'*

Figure 16. A ship with a particular damage condition and corresponding H measures. The illustration is obtained from Djupvik et al. (2015).

As mentioned in Sub-section 2.4.2 and illustrated in Figure 17, the maximal vertical damage extent is defined as d + 12.5 m. The location of watertight decks in the reserve buoyancy area and application of the v_i-factor, are also illustrated in Figure 17. Explanations to the below illustrations are provided in Table 10.

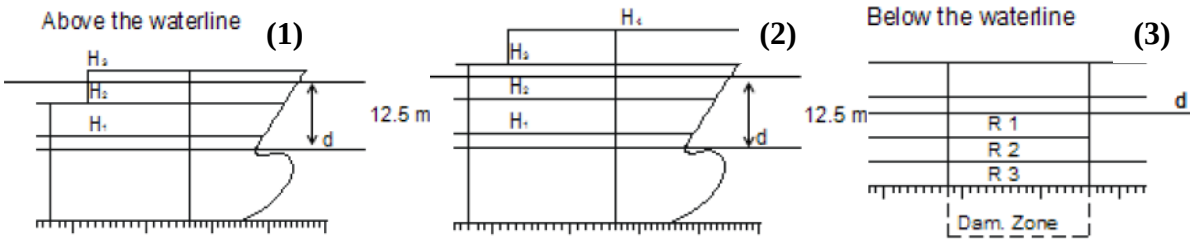

Figure 17. The use of the v_i factor for different horizontal watertight arrangements. The illustrations are adapted from IMO (2008c).

Table 10. Explanations to Figure 17 (IMO, 2008c).

Example 1	Example 2	Example 3
In example 1, three horizontal subdivisions above the water-line must be accounted for. The max. vertical damage extent, d + 12.5 m, is located between H_2 and H_3. Thus, H_1, H_2 and H_3 corresponds to v_1, $v_1 < v_2 < 1$ and $v_3 = 1$ respectively.	For this ship, the v_1 and v_2 factors are the same as for example 1. Above H_3, the reserve buoyancy should be considered undamaged in all damage cases.	Damages into the rooms R_1, R_2 and R_3, which are all below the waterline, should be combined so that the damage resulting in the lowest s_i-factor is accounted for.

The calculation of v(H,d) is carried out by using Equation 45 (IMO, 2006).

$$v(H,d) = \begin{cases} 0.8\dfrac{(H-d)}{7.8}, & if\ (H-d) \le 7.8 \\ 0.8 + 0.2\dfrac{(H-d)-7.8}{4.7}, & if\ (H-d) > 7.8 \\ 1, & if H_m\ coincides\ with\ the\ uppermost\ boundary^3 \\ 0, & if\ m = 0,\ i.e.\ v(H_{j,n,0}, d) \end{cases} \quad (45)$$

In general, if each contribution to the A-index in the event of horizontal subdivision is denoted d_A, then each contribution d_A is obtained from Equation 46. According to Equation 37, it is always the least s_i-factor obtained for all damage combinations that is to be included in the A-index. When the effect of horizontal subdivision is included, the least s_i-factor, here denoted s_{min}, is obtained under the assumption that the vertical damage extent is measured downwards from the assumed damage height H_m (IMO, 2006).

$$d_A = p_i \cdot [v_1 s_{\min 1} + (v_2 - v_1)s_{\min 2} + \ldots + (1 - v_{m-1})s_{\min m}] \quad (46)$$

Background of the v_i Factor

The principle of considering the effect of horizontal subdivision above the waterline was already implemented in the existing cargo ship regulations, before the development of the PDS

[3] 'Uppermost boundary' definition: *'…the uppermost watertight boundary of the ship within the range ($x1_j$…$x2_{j+n-1}$)'* i.e. within the range of the longitudinal damage extent (IMO, 2006).

regulations. The cargo ship rules were developed based on almost no statistics, but as time went by, a certain tendency in ship collisions eventually became evident: many ships were rammed by ships of equal size. In order to improve the old rules, it was decided to develop a formula based on the length-dependent bow height requirements in ICCL-66. This formula included an upper limit of 7 m above the waterline (Hjort & Olufsen, 2014).

Furthermore, new statistics from the HARDER project revealed that there was a significant number of ship collisions resulting in more severe vertical damage extents than assumed by the cargo ship regulations. An explanation is that the bow height requirement in ICCL-66 was a minimum requirement. The upper limit was not defined, so many ships were built with higher bows. In consequence, the new PDS regulations were developed based on all available statistics, in addition to the old regulations and 'as-built' dimensions collected from the existing world fleet. This is illustrated in Figure 18, where the red dotted line represents the formula corresponding to the v_i-factor used in the PDS regulations. With the new regulations, the maximum vertical damage extent was increased from d + 7 m to d + 12.5 m, thus providing an increased safety level (Hjort & Olufsen, 2014).

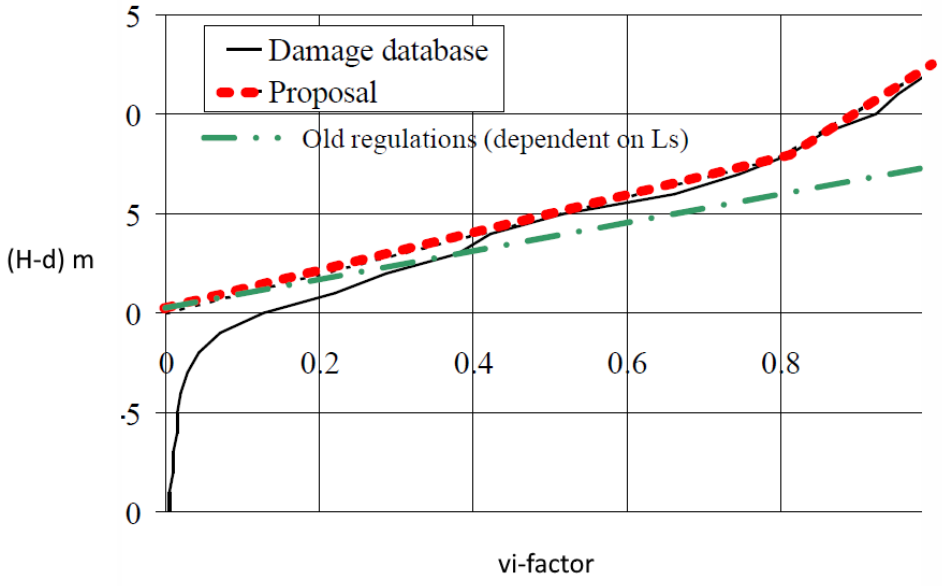

Figure 18. Vertical damage extent distribution for the old and new regulations. The figure is adapted from Hjort and Olufsen (2014).

3. Individual Study on Probabilistic Damage Stability

Based on the PDS theory presented in Chapter 0, an individual study on a given ship has been carried out in the master's thesis. The given ship is designed by Salt Ship Design with the purpose of serving wind farms. Thus, the ship will be referred to as a Wind Farm Service Vessel (WFSV). More details related to the WFSV is provided throughout Chapter 0. The methods used to investigate the objectives described in Chapter 0 of the master's thesis, are explained in the following sections.

3.1 Approach

The stepwise approach for investigating the two objectives presented in Chapter 0 is:

1. Objective 1 concerns the height of 'U-deck', i.e. the height of the horizontal surface that constitutes the bottom of the wing ballast tanks. At the same time as U-deck determines the volume of the wing ballast tanks, it also determines the volume of the so-called U-tanks that are placed below the wing ballast tanks. U-deck does in other words function as a barrier for vertical flooding between the two tanks, as illustrated in Figure 19.

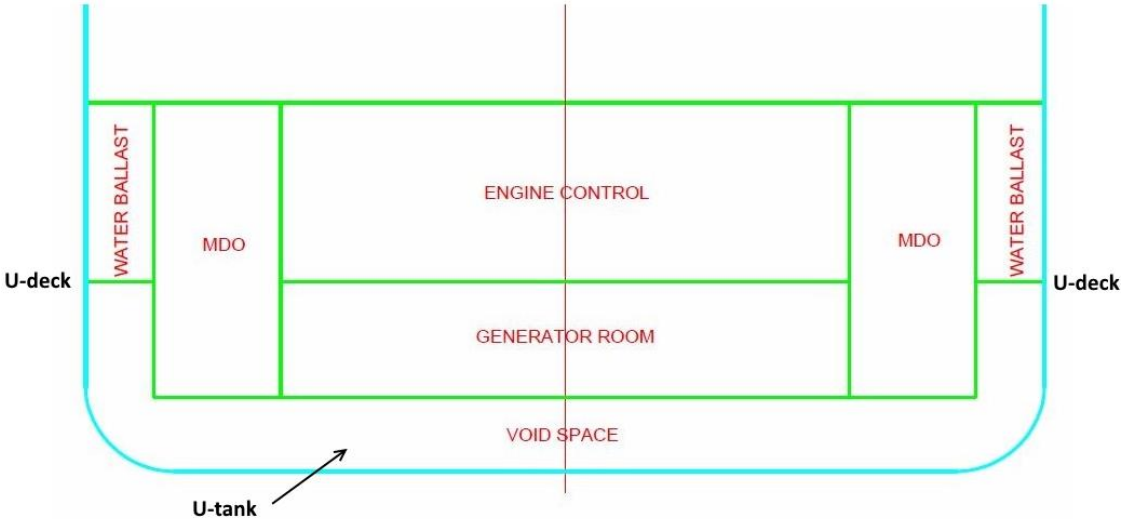

Figure 19. Illustration of wing ballast tank, U-deck and U-tank, inspired by Figure 1.

The important point with objective 1 is to attain as large A-index as reasonably practicable; it is of interest to attain a large A-index and at the same time fit a sufficient amount of water in the wing ballast tanks. This problem is investigated by changing the height of the U-deck and run multiple PDS calculations. This is explained and illustrated in more detail in Sub-section 3.5.7.

When the watertight subdivision configuration that provides the most reasonable A-index value for objective 1 is identified, the corresponding U-deck height will be used in the investigation related to objective 2.

2. Objective 2 is related to changes in the intact stability of the ship in question; the GM values for the three subdivision draughts d_S, d_P and d_L are changed with a specific interval within a certain range. Changing the GM value will surely affect the A-index, and the ultimate goal here is to understand why the A-index responds the way it does to the change in GM value. The approach used is better explained and illustrated in Sub-section 3.5.8.

3.2 Ship Particulars

The ship or WFSV used in this study is defined as an SPS, since it can host more than 12 special personnel. Thus, the WFSV is treated as a passenger ship according to the PDS regulations, except when calculating the R-index. Some information about the ship is given in Table 11, and a profile view of the ship is displayed in Figure 20. Due to confidentiality matters, only parts of the General Arrangement (GA) drawings are attached to the thesis. A link to electronic files can be found in Appendix B. These drawings are simplified in order to create a generic ship model for this study, and basically only shows the tank arrangement for a few selected decks.

Table 11. Key specifications of the ship modelled in NAPA.

Key specifications of the WFSV	
Ship type	Special Purpose Ship (SPS)
LOA / LPP	74.90 / 61.80 m
Subdivision Length L_S	72.92 m
Breadth moulded	18.20 m
Depth moulded	7.00 m
Max. number of persons on board	60
Design draught	4.5 m

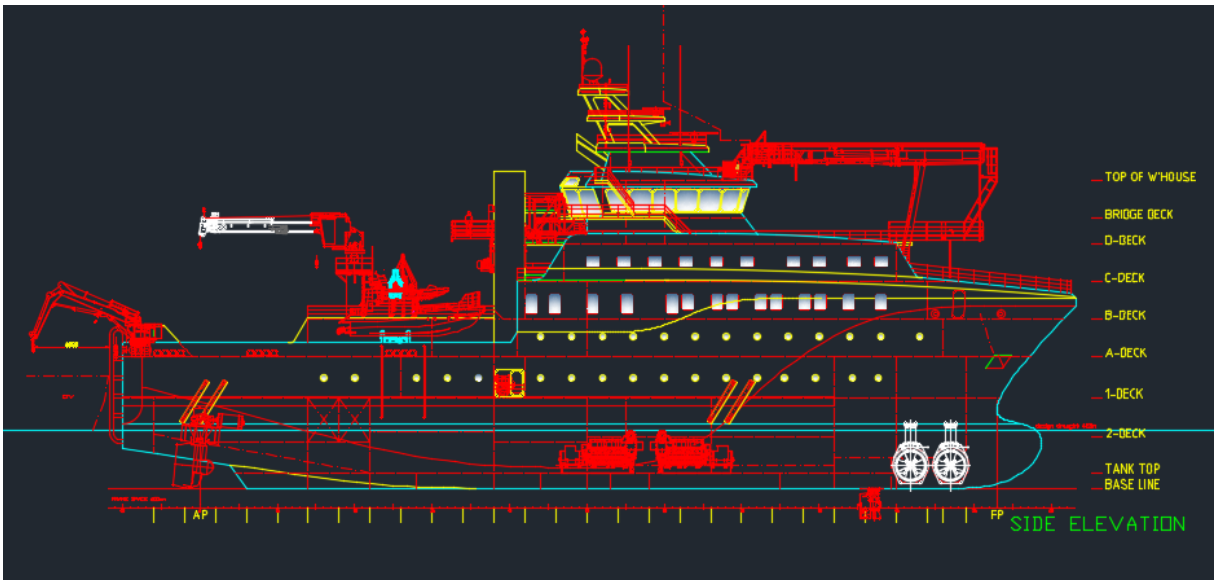

Figure 20. Profile view of the Wind Farm Service Vessel used in the study.

3.3 Software

The work that has been done to achieve the results presented in Chapter 4, has been carried out using the market-leading stability software NAPA. Salt Ship Design provided a license with access outside of normal working hours throughout the duration of the master's thesis. A laptop with pre-installed VPN and remote desktop connection was also provided, in order to be connected to the Salt Ship Design network and their databases.

In addition to the NAPA stability software, AutoCAD has been used to investigate and modify GA drawings. AutoCAD is free to use for students for non-commercial purposes. To avoid that the co-operation with Salt Ship Design could be seen as a problem, in terms of commercial use of the student license, a professional license provided by Salt Ship Design was used instead.

3.4 Modelling in NAPA

The recommendation from Salt Ship Design was to model the GA of the ship in NAPA from scratch, instead of copying the existing project from the database. This approach is time-demanding for beginners, but it was considered to be beneficial in the long run; it is easier to notice errors and analyse the results with a good understanding of the software. NAPA for Design Manuals and frequent communication with supervisors from Salt Ship Design was helpful in the process.

3.4.1 Arrangement

In the NAPA stability software, the traditional way to model the ship's arrangement is by using the 'Text Editor' tool. The Text Editor was therefore used to model the arrangement of the ship in this thesis as well, which required the author to learn the coding syntax in NAPA. For a better insight to the modelling process in this study, it is recommended to read Appendix C. The final arrangement of the WFSV's three lower decks modelled in NAPA is presented in Figure 21, and the complete arrangement can be found in Appendix C. The colour codes used in the below illustration, are explained in Table 12.

Table 12. Colour codes used in the graphical representation of the compartments arrangement in NAPA.

Colour code of compartment	Purpose description
Light grey	Void space
Dark grey	Sewage tanks
Green	Water ballast and roll-reduction tanks
Gold	Machinery spaces
Red	Fuel oil tanks
Light blue	Fresh water tanks
Pink	Storage

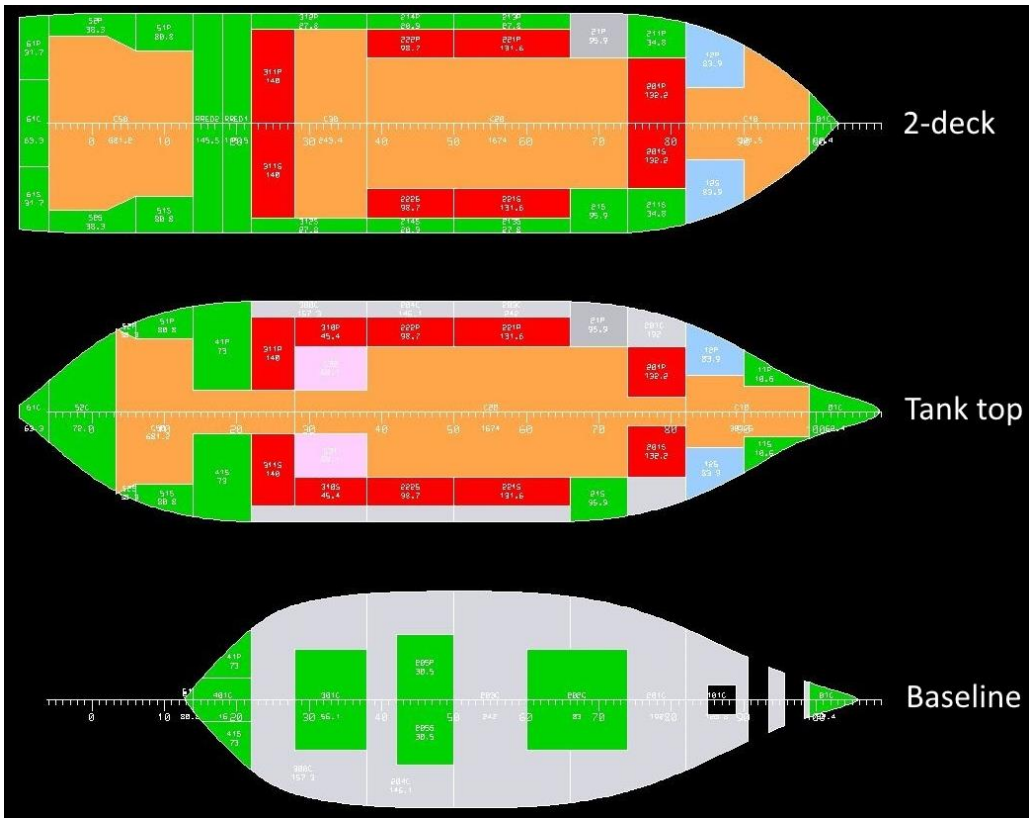

Figure 21. The three lower decks of the ship modelled in NAPA.

3.4.2 Time-Saving Measures

In 'real-life projects' the modelling of the ship in NAPA is very detailed, which means that no significant simplifications are made to ensure that the resulting A-index value is the actual one for the ship in question. This 'real-life approach' requires a large amount of computational power. Without any 'super-computer' at hand to do the work in the master's thesis, it would be too time-demanding to follow this approach. Thus, to save some valuable time in the process of carrying out the individual study, a number of measures in NAPA were taken. The ones related to the modelling of the WFSV's arrangement in NAPA are explained in this sub-section.

First of all, the hull lines of the ship in NAPA was not created by the author, but copied from an existing project to save time. An illustration of the hull lines can be found in Appendix D. A decision was made only to focus on the GA, including tanks, from the baseline upwards to deck B. To design the hull lines from scratch would not contribute to a better understanding of PDS in practice. The internal subdivision of compartments is far more important in that sense.

The complexity of the GA drawings, which are used as the basis when modelling the ship in NAPA, has been heavily reduced. An example of this is given in Appendix E, where two screenshots from AutoCAD are attached: one original and one simplified drawing of the accommodation area; all the rooms in this area are combined into only a few compartments. It is assumed that this simplification does not impact the results in a significant manner, since the original rooms are not watertight and the entire deck will anyways be flooded if a damage occurs in this area. A potential problem with this simplification, however, is the effect it may have on the s_i-factor related to the intermediate stages of flooding. As mentioned in Sub-section 2.4.7, the least $s_{intermediate}$-factor of all intermediate stages of flooding should be taken and used to calculate the A-index, if the value of $s_{intermediate}$ is smaller than the product of s_{final} and s_{mom}. The removal of several rooms might change the $s_{intermediate}$ values, but the potential difference is assumed not to be of significance.

Simplifications are also made at the lower decks; the total number of tanks, such as fuel settling tanks, bilge tanks and sewage tanks, is reduced. However, the total tank volume remains the same. This is done by combining several small tanks into larger tanks. The free surface effect (FSE) was taken into account when combining the tanks. If all tanks had been combined into one large compartment, for instance, the FSE would probably make the ship unstable.

Furthermore, curvatures in the ship model increase the computation time. With curvatures, i.e. circular surfaces and bulkheads that are not orthogonal or parallel to the centrelines, the

p_i-factor becomes more difficult to calculate because it depends on the b_k-factor. The b_k-factor must in that case be calculated according to SOLAS MSC.281(85) – 'Explanatory notes to the SOLAS Chapter II-1 subdivision and damage stability regulations'. To save computation time, most of the curvatures are therefore removed in the ship model, as illustrated in Appendix F.

3.5 Calculation Procedure in NAPA

Running PDS calculations in NAPA is a time-demanding process, even though time-saving measures are taken. The calculation process itself is relatively straightforward, by using the 'Probabilistic Manager' tool in NAPA and reading the NAPA for Design Manuals.

3.5.1 Probabilistic Manager

The Probabilistic Manager is used to calculate the PDS. As illustrated in Figure 22, the Probabilistic Manager window contains numerous macros that handles information from the input text files. Some information must also be inserted manually. This is key information such as initial loading conditions, vessel type, design draught, number of passengers, subdivision data, protected and unprotected openings, compartment connections, the regulatory framework to be applied, and not at least which text files that are used in the calculations.

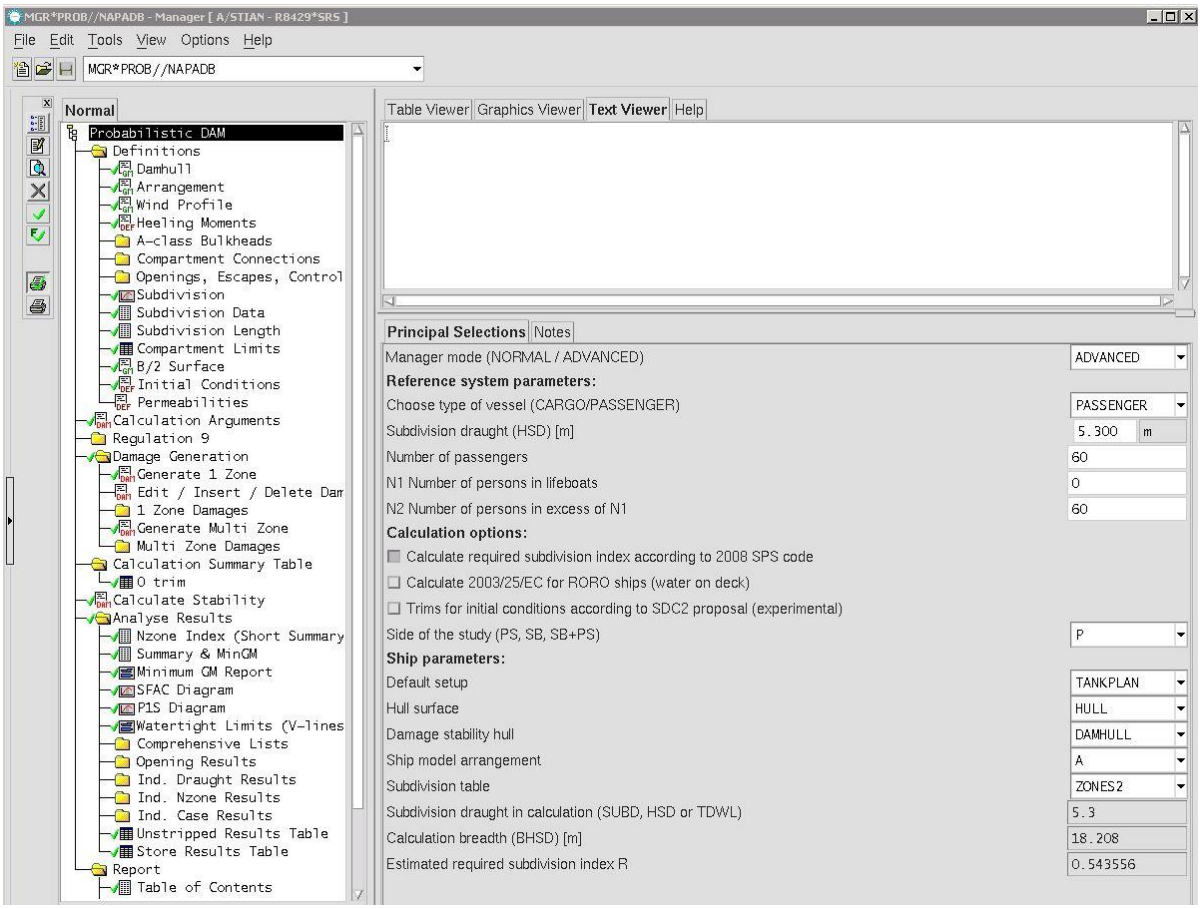

Figure 22. Probabilistic Manager in NAPA.

When updating the 'Calculate Stability' macro, as shown in Figure 22, the PDS calculations will initiate. Before this is done, the macros under the 'Definitions', 'Damage Generation' and 'Calculation Summary Table' folders must be updated in order to get correct results. The most important macros are described in the following sub-sections. Furthermore, some methods that can be used to analyse results of the PDS calculations are presented in Section 3.6. The necessary information for analysing the results is found in the 'Analyse Results' folder, and the information can be exported to a PDF file by printing the 'Report' folder.

3.5.2 Initial Conditions

The user must define three initial loading conditions in the Probabilistic Manager. The loading conditions are defined by their trim, mean draught and GM (or KG) values, as well as the three subdivision draughts that are used in the calculations – d_S, d_P and d_L. As a first attempt to obtain the required index R, the GM values are taken from the intact stability GM limit curve. This curve is illustrated in Sub-section 3.5.8. If the A-index does not meet the criteria, i.e. if A < R, a simple measure is usually to increase the GM values for the three subdivision draughts. The GM values have a large effect on the PDS, so it is important to get this right in the Probabilistic Manager. Table 13 presents the initial conditions used to solve objective 1 of the master's thesis. In objective 2, the approach is to experiment with different GM values, thus the below table is not relevant for that case.

Table 13. Intact stability and loading conditions for the WFSV in NAPA.

Initial conditions for the WFSV in NAPA			
	Deepest s. draught - d_S	Partial s. draught - d_P	Light s. draught - d_L
GM	1.3	1.1	1.0
KG	6.8	7.0	7.6
Draught, T	5.3	4.9	4.4

Additionally, the permeability of the different compartments used in this study are pre-set by NAPA. The permeability makes sure that the tanks are not completely filled with water in case of damage, because some of the space always will be occupied by something, e.g. machinery components and piping. As can be seen in Appendix G, the values are default and seem reasonable. It should also be mentioned that NAPA calculates PDS with empty tanks, e.g. there is no water in the ballast tanks, and the maximum level of water in the tanks are thus determined by the permeability (Djupvik, 2016).

3.5.3 Wind Profile and Heeling Moments

For NAPA to calculate the s_i-factor properly, a wind profile has been created in order to include wind moments in the calculations. The superstructure of the ship defines the wind profile and is automatically created in NAPA, as shown in Figure 23. The wind profile includes information about the projected lateral wind area and its area centre. With this information and default values for the wind force, the wind moment is calculated. Heeling moments due to the launching of survival crafts and due to the crowding of passengers at the mustering stations in an emergency situation, is also accounted for.

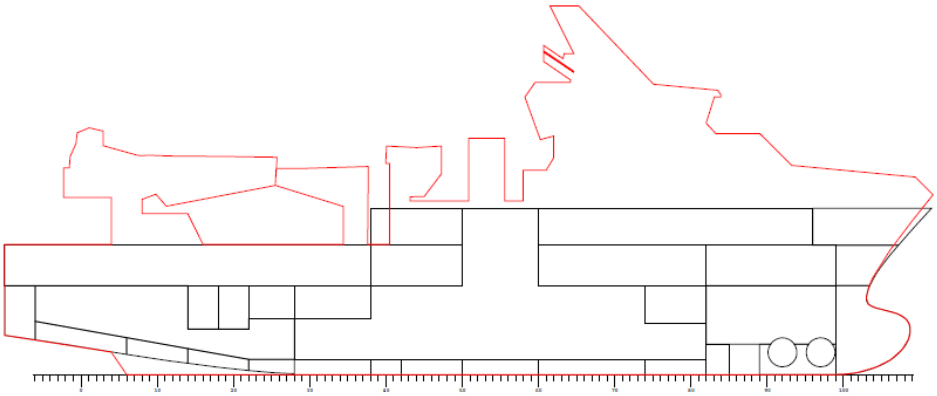

Figure 23. Wind profile of the ship created in NAPA.

3.5.4 Subdivision Data

The subdivision data is a central part of the probabilistic damage generation in NAPA; it is crucial to do the subdivision of damage zones correctly, so the calculations are performed according to the PDS regulations. As explained in Chapter 0, and illustrated in Figure 24, the subdivision represents a grid of transversal, longitudinal and vertical boundaries. These boundaries represent internal surfaces of the ship, i.e. transverse bulkheads, longitudinal bulkheads and decks, respectively. Together the boundaries define the internal structure as far as needed to get sufficiently different damage cases. The complete subdivision illustration from the NAPA results report is attached to the thesis in Appendix H. The subdivision is done in a table editor tool in NAPA and is mainly user input, as explained and illustrated in Appendix I.

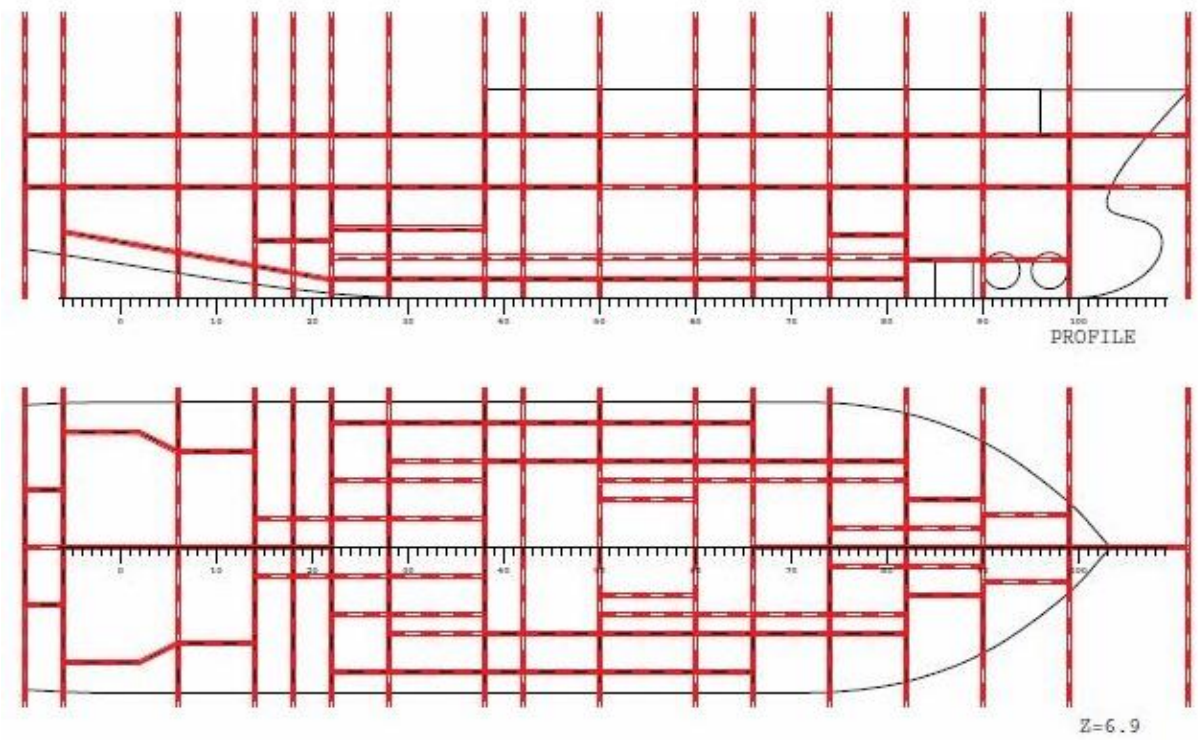

Figure 24. Subdivision illustration from the NAPA results report, for the side profile view and deck 2 of the ship.

It might be confusing when comparing the subdivision illustration above to the GA drawings made in AutoCAD. The red lines above are watertight boundaries in the subdivision table representing bulkheads and decks. However, there are more red lines than bulkheads in the plan view drawing of the deck illustrated in the above figure. Even though a bulkhead only is present at one deck, for example, the corresponding watertight boundary appears on the plan view drawing of all decks. The red lines that do not have black stripes show where subdivision occurs at other decks on the vessel.

3.5.5 Openings and Compartment Connections

To include openings and connections between compartments, i.e. non-watertight doors in practice, is critical in terms of achieving correct calculation results. Openings can be internal or external. External openings may lead to water ingress of the ship, while internal openings may lead the potential water ingress to flood several compartments. An example of a type of opening is air ventilation. If an air ventilation opening becomes submerged in a damage situation, the s_i-factor calculation will account for it; as illustrated in Figure 15 in Sub-section 2.4.7, the GZ_{max} and Range values are taken at the heel angle where the opening becomes submerged. In this study, all openings and compartment connections that are considered to be of importance to the results are included.

3.5.6 Time-Saving Measures

Reducing the number of damage zones, i.e. reducing the number of watertight boundaries in all directions, is an efficient time-saving measure. This is somehow already taken care of when modelling the ship, but it is vital to consider when doing the subdivision in the Probabilistic Manager as well. When modelling the ship, a time-saving strategy is to place similar bulkheads on adjacent decks according to each other, i.e. at the same location in either longitudinal or transverse direction. This is illustrated in Figure 25; the transverse bulkheads hidden underneath the yellow dotted lines have the exact same longitudinal placement for both deck 2 and the tank top deck. In the Probabilistic Manager, as mentioned in Sub-section 3.5.4, the subdivision procedure is to follow these bulkheads when defining the watertight boundaries.

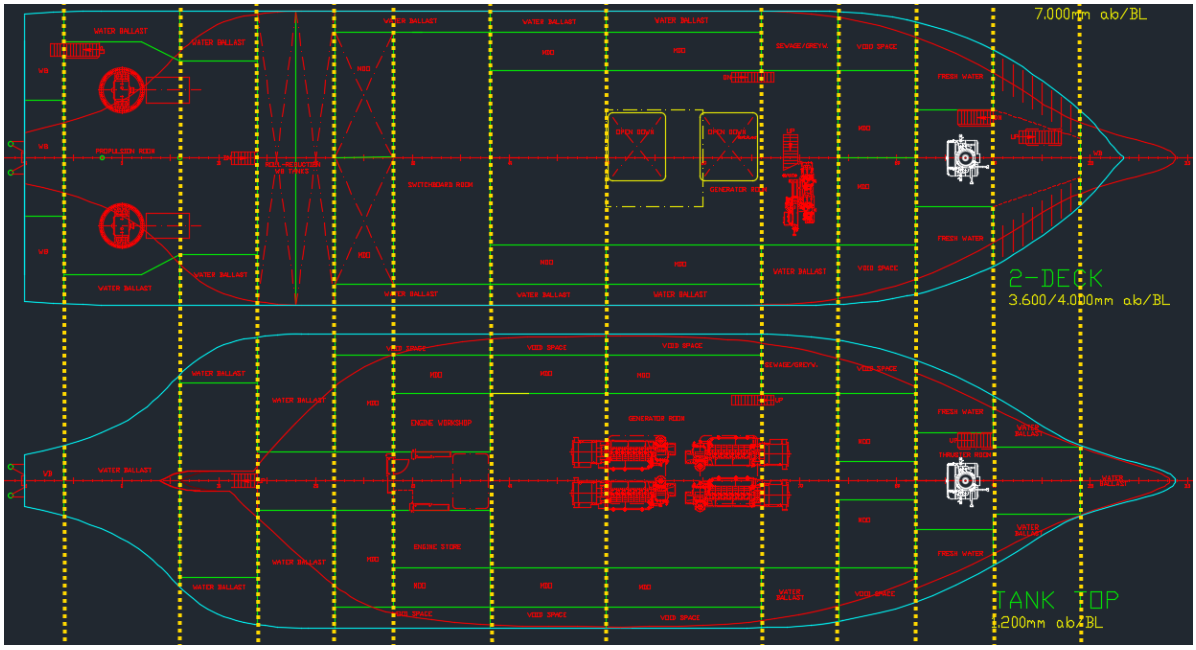

Figure 25. Illustration of how transverse bulkheads are placed at the same longitudinal location on adjacent decks.

Two other time-saving measures that have been used in this study is to exclude 5-zone damages from the calculations and to only calculate for the port side of the ship. Only single-zone, two-, three- and 4-zone damages are accounted for. It is also fine to calculate only for one ship side since the ship's arrangement is symmetrical about the longitudinal centreline.

Another measure that has been taken to save some time is related to all the macros that can be used in the Probabilistic Manager. It is not necessary to run all of them in order to obtain the desired results. The macros gathered in the sub-folders of the 'Analyse Results' folder, as illustrated in Figure 22 in Sub-section 3.5.1, can be neglected for instance.

Perhaps the second most important time-saving measure in this master's thesis study is the number of intervals used in the calculations, for instance in terms of the location of the U-deck. At first, relatively large intervals are used to locate the more critical or relevant areas on the A-index curve. Shorter intervals are eventually used to find accurate values.

The worst potential time-thief in this study is related to objective 1. It considers the horizontal watertight boundary input in the subdivision table in the Probabilistic Manager, which has to be done over again for each calculation if no measures are taken in advance. The approach to avoid that issue is described in the end of the following sub-section.

3.5.7 Objective 1

U-deck represents a horizontal surface that separates the wing ballast tanks from the so-called U-tanks. The U-tanks are located below the wing ballast tanks, as illustrated in Figure 26. Additionally, Figure 26 illustrates the vertical range of potential U-deck positions with the red coloured shaded region. In longitudinal direction, U-deck ranges from zone 6 to zone 13, i.e. from 13.2 m to 49.2 m measured from the stern reference point located at –6.0 m. This is illustrated in Figure 27.

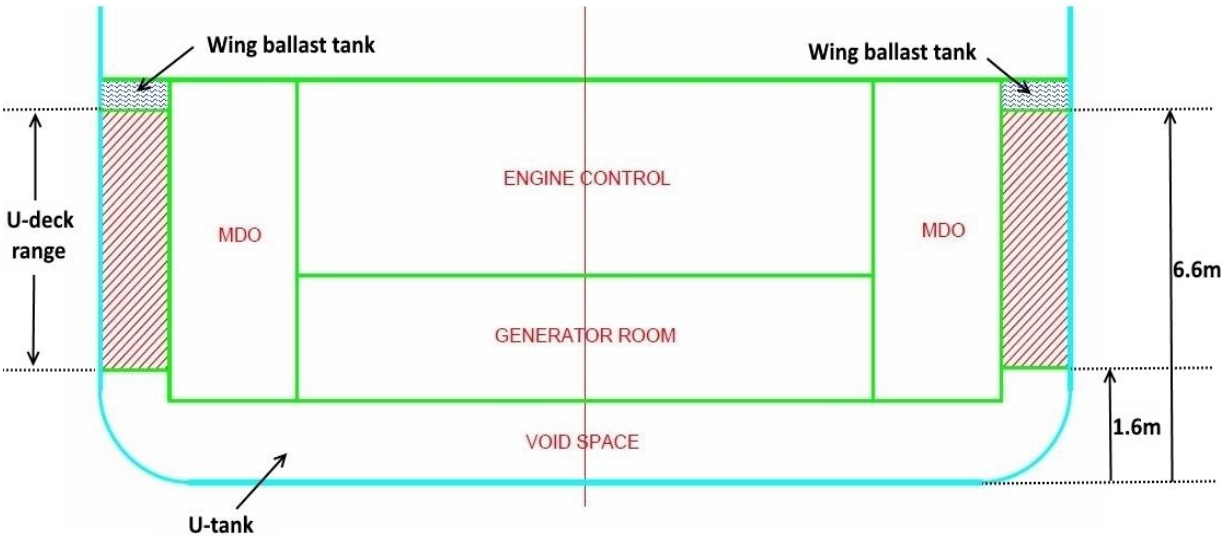

Figure 26. Cross-section of the ship illustrating the relevant placements of U-deck.

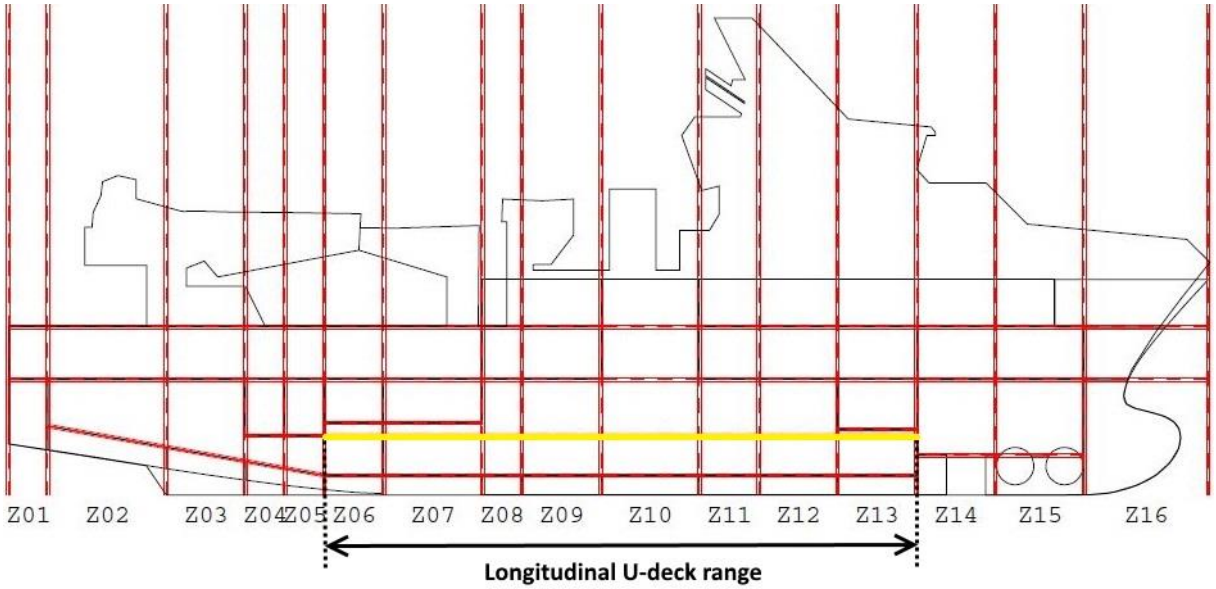

Figure 27. Illustration of the longitudinal U-deck range, which goes from zone 6 to zone 13.

Furthermore, Figure 26 also presents the procedure used to investigate objective 1: U-deck is moved in vertical direction with an interval of 0.5 m from 1.6 m up to 6.6 m – the vertical range of U-deck. Even though deck 1 and the tank top deck, with heights 7 m and 1.2 m respectively, limit the vertical placement of U-deck, it is not considered reasonable to place U-deck above 6.6 m or below 1.6 m.

U-deck was created as its own deck in the decks' text file in NAPA, to save a considerable amount of time; the height of U-deck is then changed automatically in the subdivision table by changing it once in the decks' text file, instead of having to change it manually in the subdivision table for each run.

3.5.8 Objective 2

The GM values that were used as initial conditions in the Probabilistic Manager when performing PDS calculations for objective 1, were taken from the intact stability GM limit curve. This was explained in Sub-section 3.5.2. For objective 2, the same intact stability GM limit curve is used as the starting point for the investigation, as illustrated in Figure 28.

As the below figure shows, the direction of the GM limit curve depends on the KG values; in this study, the KG values for the three subdivision draughts were changed mainly by adjusting the water levels in the double bottom ballast tanks. When filling up these tanks to obtain a deeper subdivision draught, i.e. moving to the right in the graph below, the KG value is lowered and consequently the GM value becomes higher. That explains the direction of the curves.

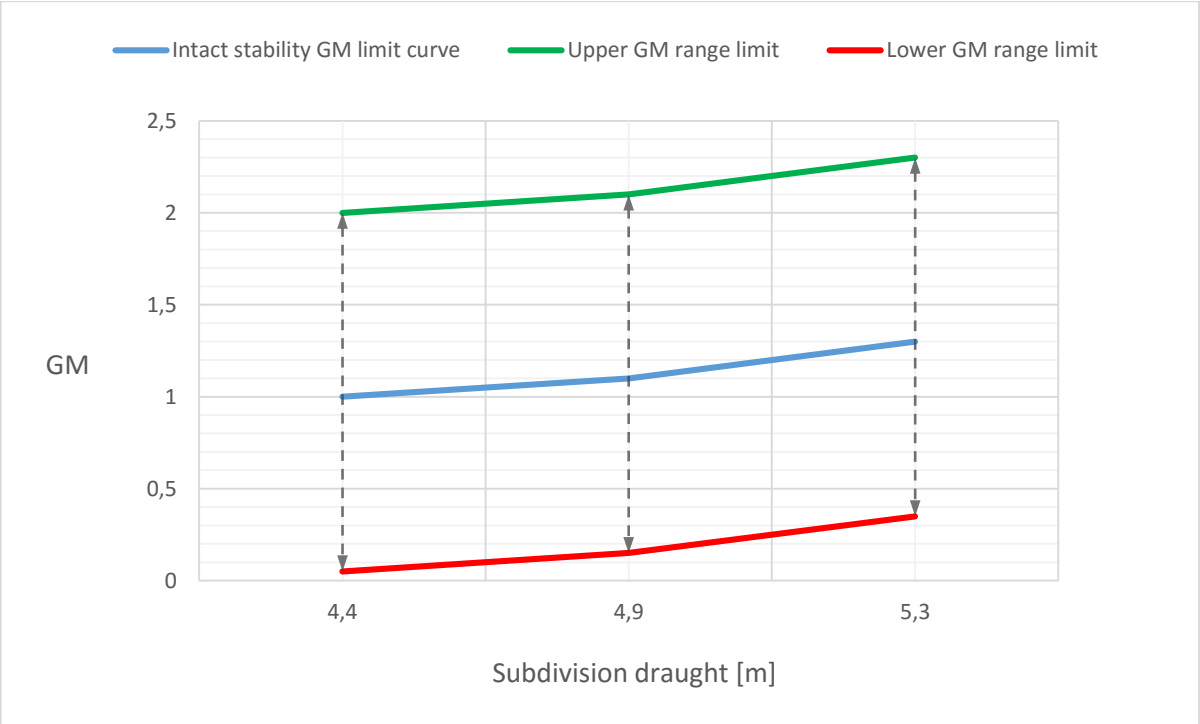

Figure 28. Intact stability GM limit curve.

The purpose with objective 2 is to investigate the behaviour of the A-index when changing the GM values corresponding to the three subdivision draughts d_L, d_P and d_S. Similar to objective 1, a relatively large interval is used: 0.2 m. The selected range is displayed in Figure 28, and goes from the deterministic requirement as the lowest value, which is equal to 0.05 m, up to 2.0 m as the upper limit. This range is considered to be sufficient in terms of identifying the A-index' behaviour.

3.6 Analysis Tools in NAPA

In the Probabilistic Manager there are multiple tools available for analysing the results. That is a strong benefit by using NAPA to do PDS calculations. These tools typically visualise the results somehow and, thus, makes the results more transparent; by only looking at the A-index value in the NAPA results report, whether it is the total A-index or the A-index for one single damage case, it is difficult to explain the result. This follows from the extensive calculations that are required to obtain the A-index value. Examples of helpful analysis tools found in the Probabilistic Manager are the SFAC and P1S diagrams.

3.6.1 SFAC Diagram

The s_i-factor (SFAC) diagram provides an overall view of the criticality with respect to the survivability of the vessel for each longitudinal zone. As shown in Figure 29, the SFAC diagram includes both single-zone and multi-zone damages. The triangles at the bottom line, i.e. the first horizontal row, represent single-zone damages. The second row, i.e. the first row of parallelograms, represent two-zone damages. The uppermost parallelograms in the SFAC diagram below thus represent 4-zone damages. In general, parallelograms represent multi-zone damages.

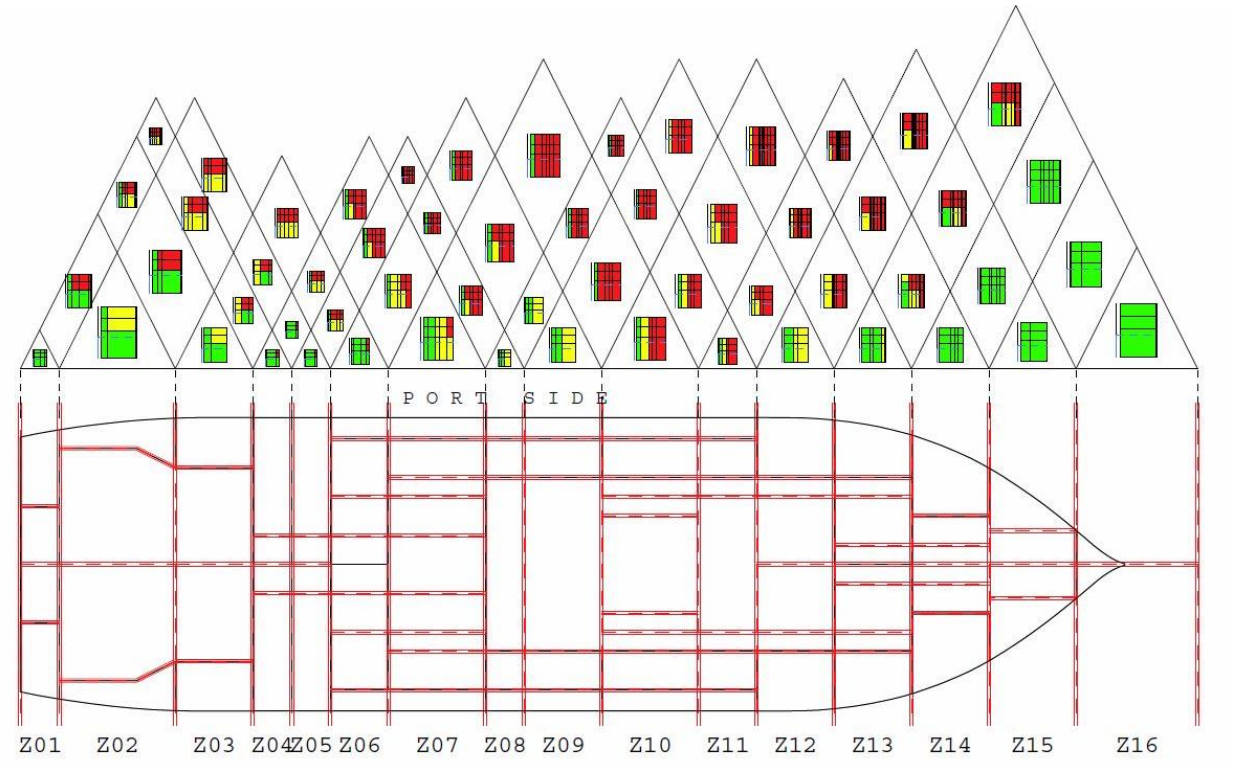

Figure 29. SFAC diagram obtained from the NAPA results report.

By taking a closer look at each triangle or parallelogram, it is possible to investigate each damage case individually. The single-zone damage case from zone 3 for the WFSV in this study is presented in Figure 30 to illustrate how it works.

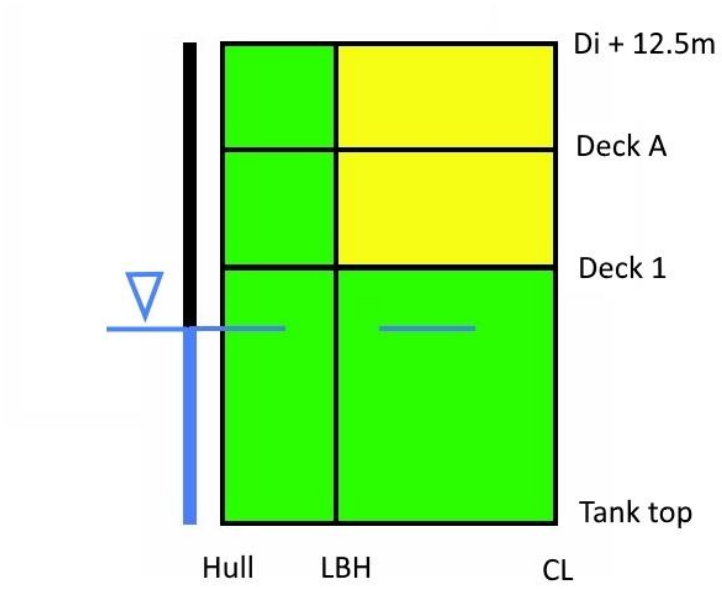

Figure 30. Single-zone damage case from zone 3. The figure is inspired by (Djupvik et al., 2015).

As visualised in Figure 30, no decks except for the tank top below the waterline are shown in the SFAC diagram. The single-zone damage case in zone 3, which is illustrated in Figure 30, deck 2 does not show. That is because the height of deck 2 in zone 3 is approximately 3 m, according to the subdivision table in Appendix J, and the PDS regulations do not account for groundings or collisions below the waterline. The waterline used in the SFAC diagram above corresponds to the light service draught, which is 4.4 m in this study.

Furthermore, the bottom horizontal line in Figure 30 represents the tank top, the uppermost horizontal line represents the maximum vertical damage extent, and the horizontal lines in between represent the decks above the light service draught. The leftmost vertical line represents the hull, the rightmost vertical line represents the centreline, and any vertical line in between the latter two lines represents a longitudinal bulkhead. Furthermore, the colour codes used in the SFAC diagrams are explained in Table 14 (Djupvik et al., 2015; Puustinen, 2012).

Table 14. Colour codes used in the SFAC diagrams (Djupvik et al., 2015; Puustinen, 2012).

Colour code	Value of the s-factor
Green	$s \geq 0.99$
Yellow	$0.05 \leq s \leq 0.99$
Red	$s \leq 0.05$
White	$p \cdot r \cdot v < 0.00001$

3.6.2 P1S Diagram

The P1S diagram is included in NAPA to make the results more transparent. Its purpose is thus to identify problematic damage cases with a low safety level. As displayed in Figure 31, p(1-s) is on the vertical axis and the non-dimensional longitudinal position x/L is on the horizontal axis (NAPA, 2015); the larger p(1-s) value, the more critical is the damage case. It is therefore easy to locate where the critical cases occur in the ship's longitudinal direction. As opposed to the SFAC diagram, the P1S diagram includes the probability of damage in addition to the survivability. The strategy that has been used in this study is to first look at the P1S diagram to identify the problematic damage cases, and then look at the SFAC diagram to investigate these damage cases in detail with respect to survivability.

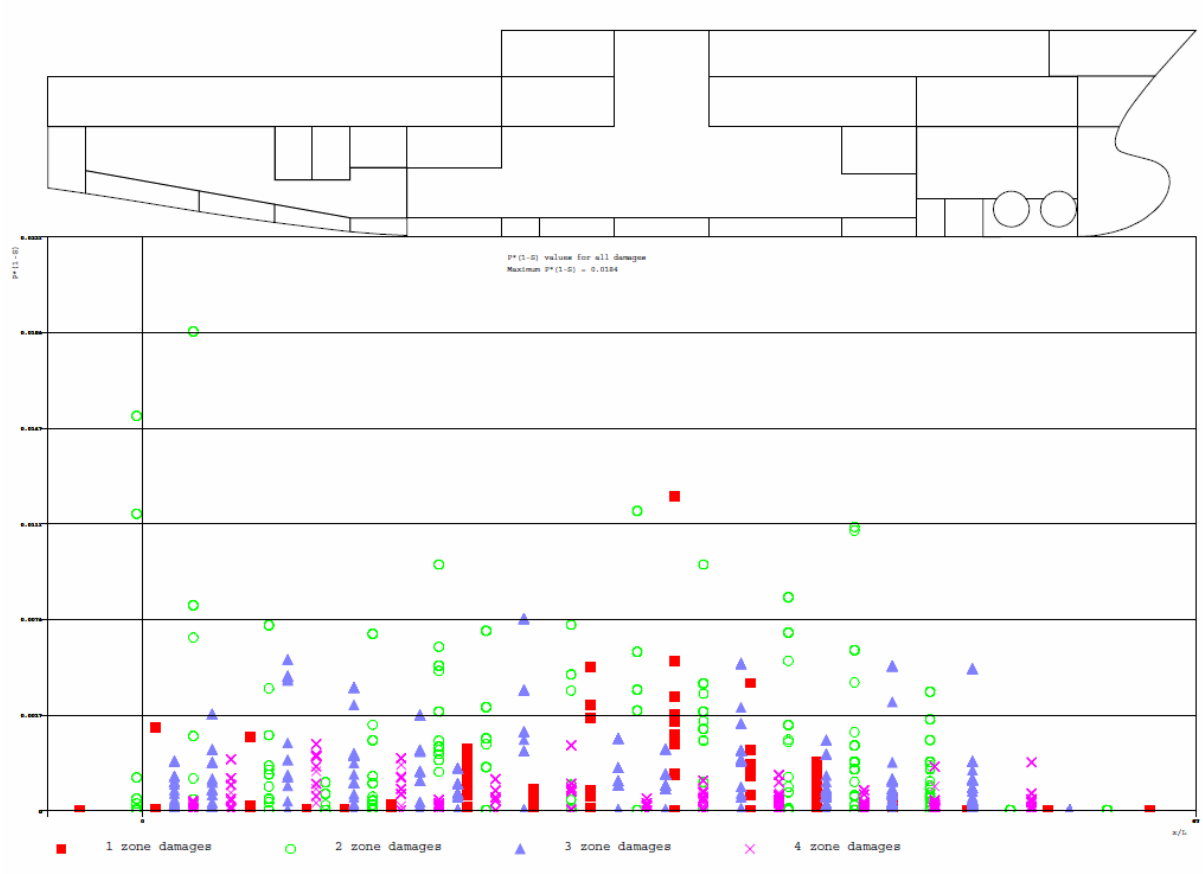

Figure 31. P1S diagram obtained from the NAPA results report.

4. Results of Individual Study

For the individual study, numerous calculations have been done in NAPA by following the methods described in Chapter 0. Each calculation provides a results report that contains more than 1000 pages of information. Considering the large number of reports in this study, these are attached electronically, and can be found through a link in Appendix B. Thus, only the most relevant information is included in the appendices, or presented in the thesis' results or discussion chapter. The results of the PDS calculations carried out for the objectives described in Chapter 0 and 0, are presented in Chapter 4.

4.1 Objective 1: Changing the Height of U-deck

Section 4.1 presents the results related to objective 1 of the thesis; the aim of this section is to show how the A-index varies with the placement of U-deck above the baseline. Graphs where the A-index is plotted against the height of the U-deck are provided for all three subdivision draughts individually, and for the total A-index. Regarding the A-index plots for the three subdivision draughts, it is important to keep in mind that these A-index values have different impact on the total A-index. As can be seen from Equation 8, which is re-presented below, A_S, A_P and A_L constitute 40%, 40% and 20% of the total A-index, respectively.

$$A = 0.4A_S + 0.4A_P + 0.2A_L > R$$

4.1.1 R-index

The method used to calculate the R-index was explained in Sub-section 2.4.3. Since the WFSV used in the study is an SPS, a modified version of Equation 4 should be applied to calculate the R-index, as re-presented in the below calculation. N is taken as 2 · 60 = 120, because survival craft moments are neglected. The 0.8 factor is included because the SPS carries not more than 60 personnel.

$$R = 0.8 \cdot \left[1 - \frac{5000}{L_s + 2.5N + 15225}\right] = 0.8 \cdot \left[1 - \frac{5000}{72.92 + 2.5 \cdot 120 + 15225}\right] = 0{,}54356$$

This R-index value is equal to the one calculated by NAPA, as can be seen in Appendix K.

4.1.2 A-index

As Figure 32 reveals, there is a clear tendency regarding the A-index' behaviour when changing the U-deck height. Below U-deck height 5.6 m, which yields the maximum A-index value, the A-index value is decreasing when reducing the height of U-deck. For larger U-deck heights than 5.6 m, the A-index curve turns direction; the value of the A-index is decreasing when increasing the height of U-deck.

The vertical lines in Figure 32 represent the decks that are located close to U-deck: deck 1, deck 2 and tank top deck. These decks are included in the plot because they function as vertical barriers for flooding and, thus, they might impact the A-index. Deck 2 occurs in three of the eight zones within the longitudinal range of U-deck, which stretches from zone 6 to zone 13, and deck 2's potential contribution will be discussed in Chapter 0.

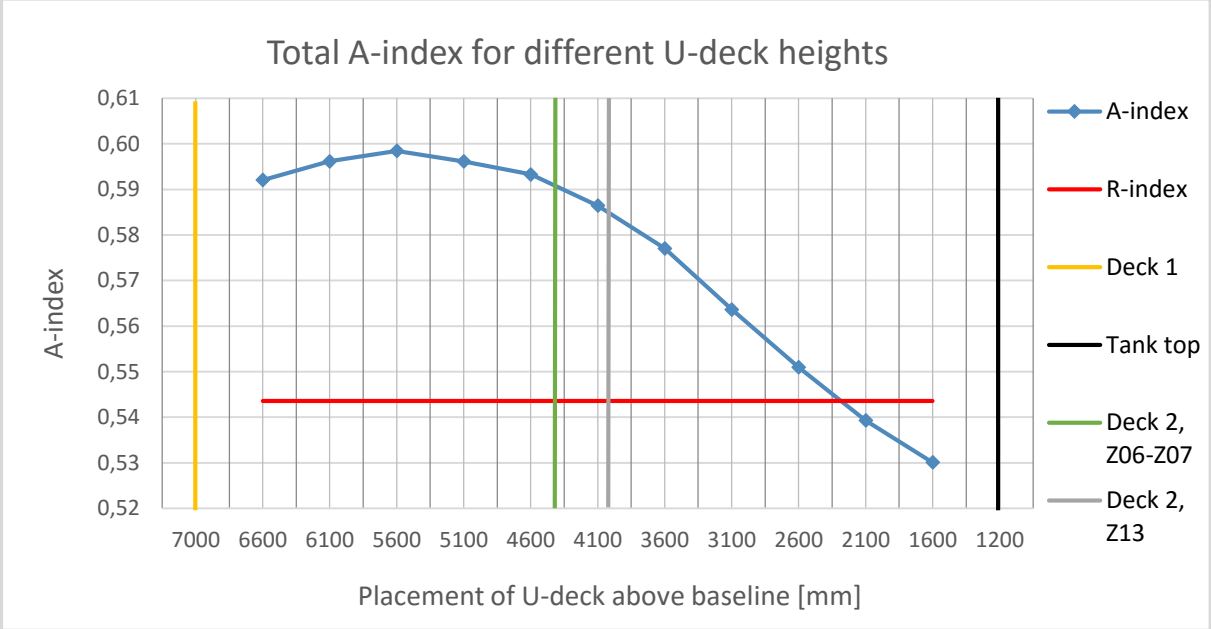

Figure 32. Plot of A-index vs. placement of U-deck.

The development of the A-index in the above plot was expected; when U-deck is lowered, the wing ballast tanks increase in volume and, consequently, a larger heeling moment can potentially be created by damages that penetrate the wing ballast tanks. A larger heeling moment reduces the survivability of the ship, which influences the A-index negatively. In the damage case discussed here, the magnitude of the heeling moment depends on the draught of the ship. As presented in Sub-section 3.5.2, the subdivision draughts used in this study are: d_L = 4.4 m, d_P = 4.9 m and d_S = 5.3 m. Bearing in mind that the A-index is equal to $0.2A_L + 0.4A_P + 0.4A_S$, it was expected that the A-index would be affected negatively by placing U-deck anywhere below d_S = 5.3 m, because sea water will flood the wing tanks below this height.

At the same time as the wing ballast tanks increase in volume, when lowering the U-deck height, the volumes of the U-tanks decrease. Offshore vessels are designed with U-tanks to increase the survivability of the ship in case of damage. The larger the size of the U-tanks, the larger effect the U-tanks have on the damage stability. U-tanks force the sea water to flood symmetrically about the centreline of the ship and, thus, the higher sea water level in the U-tanks, the bigger is the stabilizing effect. Of course, if the sea water reaches a certain level, and KG as a result becomes sufficiently low, GM could turn out negative.

The development of the A-index curve in Figure 32 confirms the above theory. Both of the two abovementioned effects drag the A-index in the same direction, when changing the U-deck height. This can be explained with a scenario where several wing ballast tanks are damaged: A larger U-deck height results in smaller wing ballast tank volumes and larger U-tank volumes, which both contribute to lower heeling moment and, consequently, larger s_i-factor. A lower U-deck height results in the opposite: larger wing ballast tank volumes and smaller U-tank volumes, which increases the heeling moment and, consequently, decreases the s_i-factor.

In other words, the goal should be to find a U-deck height that provides a reasonable balance between U-tank and wing ballast tank volumes, with respect to heeling moment in case of damages involving U-deck. At the same time, it is important to remember that it is not only the two abovementioned factors, i.e. the effect of wing ballast tanks and U-tanks, that affect the s_i-factor in case of damage. There are numerous other damage cases, which involves other compartment types and flooding scenarios. The focus in this part of the thesis is however on damages that involve U-deck.

Furthermore, the key is to have as large wing ballast tanks as reasonably practicable. I.e., the key is to maximise the A-index under the ‘restriction’ that the wing ballast tanks should have room for a desired amount of ballast water. It is assumed that U-deck height 5.6 m, which corresponds to the maximum value on the A-index curve, results in too small wing ballast tanks. Thus, it is reasonable to proceed the study in objective 2 of the thesis with another U-deck height. The relevant area on the graph from where the U-deck height shall be taken, seems to range from approximately 4.1 m to 5.6 m – depending on how much ballast water the designer wants to fit in the tanks. To improve the decision basis related to this ‘optimisation’ problem, more data points and, thus, better accuracy in the relevant area on the graph is provided in Figure 33.

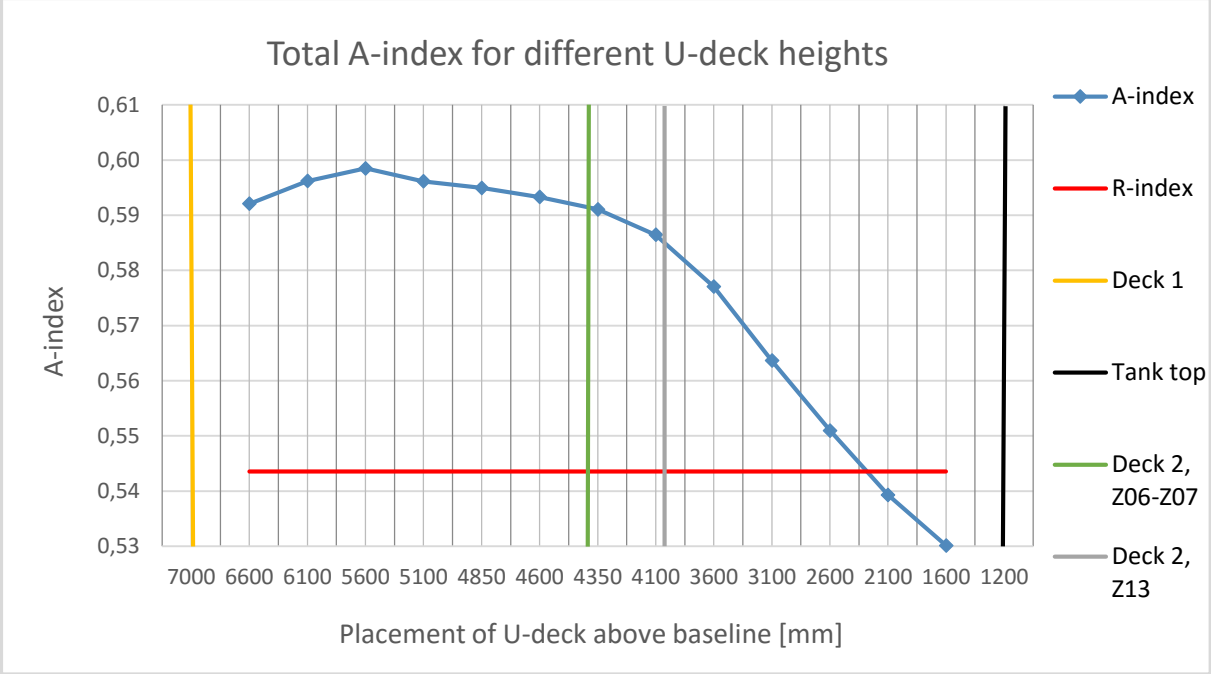

Figure 33. Plot of A-index vs. placement of U-deck.

To improve the grounds for discussion even more, Figure 34 illustrates how the A-index varies with the U-deck height for the three subdivision draughts d_L, d_P and d_S. Again, it is important to remember that the A-index is equal to $0.2A_L + 0.4A_P + 0.4A_S$.

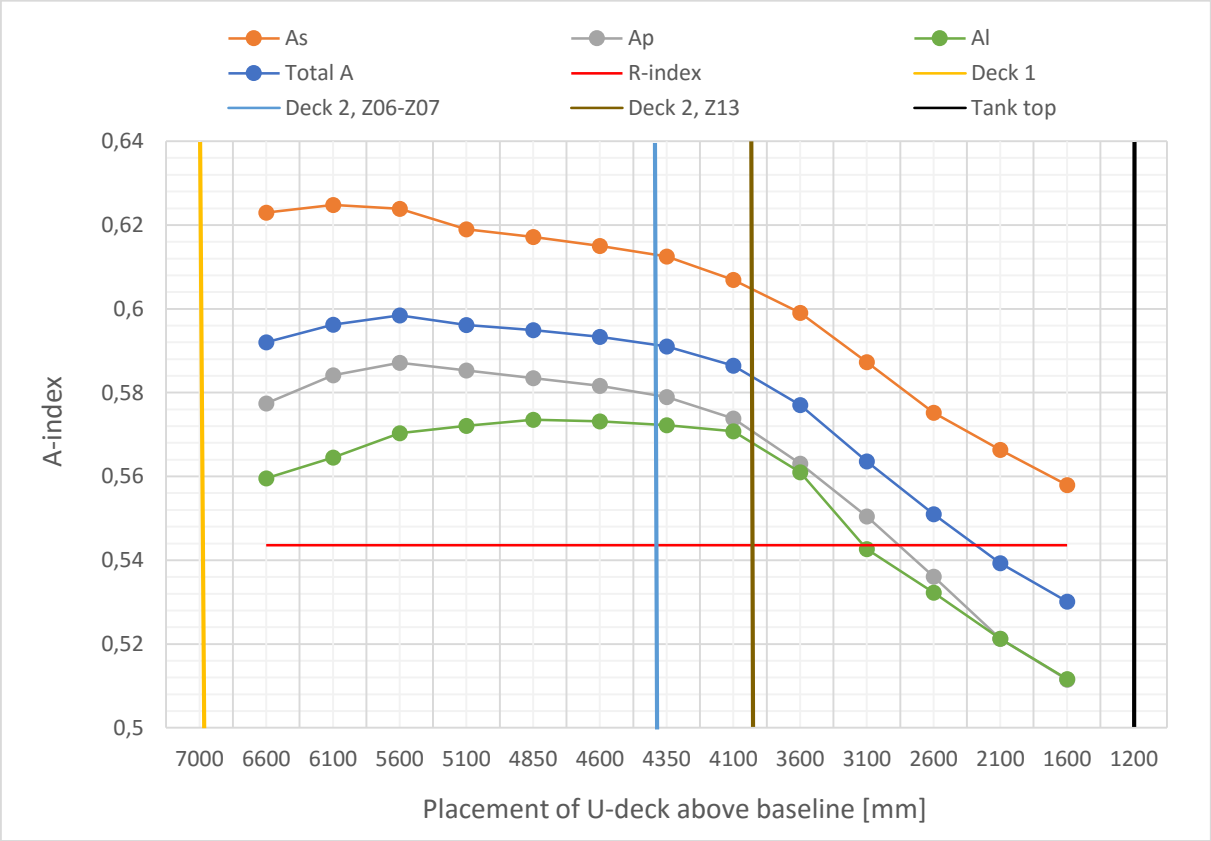

Figure 34. Plot of A_C-index vs. placement of U-deck for all subdivision draughts.

From the plot in Figure 33, it becomes evident that there is a relatively steep downhill from approximately 4.4 m and downwards in U-deck height. Any specific reasons for that are not immediately discovered, except that it probably is caused by enlarged heeling moments and smaller U-tank volumes. When U-deck is lowered beneath a subdivision draught, the wing ballast tanks will take in sea water and create a heeling moment for that subdivision draught. In this case the subdivision draught is d_L = 4.4 m, thus the wing ballast tanks will take in sea water and create a heeling moment for both A_S, A_P and A_L, in case of damage.

Furthermore, Figure 34 shows that the A_C-index for all three subdivision draughts decreases with approximately the same rate. The curve for A_L, however, is a bit flatter than the other curves until approximately 4.1 m in U-deck height. From there on, there is a noticeable declination for the A_L-index. That could be due to deck 2 in zone 13, as illustrated in the figure, but it has to be examined closer by for instance using the P1S and SFAC diagrams.

As discussed in Chapter 0, the PDS calculations are extensive and complex, and it is not easy to immediately see the effect one single change has on the whole system; one single change may affect many 'PDS-factors'. The effect of changes is also varying for different damage cases. Thus, P1S and SFAC diagrams should be used to examine the results more in-depth, which is done for critical damage cases in Chapter 0.

4.2 Objective 2: Changing the Initial GM Values

In order to investigate objective 2, the results from the PDS calculations that were conducted for a specified range of GM values, are presented in Section 4.2. The height of U-deck used in these calculations is 4.4 m, which seems like a reasonable choice when looking at Figure 33 in the previous section; there is a considerable declination in the graph to the right of U-deck height 4.35 m. U-deck height 4.4 m seems beneficial both with respect to the ship's damage stability and with respect to the size of the wing ballast tanks.

The R-index value is the same for objective 2 as for objective 1, as shown in Figure 35. The development of the A-index for a range of GM values is presented in the same figure. There is no specific reason why GM values for d_L are on the horizontal axis, instead of GM values for d_S or d_P; all three subdivision draughts will indicate the same behaviour, the only difference is that the curve will shift 0.3 and 0.1 units to the left with d_S and d_P, respectively.

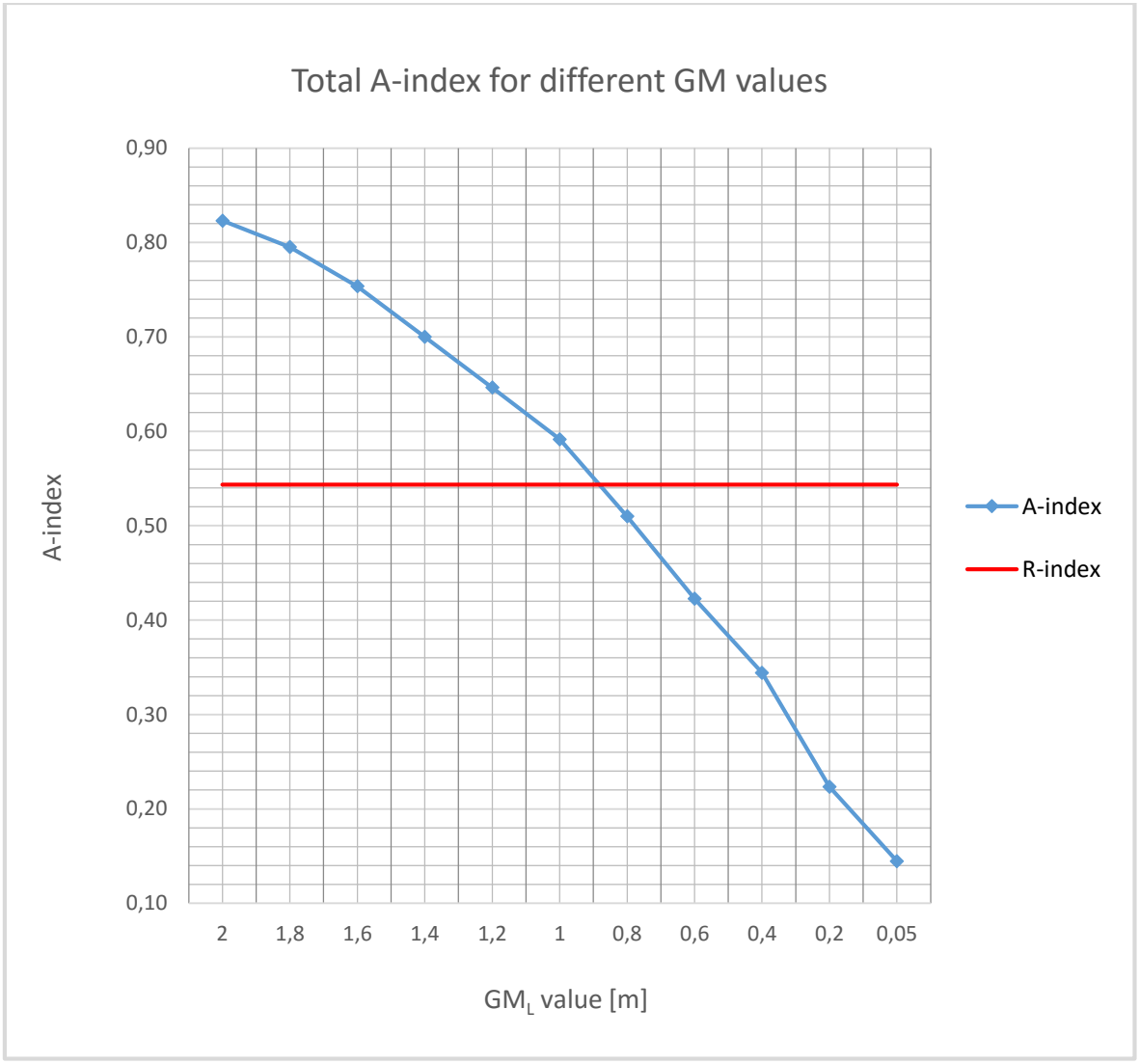

Figure 35. Plot of A-index vs. GM_L value.

As stated in Sub-section 3.5.2, a simple measure to increase the A-index is to increase GM. This is usually done if the A-index does not meet the PDS criterion, i.e. if A < R (IMO, 2008c). In other words, the direction of the A-index curve in the above plot was expected.

In Chapter 0, a discussion around the development of the A-index for varying GM values is provided. For instance, it is interesting to investigate why GM values below approximately 1 m are critical, and why GM values below 0.9 are not approved according to the PDS criterion.

Figure 36 presents how the A_C-index varies with the GM values corresponding to d_L, d_P and d_S. A conclusion that immediately can be drawn from Figure 36 is that A_L, A_P and A_S respond similarly to changes in GM.

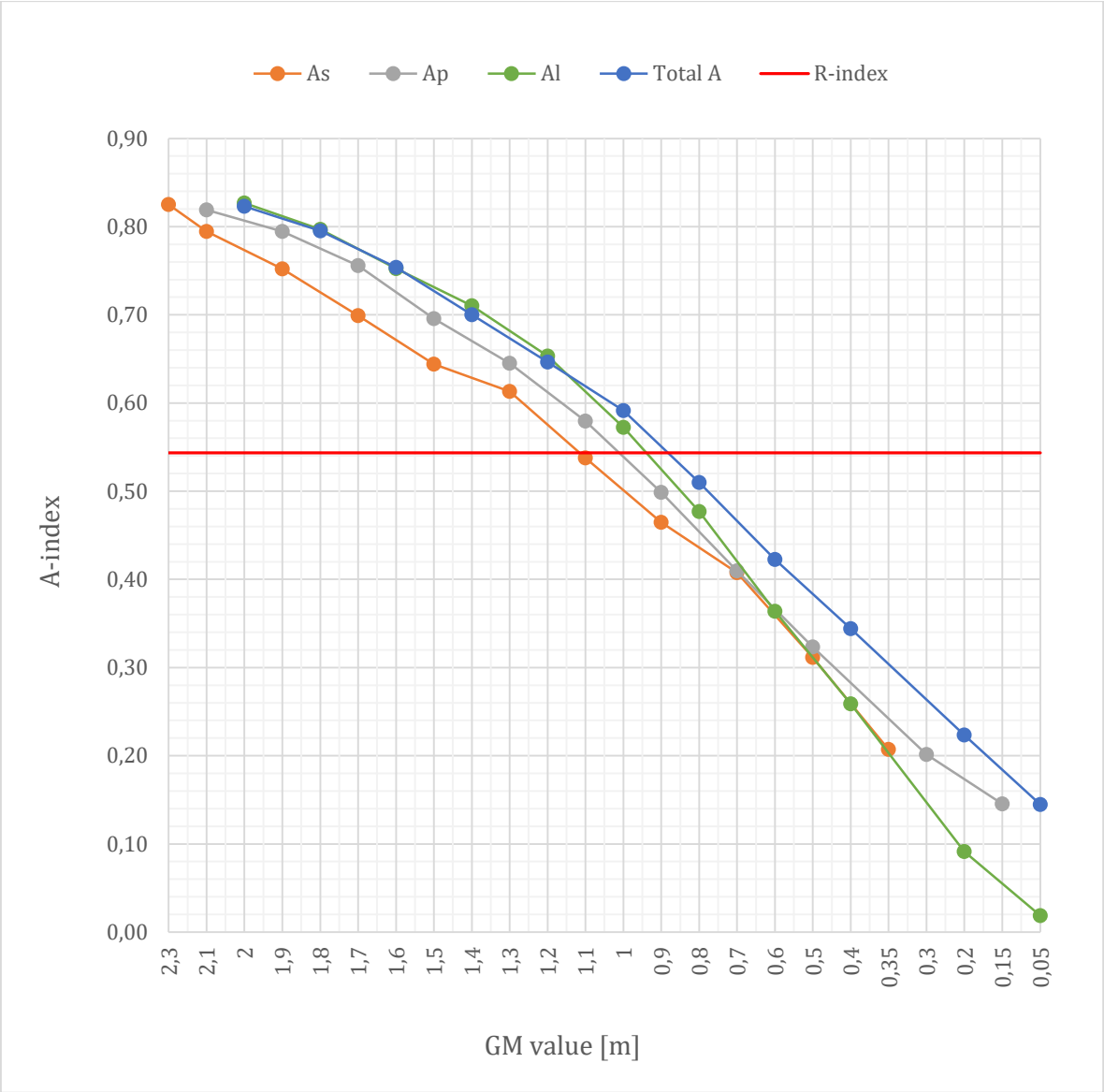

Figure 36. Plot of A_C-index vs. GM values for all subdivision draughts.

5. Analysis and Discussion

The method and results of the study conducted in this thesis were presented in Chapter 0 and 4, respectively. The results have been analysed in order to evaluate the A-index. As mentioned in previous chapters, the ship under investigation is referred to as a WFSV, which is assumed to go under the SPS Code. Since the shape and size of the WFSV are fairly similar to other offshore vessel types, it seems reasonable to assume that the results also could be valid for other offshore vessels applying to the SPS Code. Chapter 0 generally discusses how and why the A-index is affected by the changes made in the arrangement and intact stability for the WFSV.

5.1 The Effect of Changing the U-deck height

This section discusses the effect on the A-index of placing U-deck at different heights above the baseline. A definition and illustration of U-deck were given in both Section 3.1 and Sub-section 3.5.7. The following discussion includes a detailed investigation of the three probability factors p_i, s_i and v_i, which multiplied together constitute the A-index. By investigating these factors separately, it should be easier to explain the results presented in Section 4.1.

In Figure 37, there are some circled data points on the A-index curve for varying U-deck heights, which are considered to be more interesting than the other data points.

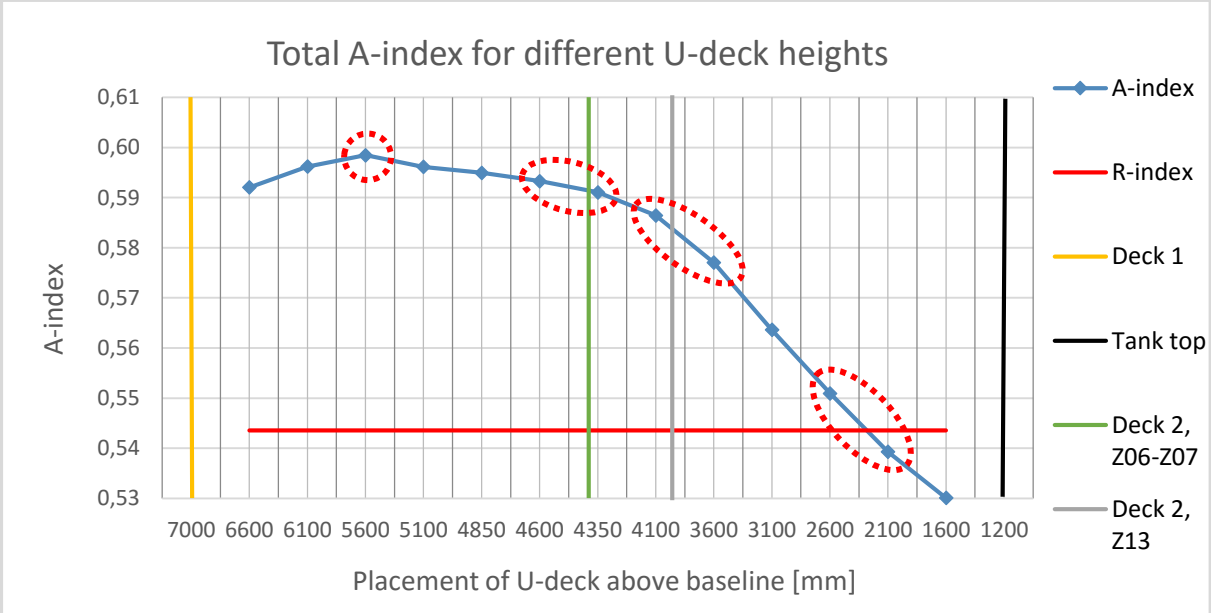

Figure 37. Areas of particular interest on the A-index curve for different U-deck heights.

A selection of only four U-deck heights will be focussed on in the following discussion: 5.6 m, 4.6 m, 3.6 m and 2.6 m. This is considered to be sufficient in terms of achieving an in-depth understanding of the results.

When investigating the U-deck heights selected above, U-deck height 2.6 m will be examined first considering it has the lowest A-index and, thus, probably contains the most critical damage cases. The strategy is to use the P1S diagram to identify critical damage cases within the longitudinal range of U-deck with height 2.6 m. Then, SFAC diagrams are used to confirm the findings from the P1S diagram, or to identify other interesting damage cases. Furthermore, the SFAC diagrams for the most critical damage cases for all of the selected U-deck heights, are studied closely to find out what happens with the s_i-, v_i- and p_i-factor.

The P1S diagram for U-deck height 2.6 m is presented in Figure 38. The black coloured square marks the relevant longitudinal range of U-deck: zone 6 to zone 13. The damage cases with the largest p(1-s) values and, thus, the lowest safety level within the longitudinal U-deck range, are marked with a red coloured square.

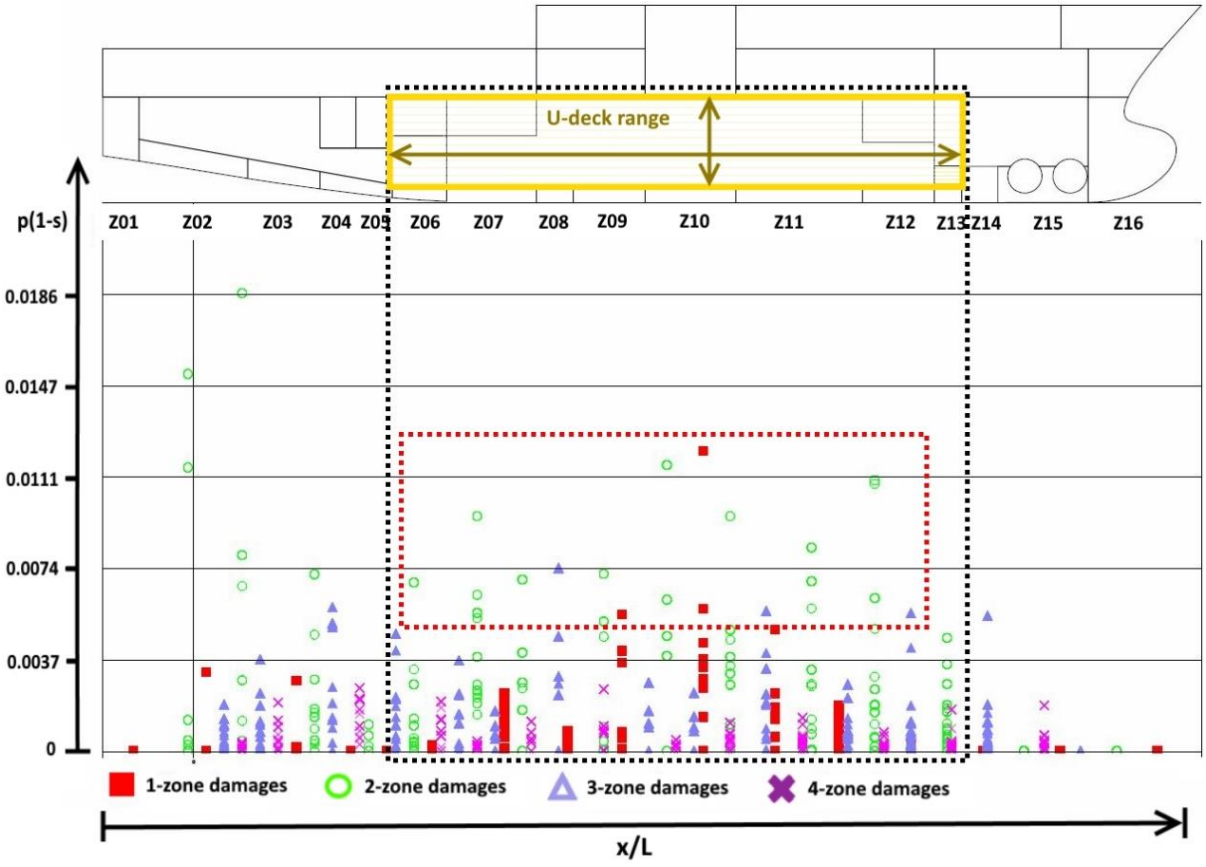

Figure 38. P1S diagram for U-deck height 2.6 m.

In Figure 38, two-zone damages appear to be generally more critical than other damage cases. It is not straightforward to find the reason for that, especially due to the complex formulas and extensive procedure used to calculate the p_i-factor both for single-zone and multi-zone damages. These formulas are attached in Appendix A. Regarding the s_i-factor, it is expected that the more zones that are involved in a damage, the more critical the damage becomes with

respect to the survivability of the ship. Thus, it seems like the p_i-factor makes the two-zone damages more problematic, compared with damages involving three or more adjacent zones. SFAC diagrams could be used to support this argumentation.

None of the zones in Figure 38 stands out with respect to criticality within the range of U-deck, but zone 9 and 10 are slightly more critical than the other zones. For instance, the single-zone damage cases in zone 10 appear in the P1S diagram as most critical within the range of U-deck. Consequently, these zones are selected for a closer examination in the following sub-sections.

5.1.1 The p_i-factor

As explained in Sub-section 2.4.6, the p_i-factor is only dependent on the longitudinal and transverse damage extent. In equation 9 from the same sub-section: $p_i = p(x1_j,x2_j)\cdot[r(x1_j,x2_j,b_k) - r(x1_j,x2_j,b_{k-1})]$, p(x1,x2) is the longitudinal contribution and r(x1,x2,b) is the transverse contribution to the p_i-factor. A damage to one of the wing ballast tanks is furthermore illustrated in Figure 39.

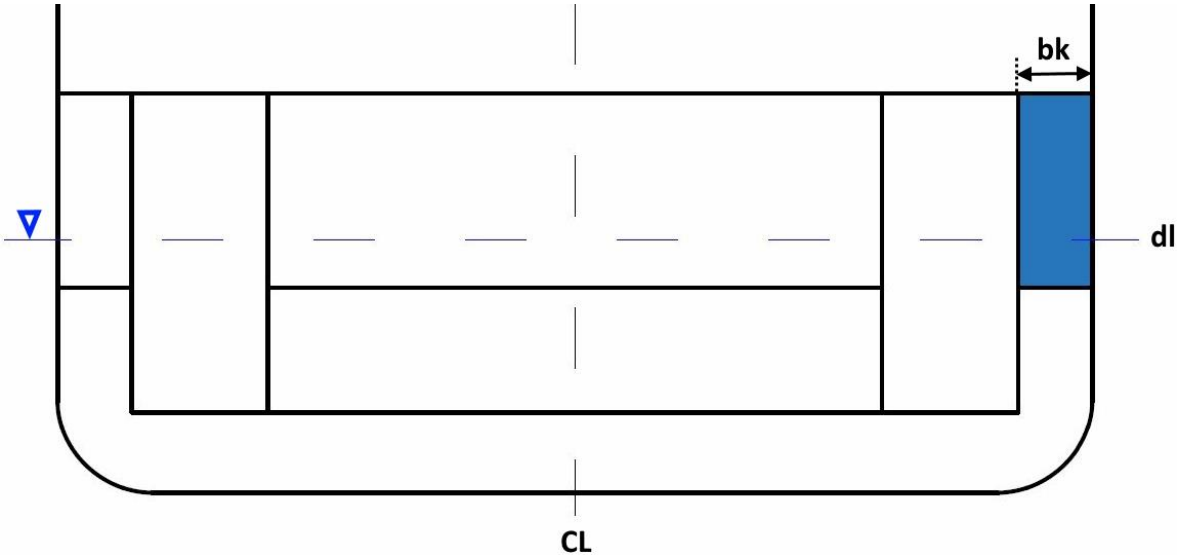

Figure 39. Illustration of a damaged wing ballast tank and corresponding b_k-factor.

In the Figure 39, b_{k-1} does not exist, because there is only one longitudinal bulkhead that limits the flooding in transverse direction. Since the number of longitudinal bulkheads is not the same for all zones within the longitudinal range of U-deck, the b_k and b_{k-1} values and the r(x1,x2,b)-factor will vary from zone to zone. The p(x1,x1)-factor is also changing from zone to zone, since the distance between the transverse bulkheads varies. However, neither p(x1,x1) nor r(x1,x2,b) is affected by the distance between decks, which is the only changing parameter

regarding objective 1 of the thesis. In other words, the height of U-deck will not affect the p_i-factor.

5.1.2 The s_i-factor

As discussed in Sub-section 4.1.2, damages to the wing ballast tanks might have a considerable effect on the s_i-factor; this type of damage can potentially create a heeling moment that makes the ship heel over. In such case, the GZ curve changes and results in a reduced K value for heel angles larger than 7 degrees. This can be seen from Equation 38 and 39 in Sub-section 2.4.7: θ_{min} is equal to 7 degrees, since the WFSV is treated as a passenger ship by the PDS regulations. Thus an increase in θ_e reduces K and, consequently, the s_i-factor for heel angles larger than 7 degrees. On top of this, if the GZ_{max} and range values are reduced below 0.12 and 16, respectively, the s_i-factor will be reduced even more.

The abovementioned potential effects influence the A-index negatively. The magnitude of the impact depends on the height of U-deck, as was thoroughly explained in Sub-section 4.1.2. It should be added that the survivability, or the s_i-factor, of the ship depends on a number of other factors than the height of U-deck. It is however the U-deck height that is in focus in Sub-section 5.1.2, and in Section 5.1.

The survivability of the ship for every single damage case is illustrated in SFAC diagrams in the NAPA results report. NAPA creates one SFAC diagram for each subdivision draught. It seems like d_L is most critical with respect to survivability in this study, which is illustrated and explained in Appendix L. The SFAC diagrams for d_L for the selected U-deck heights are therefore used as the basis in the following discussion, in order to be conservative.

Figure 40 furthermore presents the SFAC diagram for U-deck height 2.6 m. This U-deck height is the most problematic of the selected U-deck heights in terms of A-index value. There is a dotted circle in Figure 40, highlighting the damage zones considered to be most critical within the U-deck range. The SFAC diagrams for the other selected U-deck heights can be found in Appendix M.

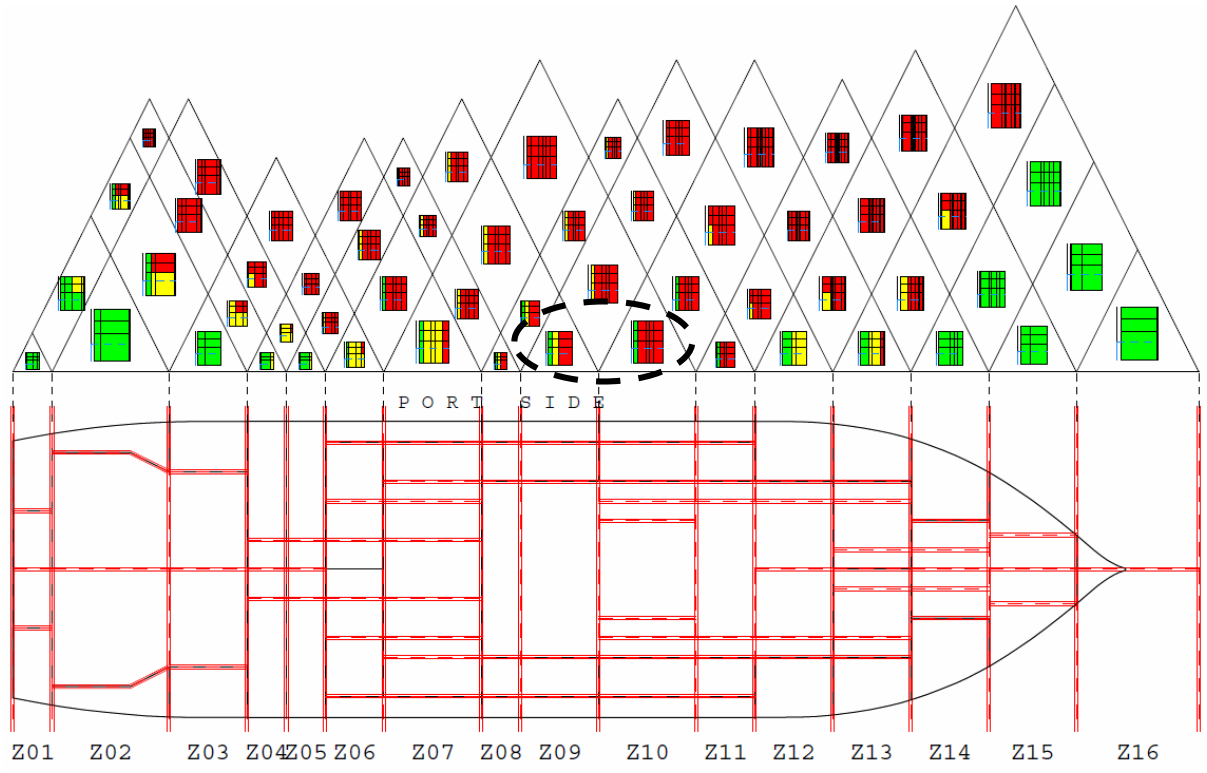

Figure 40. SFAC diagram for d_L, with U-deck height 2.6 m.

Furthermore, Figure 41, Figure 42, Figure 43 and Figure 44 present up-scaled SFAC diagrams for the single-zone damages in zone 9 and 10 for all four selected U-deck heights, in declining order: from U-deck height 5.6 m and downwards to U-deck height 2.6 m.

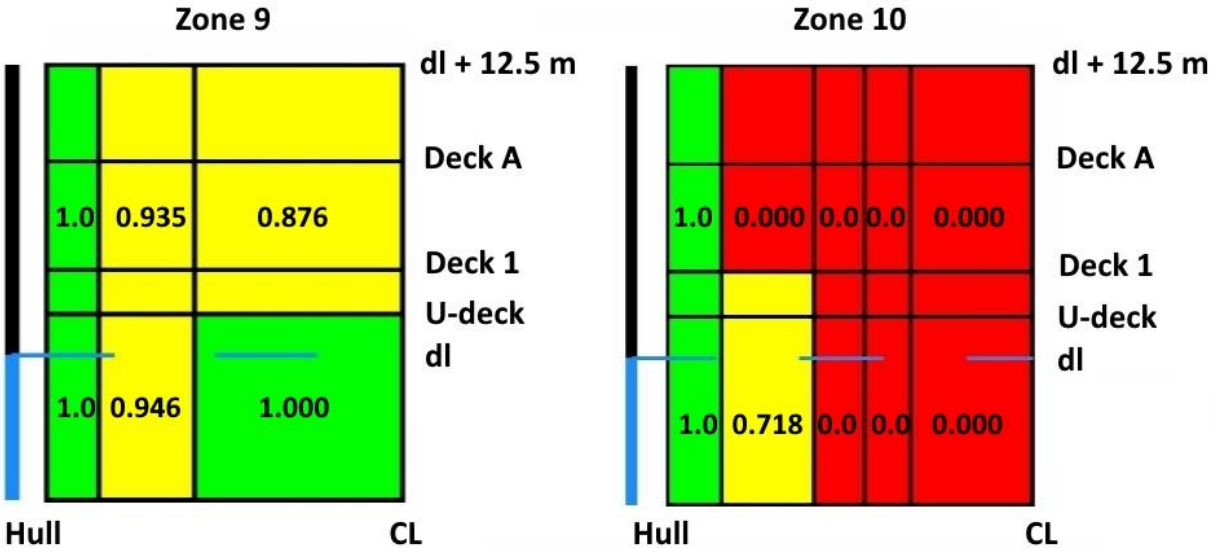

Figure 41. Up-scaled SFAC diagrams for the single-zone damages in zone 9 and 10, with U-deck height 5.6 m.

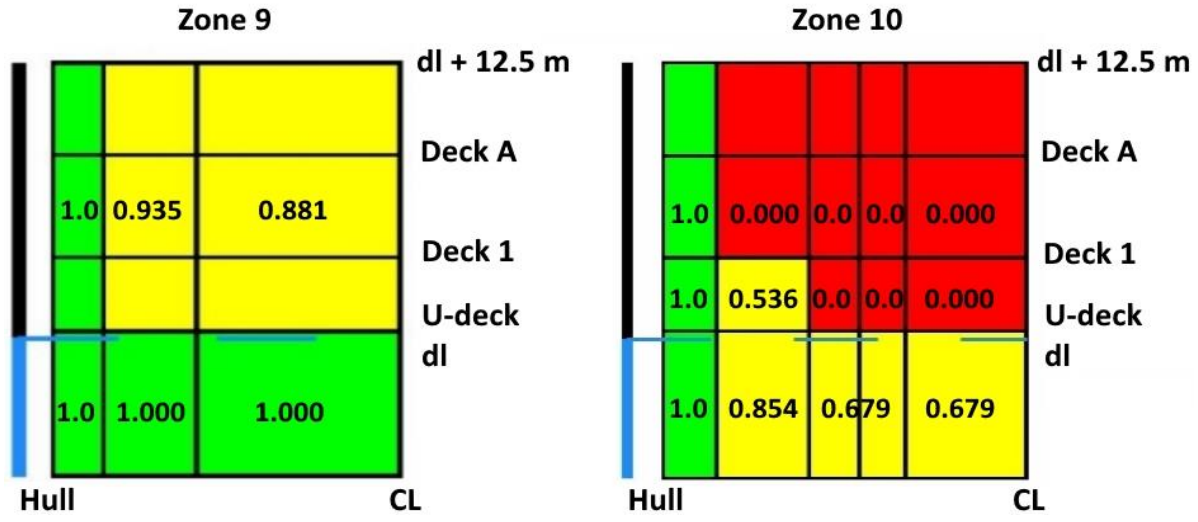

Figure 42. Up-scaled SFAC diagrams for the single-zone damages in zone 9 and 10, with U-deck height 4.6 m.

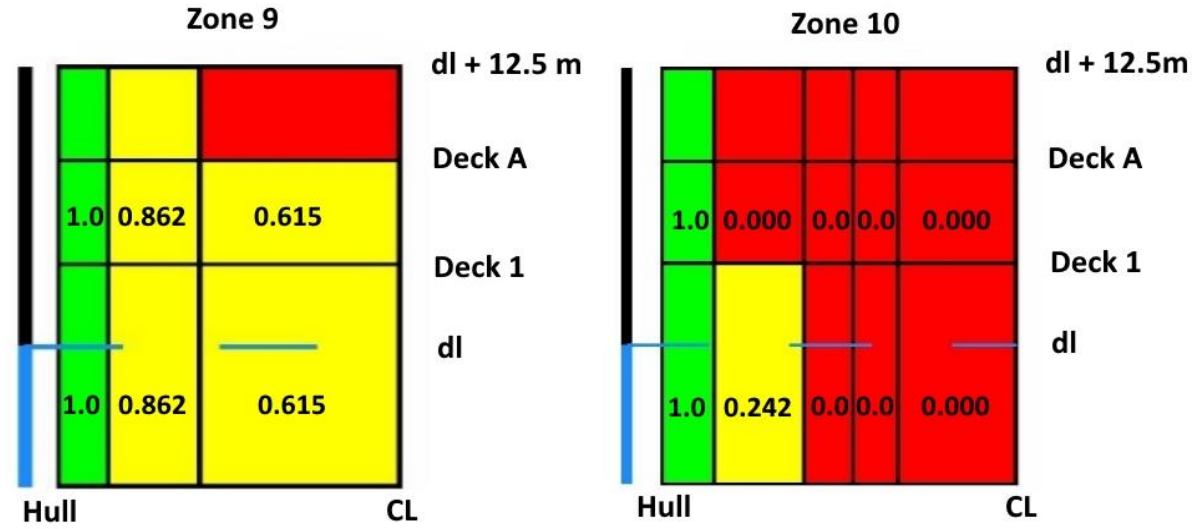

Figure 43. Up-scaled SFAC diagrams for the single-zone damages in zone 9 and 10, with U-deck height 3.6 m.

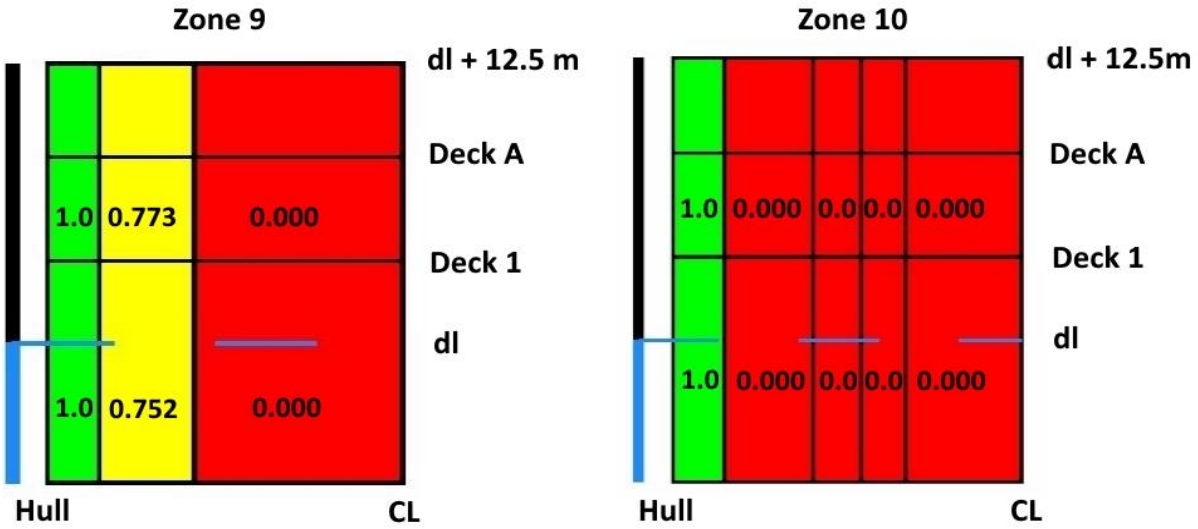

Figure 44. Up-scaled SFAC diagrams for the single-zone damages in zone 9 and 10, with U-deck height 2.6 m.

Only the SFAC diagrams in Figure 41 and Figure 42 display U-deck. That is because the PDS regulations do not account for groundings or collisions below the waterline, which is 4.4 m in this case. The numbers given in the SFAC diagrams are the s_i-factor values connected to specific damage cases within zone 9 or 10. From these values it can be concluded that the s_i-factor generally becomes lower with decreasing U-deck height. This coincides with the expectations that were discussed in Sub-section 4.1.2 and in the introduction to this sub-section.

There is one exception that immediately seems to undermine the 'confirmation': the opposite development of the s_i-factor occurs under the transition from U-deck height 5.6 m to 4.6 m for the single-zone damages in zone 10; the s_i-factor decreases when U-deck is placed higher. This is however not strange: Figure 34 in Sub-section 4.1.2 shows that the peak on the A_L-index curve does not occur at 5.6 m, as it does for the A-index curve. The maximum A_L-index occurs approximately at U-deck height 4.8 m, which is closer to U-deck height 4.6 m, where the survivability is better for loading condition d_L. For the two other subdivision draughts, d_P and d_S, this is however not the case: their peaks are located at approximately 5.6 m in U-deck height. Since the total weight of the A_C-indexes corresponding to loading conditions d_P and d_S is 80% of the A-index, the peak of the A-index curve is naturally in the same area.

Furthermore, the decline in s_i-factor is quite significant for some compartments. Damages close to the centreline are naturally the worst ones with respect to survivability, and also the ones with the heaviest declination. In zone 9, these damages reduce the s_i-factor with approximately 30-40% from U-deck height 4.6 m to 3.6 m. Then, the s_i-factor goes all the way to zero for U-deck height 2.6 m. In zone 10, the damages close to the centre line are even more critical with respect to survivability, as compared to zone 9; except for the bottom damage case closest to the centreline for U-deck height 4.6 m, all the s_i-factors are equal to zero in zone 10.

Within the longitudinal range of U-deck, there are three damage zones that include an extra deck within the vertical range of U-deck: deck 2. These damage zones are 6, 7 and 13, which are not represented by the SFAC diagrams presented above. In order to investigate the impact that deck 2 might have on the s_i-factor, SFAC diagrams for the single-zone damages in zone 6, 7 and 13 are attached in Appendix N. Furthermore, the height of deck 2 is 4.4 m in zone 6 and 7, and 4 m in zone 13. Deck 2 is in other words never placed higher than the waterline for any of the subdivision draughts in the abovementioned zones. However, the s_i-factor could be affected, since deck 2 can prevent down-flooding and, thus, reduce the heeling moment.

First of all, by looking at the P1S diagram in Figure 38, it does not seem like the single-zone damages in zone 6, 7 and 13 are critical at all. This could be a result of a low p_i-factor or a large s_i-factor, or both. The SFAC diagrams in Appendix N furthermore indicate that the survivability in general decreases when lowering the U-deck height in these zones, however not in the same order of magnitude as for the single-zone damages in zone 9 and 10. In addition, it is assumed that the p_i-factor is fairly similar for all of the abovementioned damage cases. Thus, it seems like deck 2 has a positive, minor effect on the s_i-factor, but not significant enough to prevent the declination when lowering the U-deck height.

Based on the above discussion, it seems safe to conclude that the s_i-factors generally decrease when the U-deck height is lowered beneath 5.6 m. As mentioned earlier, U-deck will probably never be placed above this height anyway, due to practical reasons. Additionally, since the development of the s_i-factor correlates quite well with the development of the A-index, the results may indicate that the s_i-factor in general contributes significantly to the A-index. This will be discussed further in Sub-section 5.1.4.

5.1.3 The v_i-factor

U-deck is a horizontal surface that may, depending on its height and the damage scenario, limit flooding vertically in case of damage. Either way, the v_i-factor will change when U-deck is moved in vertical direction, as long as the change in height occurs above the waterline. For U-deck heights below the waterline, any changes will not influence the v_i-factor. This is illustrated below, where U-deck is placed above the waterline in Figure 45 and below the waterline in Figure 46. Supporting literature can be found in Sub-section 2.4.8 of the thesis.

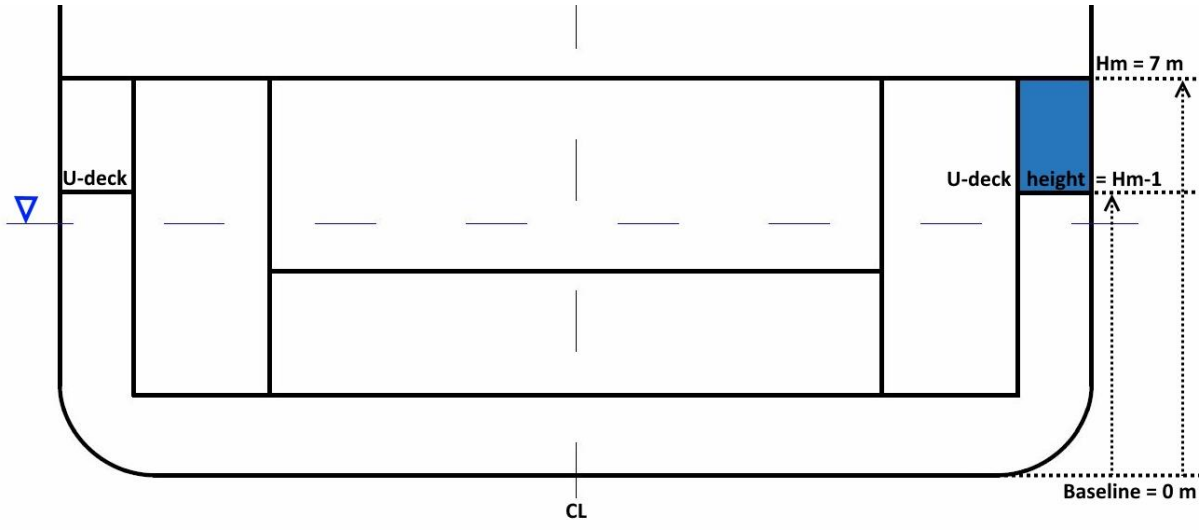

Figure 45. v_i-factor for wing tank damage, with U-deck placed above the waterline.

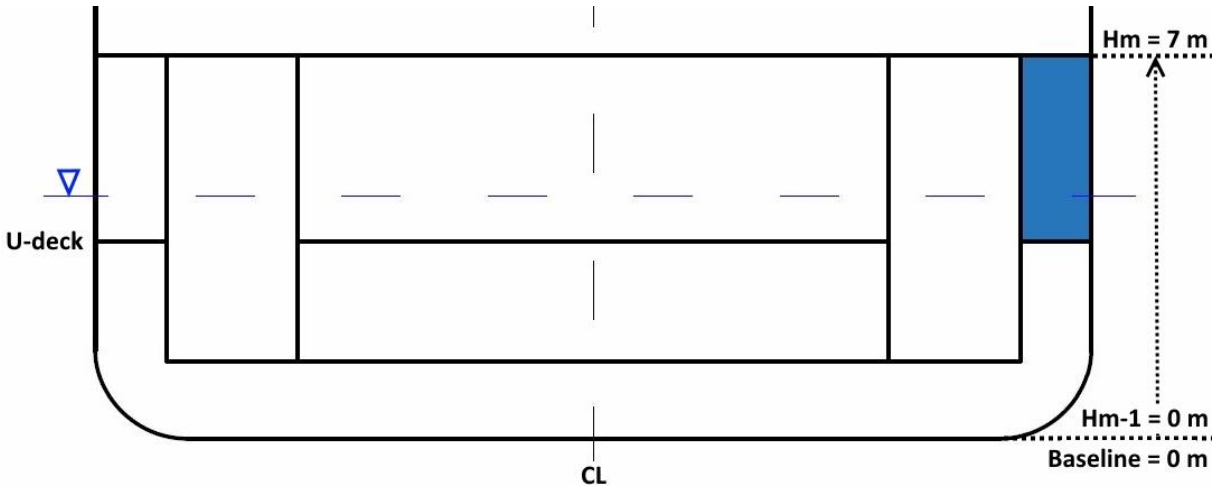

Figure 46. v_i-factor for wing tank damage, with U-deck placed below the waterline.

Since the PDS regulations do not account for damages below the waterline, damages to the U-tanks will not be included in the calculations for the arrangement displayed in Figure 46. For U-deck heights above the waterline however, as shown in Figure 45, there will be v_i-factor contributions to the A-index for both wing ballast tank and U-tank damages. The latter damage scenario is illustrated in Figure 47. Additionally, it should be noted that the wing ballast tanks and U-tanks can be damaged at the same time, for U-deck heights above the waterline. This is illustrated in Appendix O.

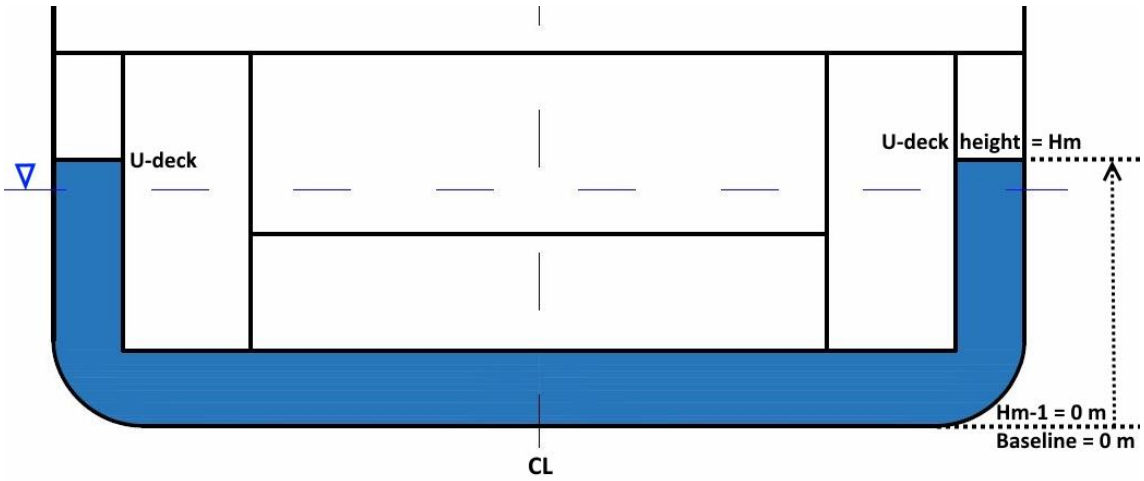

Figure 47. v_i-factor for U-tank damage, with U-deck placed above the waterline.

Based on the above illustrations and discussion, it is not immediately possible to conclude which U-deck heights contribute most to the total A-index in terms of the v_i-factor. The declination in A-index below 4.4 m in U-deck height, as can be seen in Figure 33 in Sub-section 4.1.2, may however indicate that the v_i-factor has a significant effect; the waterline in the above

illustrations corresponds to d_L = 4.4 m, and the overall v_i-factor contribution is assumed to be smaller for U-deck heights below the waterline. At the same time, the declination could also be solely due to the reduction in s_i-factor. Hence, it is not easy to tell straight away which of the v_i- and s_i-factor that is most influential with respect to the A-index. This issue will be discussed further in Sub-section 0.

To provide greater insight related to the v_i-factors, calculations for the abovementioned damage cases have been carried out according to the theory presented in Sub-section 2.4.8. The calculations are conducted for all three loading conditions: d_S, d_P and d_L. The damage cases used in the calculations are presented in Table 15, and the corresponding H_m and H_{m-1} values for the selected U-deck heights can be found in Appendix P. For all three loading conditions, a calculation of the v_i-factor is done for each damage case listed in Table 15. The mean v_i-factor of the three damage cases, is then plotted for each loading condition against the selected U-deck heights in Figure 48.

Table 15. The damage cases used to investigate the v_i-factor for objective 1.

Damage case	Damaged compartments	Illustration of damage case
A	Wing ballast tank	Figure 45 / Figure 46
B	U-tank	Figure 47
C	Wing ballast tank + U-tank	Appendix O

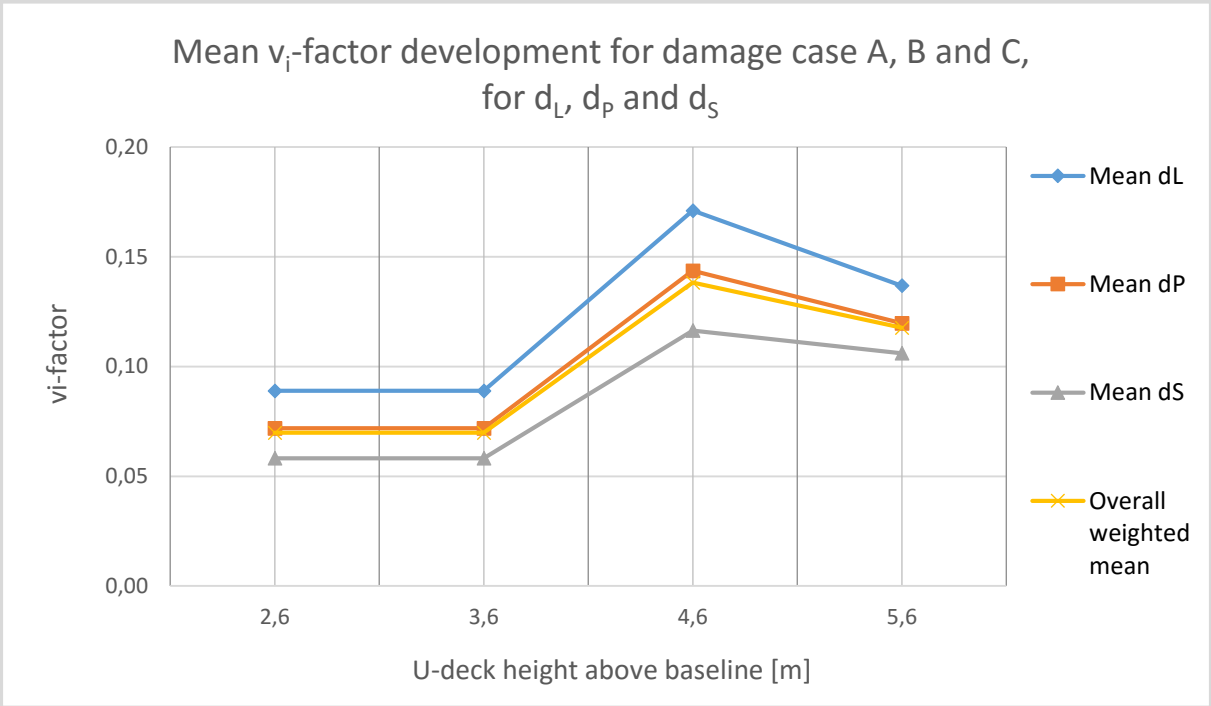

Figure 48. Mean development of the v_i-factor for damage case A, B and C, for all three subdivision draughts.

The trend lines in Figure 48 indicate how the v_i-factor for the ship 'behaves' within the longitudinal range of U-deck. Even though the above results only represent one specific damage zone, the majority of the zones from zone 6 to 13 have fairly similar arrangements. The yellow trend line is furthermore the overall weighted mean value for the v_i-factor of all three subdivision draughts, where the mean v_i-factor development for d_L, d_P and d_S counts 20%, 40% and 40% respectively. According to these trend lines, there is a significant percentual change in v_i-factor when reducing the U-deck height from 5.6 m to 2.6 m: approximately 40% reduction. This reduction is of equal size order as for the s_i-factor for certain damaged compartments in the SFAC diagrams in Sub-section 5.1.2.

Furthermore, it could be presumed the presence of deck 2 in zone 6, 7 and 13 has an impact on the v_i-factor, since decks function as horizontal boundaries that limit flooding in vertical direction. However, since the height of deck 2 never is higher than 4.4 m, which corresponds to loading condition d_L, deck 2 will not contribute to the v_i-factor within the range of U-deck. That is because the $v(H_m,d)$ or $v(H_{m-1},d)$ value for deck 2 is zero in all damage cases. The author assumes, since it is not completely clear in the PDS regulations, that a horizontal boundary or deck must be placed above the waterline in order to attain a $v(H_m,d)$ or $v(H_{m-1},d)$ value larger than zero.

5.1.4 Total A-index

The total A-index is a weighted sum of the three A_C-indexes corresponding to the three subdivision draughts d_S, d_P and d_L, as shown in the re-presentation of Equation 8 below:

$$A = 0.4A_S + 0.4A_P + 0.2A_L$$

Furthermore, the below re-presentation of Equation 7 shows how the A_C-indexes are calculated, where N is the number of damage cases.

$$A_c = \sum_{i=1}^{N} p_i s_i v_i$$

When U-deck is placed below the waterline, there are fewer damage cases which will contribute to the total A-index. Thus, there are fewer contributions to the A_C-indexes from both the p_i-, s_i- and v_i-factors. This does not necessarily mean that the A-index gets a lower value, but the results from this study could indicate this.

In this study, the A-index is declining below 5.6 m in U-deck height. From a U-deck height approximately 4.4 m and downwards, which corresponds to waterline d_L, the declination gets steeper for the A-index. This strengthens the theory that the number of damage cases could be of importance; when U-deck is placed below the waterline, the number of damage zones is reduced, which in turn leads to fewer A_C-index contributions. On the other hand, the A-index continues to decline below all three subdivision draughts, i.e. below d_L = 4.4 m, where the number of damage zones will be constant for all U-deck heights. This weakens the theory in the previous paragraph.

Furthermore, by knowing the p_i-factor is constant for all U-deck heights, it is obvious that either the s_i- or v_i-factor, or both, contribute to the reduction in A-index for U-deck heights lower than 5.6 m. Based on the analysis and discussion in Sub-section 5.1.2 and 5.1.3, it seems safe to state that both factors contribute to the reduction. Which of the factors that is most influential, however, is harder to say.

One potential indicator, which leads the author to think that the s_i-factor might be more influential, is the mean v_i-factor curves presented in Figure 48. These trend lines only represent the majority of the damage zones within the range of U-deck. Additionally, they do not represent any other damage cases than the ones closest to the hull. This means that it might be wrong to draw a conclusion based on this data. Irrespective of the latter uncertainty, the abovementioned trend lines do not correspond very well with the A-index curve. For instance, there does not seem to be a development for the v_i-factor when moving U-deck from 3.6 m to 2.6 m. This is not the case with the s_i-factor, which is reduced all the way down from U-deck height 5.6 m to 2.6 m for zone 6, 7, 9, 10 and 13 at least. In conclusion, the s_i-factor seems to be more influential, under the assumption that the v_i-factor development is valid.

5.2 The Effect of Changing the Initial GM Values

This section discusses the influence changes in GM values have on the A-index for the three subdivision draughts d_L, d_P and d_S. The GM values will thus be referred to as the GM_L, GM_P and GM_S, when discussing the change in A-index or A_C-index for the different subdivision draughts. Sub-section 3.5.8 and Section 4.2 constitute the basis for the following discussion. Furthermore, by investigating the p_i-, s_i- and v_i-factors individually, it should be easier to break down and understand the results.

Figure 49 re-presents the results from Section 4.2, but now the figure includes two circles that indicate interesting areas on the graph with respect to further investigation. Additionally, it is important to note that the results presented below and discussed in this section only are relevant for U-deck height 4.4 m, as explained in Chapter 4.

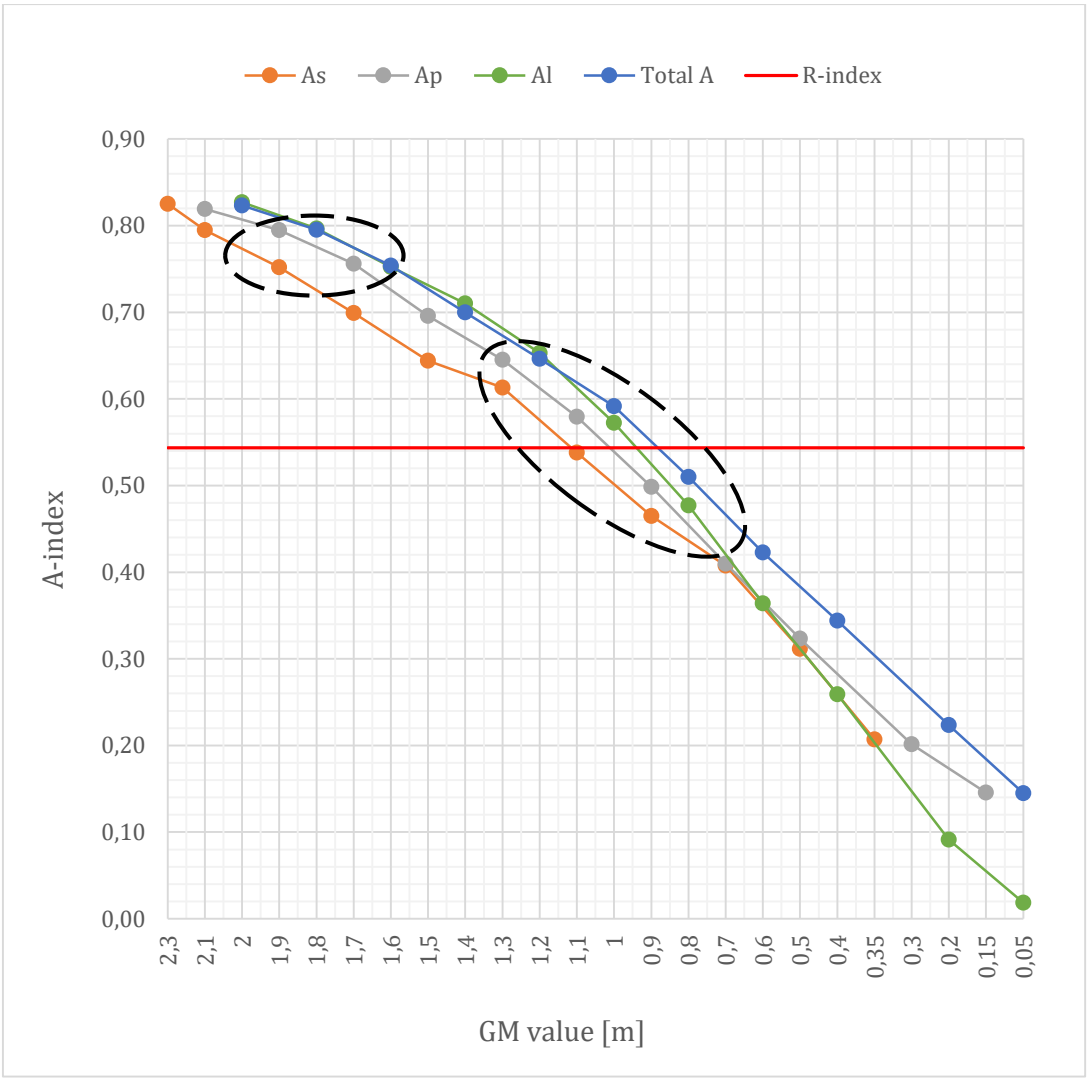

Figure 49. Areas of particular interest on the A-index curve for different GM values.

From Figure 49 it seems like the loading condition d_S is most critical with respect to the A-index, knowing that the A_S-index weighs 40% of the A-index. Three different GM_S values have therefore been selected for a closer investigation: 0.9 m, 1.3 m and 1.9 m. GM values lower than 0.9 m are not considered relevant, because their corresponding A-indexes are far from being in compliance with the 'PDS criteria', i.e. A > R. Furthermore, the GM_P and GM_L values corresponding to the selected GM_S values, are listed in Table 16.

Table 16. GM values selected for in-depth analysis and discussion.

GM_S	GM_P	GM_L
0.9 m	0.7 m	0.6 m
1.3 m	1.1 m	1.0 m
1.9 m	1.7 m	1.6 m

The same approach that was used to identify critical damage cases in Section 5.1, will be followed in this section: the P1S diagram for GM_S = 0.9 m will be used to find critical damage cases, which subsequently will be studied in detail using SFAC diagrams. Additionally, the s_i-, v_i- and p_i-factors are analysed individually. The P1S diagram for GM_S = 0.9 m, with U-deck height 4.4 m, is given in Figure 50.

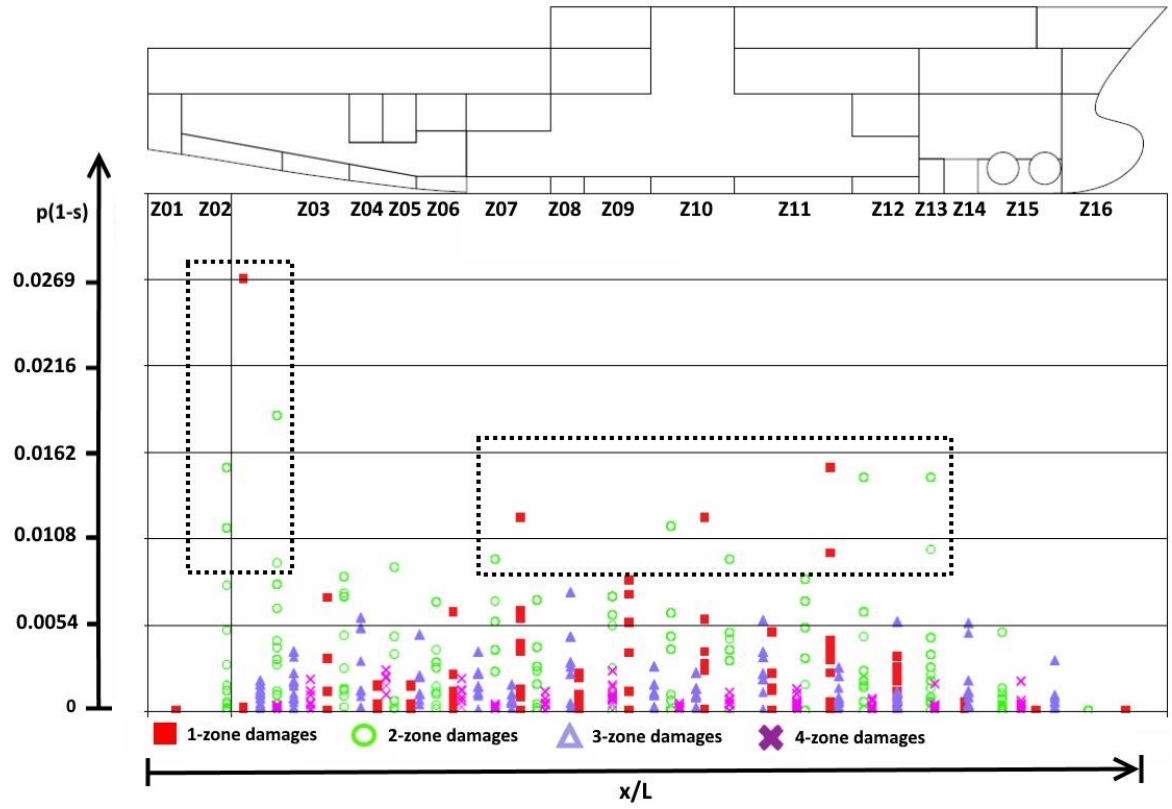

Figure 50. P1S diagram for GM_S = 0.9 m and U-deck height 4.4 m.

The squares in Figure 50 enclose a selection of damage cases that may be considered critical, where the single-zone damages in zone 2 clearly stand out as most severe. There are in addition some relatively critical two-zone damages evenly distributed over the entire ship length, with the majority encapsulated in the square to the right. The following damage cases will therefore be subject to analysis: the single-zone damages in zone 2 and the two-zone damages involving zone 10 and 11.

5.2.1 The p_i- and v_i-factor

There are no changes in the arrangement of the WFSV in objective 2 of the master's thesis. Thus, in similarity with objective 1 of the thesis, the p_i-factor does not change. Additionally, as opposed to objective 1 of the thesis, the v_i-factor does not change since the height of all horizontal surfaces remain the same. Consequently, the development of the A-index corresponding to objective 2 of the thesis, must therefore be a result of changes in the s_i-factor. This will be discussed in the following sub-section.

5.2.2 The s_i-factor

Up-scaled SFAC diagrams for the selected damage cases corresponding to objective 2 of the thesis, for loading condition d_S and the GM_S values in Table 16, are provided in Figure 51 and Figure 53. The complete SFAC diagrams are attached to the thesis in Appendix Q. The single-zone damages in zone 2 will be investigated first, followed by the two-zone damage cases involving zone 10 and 11.

- Investigating the s_i-factor for the single-zone damages in zone 2:

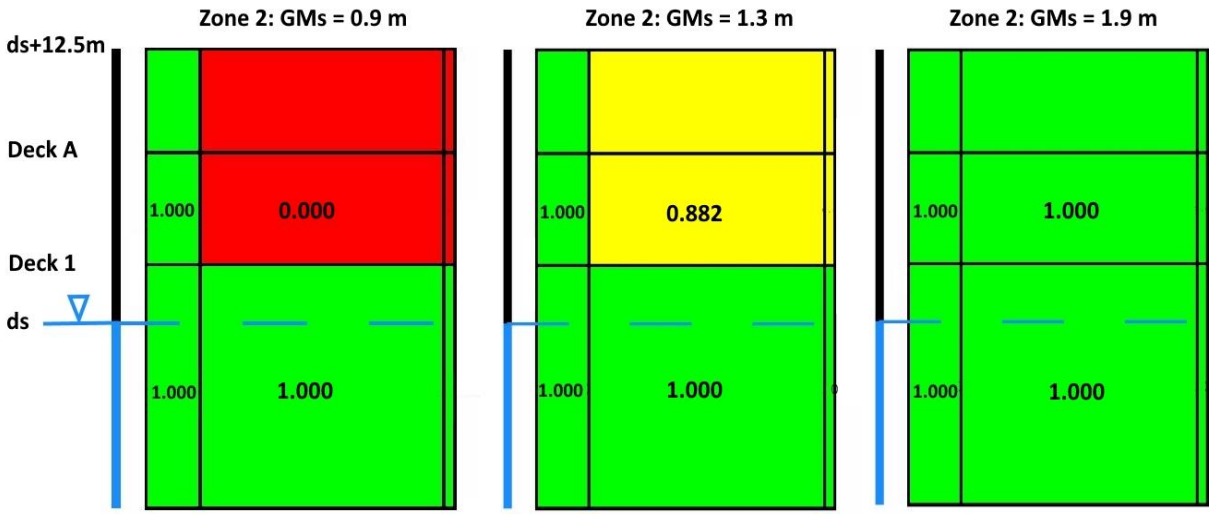

Figure 51. Development of the s_i-factor in zone 2, for loading condition d_S and varying GM_S values.

The above SFAC diagrams show a clear tendency: the survivability connected to the single-zone damage cases under investigation is generally better for larger GM_S values. As illustrated with numbers for the s_i-factor in Figure 51, the increase in s_i-factor is quite drastic for the center compartment damage at deck 1 in zone 2: the s_i-factor increases from 0 at GM_S = 0.9 m to 0.882 at GM_S = 1.3 m, and further on with 13.4%, from 0.882 at GM_S = 1.3 m to 1.0 at GM_S = 1.9 m.

In NAPA, the damage case discussed above is referred to as 'DS/SDSP2.2.2'. For convenience, this damage case is illustrated in Figure 52. Additionally, a damage drawing from NAPA can be found in Appendix R, together with the damage drawing for the two-zone damage case in zone 10 and 11. The latter drawings are more descriptive and illustrative than the one below. The ship's equilibrium floating positions for all six damage scenarios discussed in this sub-section, are also attached to the thesis, in Appendix S.

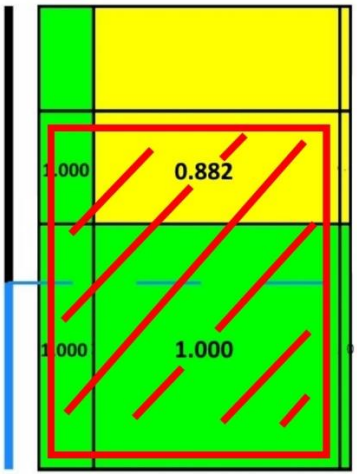

Figure 52. Damage case DS/SDSP2.2.2.

In order to explain the behavior of the s_i-factor for damage case DS/SDSP2.2.2, it is necessary to utilize the PDS theory presented in Sub-section 2.4.6. Since NAPA uses $s_{final,i}$ as the s_i-factor for both damage cases under investigation, and for all GM_S values, Equation 38 and 39 are re-presented below:

$$s_{final,i} = K \cdot \left[\frac{GZ_{max}}{0.12} \cdot \frac{Range}{16}\right]^{\frac{1}{4}}$$

$$K = \begin{cases} \sqrt{\dfrac{\theta_{max} - \theta_e}{\theta_{max} - \theta_{min}}}, & if\ \theta_{min} < \theta_e < \theta_{max} \\ 1, & if\ \theta_e \leq \theta_{min} \\ 0, & if\ \theta_e \geq \theta_{max} \end{cases}$$

Furthermore, the GZ_{max}, equilibrium heel angle θ_e, Range and s_i-factor values for damage case DS/SDSP2.2.2 is obtained from NAPA, and presented in Table 17 for the three selected GM_S values.

Table 17. NAPA results for damage case DS/SDSP2.2.2.

GM_S [m]	s_i-factor	Heel angle θ_e [degrees]	GZ_{max} [m]	Range [degrees]
0.9	0.000	-	-	-
1.3	0.882	8.8	0.24	41.2
1.9	1.000	2.8	0.64	47.2

According to the results in Table 17, the ship will capsize for damage case DS/SDSP2.2.2 when the GM_S value is 0.9 m. It is assumed that the ship also capsizes for lower GM_S values if this damage occurs. In other words, damage case DS/SDSP2.2.2 will not contribute to the A-index when $GM_S \leq 0.9$ m. Furthermore, there is some uncertainty in the range 0.9 - 1.3 m for GM_S, but damage case DS/SDSP2.2.2 will definitely contribute to the A-index for $GM_S \geq 1.3$ m.

The floating positions for the damaged ship, which is illustrated in Appendix S, confirms the development of the equilibrium heel angle in Table 17; for lower GM_S values, the ship will heel more. This development was expected from evaluating the SFAC diagrams; when the heel angle increases, the s_i-factor decreases, and vice versa. This can also be explained by utilizing the formula for $s_{final,i}$. Since the values for GZ_{max} and range never should be taken as larger than 0.12 and 16, respectively, the following occurs for both $GM_S = 1.3$ m and $GM_S = 1.9$ m:

$$s_{final,i} = K \cdot \left[\frac{GZ_{max}}{0.12} \cdot \frac{Range}{16}\right]^{\frac{1}{4}} = K \cdot \left[\frac{0.12}{0.12} \cdot \frac{16}{16}\right]^{\frac{1}{4}} = K$$

It must therefore be the K-value, or more precisely the equilibrium heel angle θ_e, which influences the s_i-factor. Since the ship in this study is considered a passenger ship in the PDS regulations, the following applies for the results presented in Table 17: $\theta_{min} = 7°$ and $\theta_{max} = 15°$.

This leads to:

- For $GM_S = 1.9$ m: $K = 1$, since $\theta_e < \theta_{min}$
- For $GM_S = 1.3$ m: $K = \sqrt{\frac{\theta_{max} - \theta_e}{\theta_{max} - \theta_{min}}} = \sqrt{\frac{15 - 8.8}{15 - 7}} = 0.88$, since $\theta_{min} < \theta_e < \theta_{max}$

Based on the discussion and calculations above, it should be safe to conclude that the heeling moment has a large effect on the s_i-factor for damage case DS/SDSP2.2.2.

- Investigating the s_i-factor for the two-zone damages involving zone 10 and 11:

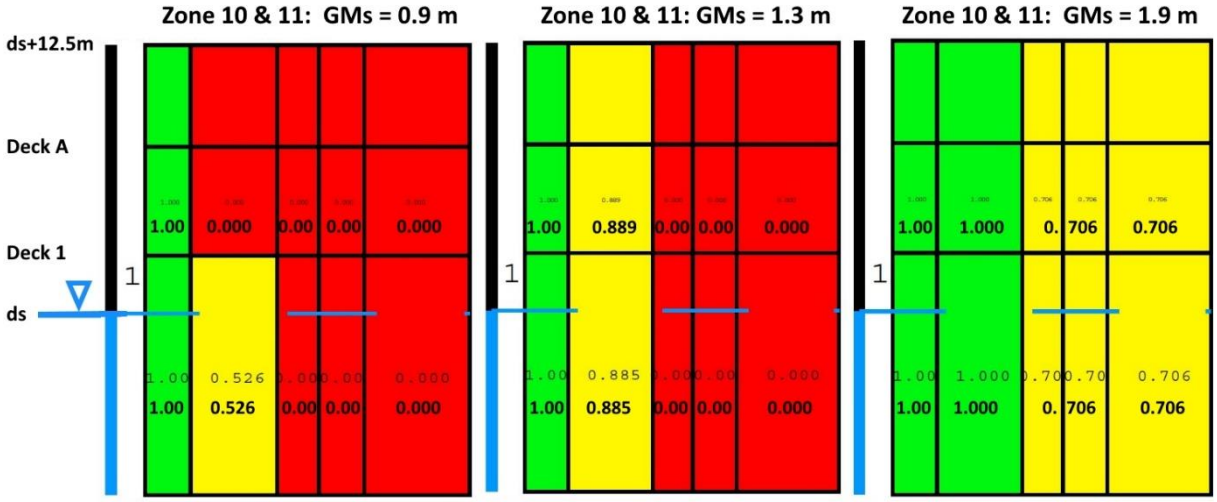

Figure 53. Development of the s_i-factor for two-zone damages involving zone 10 and 11, for loading condition d_S and varying GM_S values.

The same approach used to investigate the s_i-factor in zone 2, is also used to investigate the s_i-factor for the two-zone damages illustrated in Figure 53. The damage case examined is named DS/SDSP10-11.2.3-2 in NAPA, and is furthermore illustrated in Figure 54 and in Appendix R. The PDS calculation results from NAPA that are relevant for the s_i-factor, are presented in Table 18 for each of the selected GM_S values.

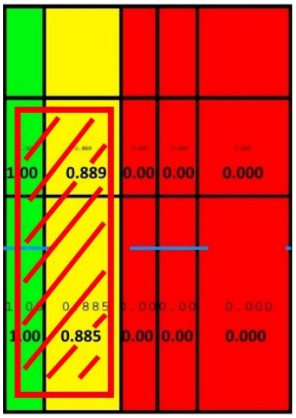

Figure 54. Damage case DS/SDSP10-11.2.3-2.

Table 18. NAPA results for damage case DS/SDSP10-11.2.3-2.

GM_S [m]	s_i-factor	Heel angle θ_e [degrees]	GZ_{max} [m]	Range [degrees]
0.9	0.000	-	-	-
1.3	0.889	8.7	0.49	41.3
1.9	1.000	6.2	0.66	43.8

Similar to the single-zone damage case that was investigated in zone 2, namely DS/SDSP2.2.2, the ship tends to heel less for larger GM_S values. Additionally, the development of the s_i-factor is almost identical for the two damage cases DS/SDSP2.2.2 and DS/SDSP10-11.2.3-2. Furthermore, both the GZ_{max} and Range values for DS/SDSP10-11.2.3-2 are larger than their respective maximum values, with respect to the $s_{final,i}$ calculation. Thus, it is once again the K-value that influences the s_i-factor. In similarity with damage case DS/SDSP2.2.2, K = 1 for GM_S = 1.9 m. In addition, the K-value for GM_S = 1.3 m is approximately in the same order of magnitude as for the two damage cases.

Based on the discussion on both damage case DS/SDSP2.2.2 and damage case DS/SDSP10-11.2.3-2, it seems reasonable to assume that the 'trend' with increasing survivability for larger GM values could be universal. Additionally, it looks like the K-factor, or more specifically the equilibrium heel angle θ_e, is most influential with respect to the s_i-factor. In other words, the heeling moment that occurs when the ship is damaged, has a significant impact on the s_i-factor.

5.2.3 Total A-index

Since both the p_i- and v_i-factors are constant, as mentioned in Sub-section 5.2.1, it is only the s_i-factor that can influence the A-index in this study. Thus, as indirectly stated in the previous sub-section, the 'total' A-index is more or less only dependent on the heeling moment in case of damage. This heeling moment gives the ship a new floating position, i.e. the ship obtains an equilibrium heel angle larger than zero degrees. This heel angle reduces the s_i-factor – the survivability of the ship, which in turn reduces the A-index – the damage stability of the ship.

5.3 Uncertainties

There are naturally uncertainties related to the results of the individual study in this thesis. Sources of uncertainty could for example be limitations, simplifications and assumptions made by the author. Thus, the following question arises: are the results and the post-analysis of the results in this thesis valid, despite of the uncertainties?

It seems reasonable to begin the discussion related to the important question above, with the simplifications made in the ship modelling process in NAPA. In this process, the internal arrangement of the ship was heavily simplified as compared to the original GA drawings from AutoCAD. The CAD-drawing of the simplified GA is the one that is attached to the thesis electronically – a link is provided in Appendix B. Furthermore, the simplification of the arrangement was a measure to save time. The author has been told that this is a standard approach used by ship designers in real life. However, in real-life projects the tank arrangement created in NAPA is a bit more detailed than in this study, and it usually includes more curvatures (Djupvik, 2016). That makes the PDS calculations more time-consuming, but more accurate. Despite this, it is assumed that none of the simplifications made in the arrangement have had any significant effects on the results.

There are some uncertainties connected to the calculations conducted in NAPA, as well. For instance, survival craft moments were neglected in all calculations. The effect of this measure can be seen by looking at Equation 41 and Equation 37 from Sub-section 2.4.7, which are re-presented below, respectively:

$$s_{mom,i} = \frac{(GZ_{max} - 0.04) \cdot Displacement}{M_{heel} = max\left(M_{passenger}, M_{wind}, M_{survivalcraft}\right)} \leq 1$$

$$s_i = min\left[s_{intermediate,i}, (s_{final,i} \cdot s_{mom,i})\right]$$

The results reports from NAPA, which also are attached to the thesis electronically, reveal that the s_i-factors used in the calculations are $s_{final,i}$. Additionally, the author could find no information about $s_{mom,i}$ in NAPA. Thus, supported by the above equation for s_i, the author therefore assumes that $s_{mom,i} = 1$ for the damage cases in this study; i.e. numerator ≥ denominator in the equation for $s_{mom,i}$. Furthermore, since $M_{survivalcraft}$ is ignored in this study, the denominator in the $s_{mom,i}$ equation will take the maximum value of M_{wind} and $M_{passenger}$ in all damage cases. Unless the value of $M_{survivalcraft}$ is significantly larger than the other two heeling moments, neglecting $M_{survivalcraft}$ does not seem to influence the results, because $s_{mom,i} = 1$ in any other case.

The analysis and discussion that the author is most uncertain on, is furthermore related to the v_i-factor in Sub-section 5.1.3, i.e. for objective 1 of the thesis. The plots for the mean v_i-factor development presented in this sub-section, is in fact only valid for the damage cases in a couple of zones within the range of U-deck. It is however assumed that the results will be fairly similar for most of the other zones, within the abovementioned range, but that is not certain. This uncertainty is thus a possible objective for further work related to this thesis.

Another uncertainty related to the v_i-factor analysis in Sub-section 5.1.3, is that only the damage cases closest to the hull are investigated. Based on the author's understanding of the PDS regulations, the v_i-factor for U-deck will not contribute to the A-index for damages that breaches the first longitudinal bulkhead (LBH) both below and above U-deck. There are however other damage cases where the v_i-factor will contribute to the A-index, for the latter scenario, when U-deck is placed higher than d_L = 4.4 m. These damages breach the first LBH below U-deck only. In that case, according to the above sense of logic, the v_i-factor for U-deck will contribute to the A-index. In other words, the v_i-factor for U-deck also contributes to the A-index for damage cases that penetrates the first – and perhaps the second – LBH. Thus, any conclusions drawn related to the v_i-factor for objective 1 in this study, might not be valid for damage cases that penetrate LBHs. These cases and damage cases in other zones where the arrangement is slightly different, are potential research objectives for further work related to changes in v_i-factor for different U-deck heights.

A third uncertainty related to the v_i-factor discussion, is the potential contribution from deck 2 within the range of U-deck. It has been assumed that deck 2 does not influence the v_i-factor in any damage cases within this range, since deck 2 never is placed higher than d_L = 4.4 m above the baseline. As mentioned in Sub-section 5.1.3, deck 2 must according to the author's understanding be placed higher than the lowest waterline in order to contribute to the v_i-factor in any damage case. The formulations in the PDS regulations are not clear on this matter, and neither are the instructions in the NAPA for Design Manuals. However, if deck 2 contributes, it is only for the light service draught d_L, which in turn only contributes 20% to the A-index. Thus, the influence is either way considered not to be of significance; the conclusions made in Section 5.1 will not be altered by this potentially wrong assumption made by the author.

Obviously, there are a number of uncertainties related to this study. However, based on the above discussion, the author would like to conclude that none of the uncertainties is of a size that threatens the validity of the results – or the conclusions made in the analysis and discussion chapter.

6. Conclusion

This master's thesis investigates how changes in size of the wing ballast tanks and changes in the initial GM values, for a WFSV designed by Salt Ship Design, influences the A-index. The presentation of results, along with the analysis and discussion of these results, are based on PDS calculations conducted in NAPA.

The results for objective 1 show that the A-index generally increases for larger U-deck heights, all the way up to 5.6 m above the baseline. Thus it can be concluded that the height of U-deck certainly influences the A-index, whereas positively when the height is increased up to 5.6 m. It is not considered realistic to place U-deck above this height, considering that the wing ballast tanks should have room for a sufficient amount of ballast water. The main contributions to the A-index come from the s_i-factor, most likely due to heeling moments that causes changes in the equilibrium heel angle. However, the v_i-factor is also influential, but the impact is not as consistent for all U-deck heights as compared to the s_i-factor. The p_i-factor does not contribute to changes in A-index for objective 1, since changes to the arrangement only are made in vertical direction.

For objective 2, no changes are made to the arrangement of the ship in question. The selected U-deck height for the study is 4.4 m, because of the corresponding trade-off between sufficient A-index and sufficiently large wing ballast tanks is considered to be beneficial. Furthermore, the results of the study reveal that the A-index increases almost proportionally with the GM values, i.e. the A-index curve behaves linearly. Additionally, it can be concluded that GM values around 1 m are critical with respect to the A-index, while GM values lower than this will result in an A-index which does not meet the 'PDS criterion', i.e. A > R. The only factor that contributes to changes in A-index, when varying the initial GM values for the ship, is the s_i-factor; in such cases the A-index is heavily dependent on the heeling moment caused by potential damage. The heeling moment causes a change in equilibrium heel angle, which in turn affects the s_i-factor. I.e., when the initial GM values are increased, the heeling moment in case of damage decreases. The s_i-factor thus increases and, consequently, the A-index is improved. Neither of the p_i- or v_i-factors influence the changes in A-index in the study related to objective 2, because there are no changes in the arrangement.

6.1 Uncertainties

The most important uncertainties related to the studies conducted, were discussed in Section 5.3. As the reader might have noticed, none of the uncertainties, except for the arrangement simplifications, were related to objective 2 of the thesis. This is because the only possible uncertainties regarding objective 2 would be related to the s_i-factor. For the s_i-factor, the analysis tools in NAPA make the results more transparent, as compared to the p_i- and v_i-factor. The development of the s_i-factor for different GM values was clear, as mentioned introductorily in this chapter: the s_i-factor changes when the heeling moment changes; a larger heeling moment causes a reduction in the s_i-factor. In other words, there are no uncertainties related to objective 2 that threaten the validity of the results, the analysis and discussion of the results, or conclusions drawn.

For objective 1, there are a few uncertainties related to the analysis of the results. The results themselves should be correct; the A-index decreases when the U-deck height is lowered beneath 5.6 m, which is considered realistic. The uncertainties discussed in Section 5.3 are mainly related to further work; investigations related to these uncertainties could be done in order to further raise the confidence level on the conclusions made for objective 1.

6.2 Key Findings

The goal of the thesis is to contribute with more insight as to how changes made in the arrangement and intact stability of offshore vessels impact the A-index. In order to achieve this goal, the produced results were analysed in-depth and conclusions have been based on discussion regarding these results. Arguably, this is done successfully; the results and conclusions are not valid for all offshore vessels, but they are assumed to be valid for offshore vessels with fairly similar arrangements as the WFSV used in this study. Finally, the key findings in this thesis are:

- The A-index does in general obtain a larger value when the size of the wing ballast tanks is reduced – to a certain extent; when U-deck is placed above 5.6 m for the WFSV, the A-index will not be improved anymore. However, it is not considered relevant to install smaller wing ballast tanks than the size corresponding to this U-deck height.
- The A-index is generally better for larger initial GM values, because the increase in GM values results in smaller heeling moments in case of damage.

6.3 Further Work

- Some suggestions to further work are already mentioned in Section 5.3, where uncertainties related to this study were discussed. For instance, there are uncertainties related to the analysis of the v_i-factor for objective 1 of the thesis. In order to increase the reliability of the results for the v_i-factor development, for different U-deck heights, the following could be done:
  - Investigate more damage zones in general; and
  - Investigate damage cases penetrating longitudinal bulkheads within each zone.
- Additionally, it could be investigated as to why the A_S-index is most critical in the study conducted for objective 2, while the A_L-index seems to be most critical for objective 1.
- Furthermore, the studies carried out for objective 1 and 2 in this thesis, could be carried out for other types of offshore vessels as well. This would provide more generic results which, consequently, could lead to conclusions valid for a wider range of vessels.

7. Bibliography

DELFTship. Single and Multizone Damages. In probabilistic-damage-stability_zone-damage.png (Ed.): DELFTship.

Djupvik, O. M. (2015). [Phone conversation with Ole Martin Djupvik, 'Naval Architect' at Wärtsilä Ship Design (previously)/Salt Ship Design (from 2016 and onwards)].

Djupvik, O. M. (2016). [Phone and email conversations with Ole Martin Djupvik, 'Naval Architect' at Salt Ship Design (from 2016 and onwards)].

Djupvik, O. M., Aanondsen, S. A., & Asbjørnslett, B. E. (2015). Probabilistic Damage Stability - Maximizing the Attained Index by Analyzing the Effects of Changes in the Arrangement for Offshore Vessels: NTNU.

Eklund, R., & Lindroth, D. (2009). *Workshop N2 - Damage Stability According to SOLAS 2009, NAPA User Meeting 2009*. NAPA Ltd.

Hjort, G. (2015). [Email correspondence with Gunnar Hjort, Principal Approval Engineer, Stability section, DNV GL].

Hjort, G., & Olufsen, O. (2014). Probabilistic damage stability: DNV GL AS.

IMO. (1966). Load Lines, 1966/1988 - International Convention on Load Lines, 1966, as Amended by the Protocol of 1988 - Articles of the International

Convention on Load Lines, 1966 - Article 2 - Definitions In I. M. Organization (Ed.).

IMO. (2006). SOLAS Chapter II-1 Construction - structure, Subdivision and Stability, Machinery and Electrical Installations, Part B-1 Stability.: International Maritime Organization.

IMO. (2008a). International Code on Intact Stability (2008 IS Code): International Maritime Organization.

IMO. (2008b). Resolution MSC.266(84) - Code of safety for special purpose ships, 2008: International Maritime Organization.

IMO. (2008c). Resolution MSC.281(85), Explanatory notes to the SOLAS Chapter II-1, Subdivision and damage stability regulations, Part B.: International Maritime Organization.

Kirchsteiger, C. (1999). On the use of probabilistic and deterministic methods in risk analysis. *Journal of Loss Prevention in the Process Industries, 12*(5), 399-419. doi: 10.1016/S0950-4230(99)00012-1

Lützen, M. (2001). *PhD thesis: Ship Collision Damage.*, Lyngby, Denmark.

Magnussen, E., Amdahl, J., & Fuglerud, G. (2014). *Marin teknikk grunnlag : TMR4105 : kompendium* (5. utg. ed.). Trondheim: Akademika forlag Kompendieforlaget.

MCA. (1998). MSN 1698 (M) - The Merchant Shipping (Passenger Ship Construction: Ships of Classes I, II and II(A)) Regulations 1998: Maritime and Coastguard Agency (MCA).

NAPA. (2015). NAPA for Design Manuals 2015.3.

Papanikolaou, A., & Eliopoulou, E. (2008). On the development of the new harmonised damage stability regulations for dry cargo and passenger ships. *Reliability Engineering and System Safety*, *93*(9), 1305-1316. doi: 10.1016/j.ress.2007.07.009

Patterson, C. J., & Ridley, J. D. (2014). *Ship stability, powering and resistance* (Vol. 13). London: Adlard Coles Nautical.

Puisa, R., Tsakalakis, N., & Vassalos, D. (2012). Reducing Uncertainty in Subdivision Optimization. *Journal of Shipping and Ocean Engineering 2*.

Puustinen, O. (2012). Workshop 7, FAQ in NAPA Damage Stability. In N. Ltd. (Ed.): NAPA.

Ravn, E. S. (February 2003). *Probabilistic Damage Stability of Ro-Ro Ships.* (PhD Thesis), Technical University of Denmark, Denmark.

Vassalos, D. (2014). Damage stability and survivability – 'nailing' passenger ship safety problems. *Ships and Offshore Structures*, *9*(3), 237-256. doi: 10.1080/17445302.2013.780397

Wärtsilä. Damage stability calculations. In f62e80491998c3f2a37e620b5dd160668285bc88 (Ed.). Encyclopedia of Ship Technology by Wärtsilä: http://www.shippingencyclopedia.com/term/damage-stability-calculations: Wärtsilä.

List of Appendices

Appendix A – How p_i is calculated for multi-zone damages

According to SOLAS Chapter II-1, Part B-1, Regulation 7-1, the below equations should be used to calculate the p_i-factor in case of multi-zone damages (IMO, 2006).

- If the damage involves two adjacent zones:

$$p_i = p\,(x1_j, x2_{j+1}) \cdot [r(x1_j, x2_{j+1}, b_k) - r(x1_j, x2_{j+1}, b_{k-1})]$$

$$- \; p\,(x1_j, x2_j) \cdot [r(x1_j, x2_j, b_k) - r(x1_j, x2_j, b_{k-1})]$$

$$- \; p\,(x1_{j+1}, x2_{j+1}) \cdot [r(x1_{j+1}, x2_{j+1}, b_k) - r(x1_{j+1}, x2_{j+1}, b_{k-1})]$$

- If the damage involves three or more adjacent zones:

$$\begin{aligned} p_i = {} & p(x1_j, x2_{j+n-1}) \cdot [r(x1_j, x2_{j+n-1}, b_k) - r(x1_j, x2_{j+n-1}, b_{k-1})] \\ & - p(x1_j, x2_{j+n-2}) \cdot [r(x1_j, x2_{j+n-2}, b_k) - r(x1_j, x2_{j+n-2}, b_{k-1})] \\ & - p(x1_{j+1}, x2_{j+n-1}) \cdot [r(x1_{j+1}, x2_{j+n-1}, b_k) - r(x1_{j+1}, x2_{j+n-1}, b_{k-1})] \\ & + p(x1_{j+1}, x2_{j+n-2}) \cdot [r(x1_{j+1}, x2_{j+n-2}, b_k) - r(x1_{j+1}, x2_{j+n-2}, b_{k-1})] \end{aligned}$$

and where $r(x1, x2, b_0) = 0$

Appendix B – Electronic files

The electronic files attached to this master's thesis are:

- Simplified GA drawings from AutoCAD, for the generic ship model used in this study. These drawings do not represent the authentic vessel designed by Salt Ship Design.
- NAPA results report from all PDS calculations, for both objectives of the thesis.
- The author's poster contribution to the Master Poster Exhibition at the Department of Marine Technology, NTNU, in the spring semester of 2016.

The electronic files can be found by clicking on the following link https://daim.idi.ntnu.no/soek and searching for the title of this thesis or name of the thesis' author, for instance.

Appendix C – Modelling of ship arrangement in NAPA

In the NAPA stability software, the traditional way to model the ship's arrangement is by using the 'Text Editor' tool. This method provides the possibility to organise the coding in separate text files. Examples of names of such text files used in the master's thesis are 'Decks', 'Tanks', 'Tankplan', 'Damcomp' and 'Stabhull'. There are several other text files in a 'real-life project', and it is left to the user to define the names, do all the coding and organise the coding in appropriate files. A 'room' as defined by the Text Editor, i.e. tanks and rooms, is referred to as a compartment. For any type of compartment, the coding syntax is similar. This is illustrated in the below figure. Their respective codes are located in different text files, however.

```
!end;def
room C20 'Engine room'
lim #38 #74 0 5.4 ttop 1dk
add #28 #38 0 1.8 ttop 2dk
add #74 #82 0 1.2 ttop 2dk
add #50 #60 0 3 2dk bdk
sym
ok
```

```
!end;def
room 11p 'WB'
lim #90 #99 -hull -lbh1 ttop 2dk >thr1f >thr2f
ok

!end;def
room 12s 'Fresh water'
lim #82 #90 lbh1 hull ttop 1dk
ok
```

All compartments must be added to the 'Arrangement Table' in NAPA. If this is not done, the compartments will not be included in the calculations. The only user input here is the name of the compartment that has already been defined in the text file, as well as the 'purpose description' of the compartment like for instance 'Water ballast', 'Accommodation' or 'Fuel oil'. The 'purpose description' automatically defines the permeability of the compartment. These are pre-set standard values in NAPA. Additionally, information such as location of the compartment relative to the reference system, density of the content of the compartment and volume of the compartment are filled in automatically. With this information given, NAPA also calculates the mass attached to each compartment.

Especially the volume of the compartments is useful information; if this value is zero, then the user can be certain that an error has been made. Most likely this error comes from the coding, i.e. definition of the compartment in the text file, or maybe the decks or the hull of the ship is defined wrongly in their respective text files.

The final watertight arrangement modelled in NAPA is presented in the figures below. In respective order, the figures show: the ship in profile view, 'A-deck', '1-deck', '2-deck', 'Tank top' and 'Baseline'. The colour codes are explained in table that follows after the figures.

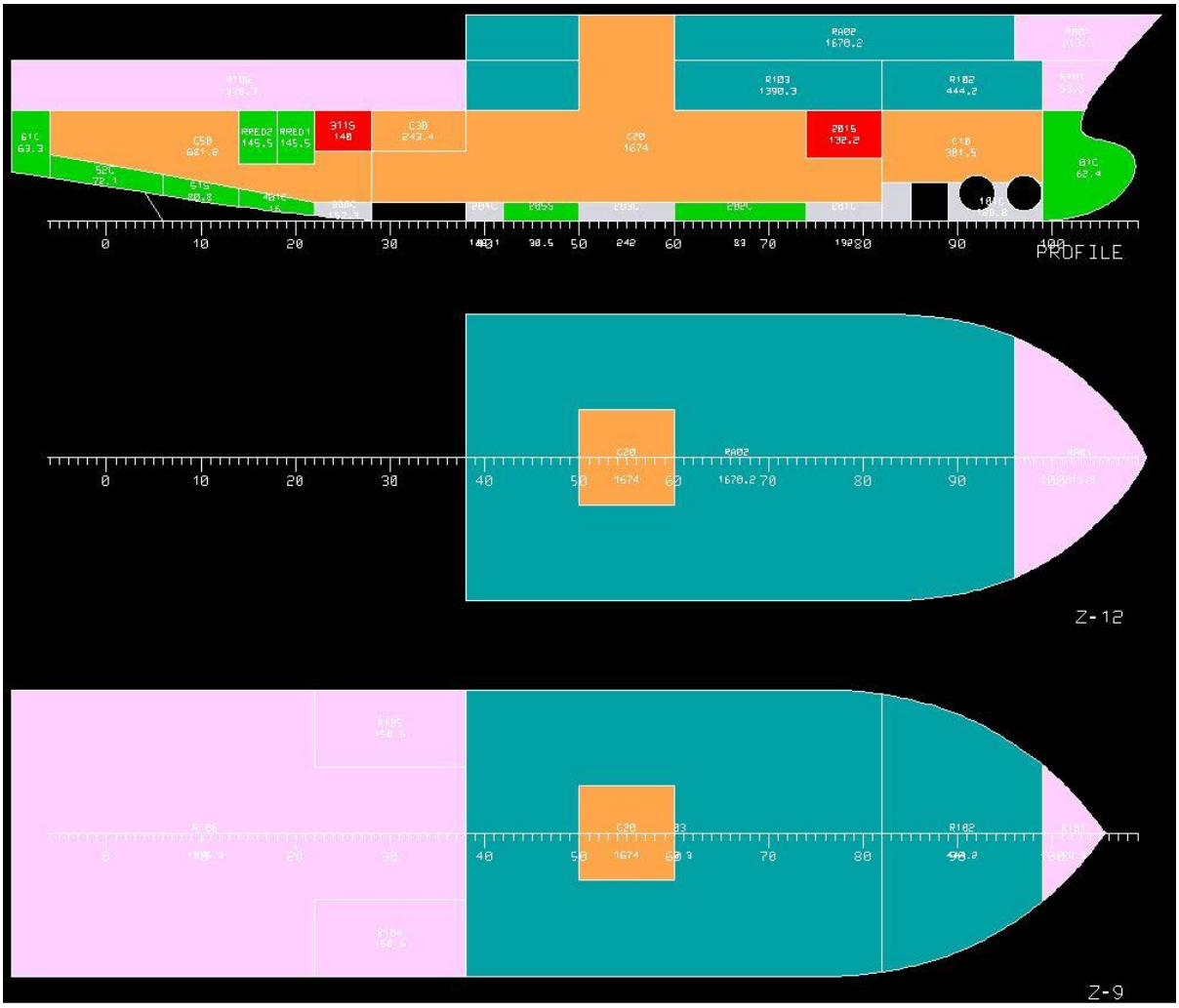
PROFILE
Z-12
Z-9


Z-6.5

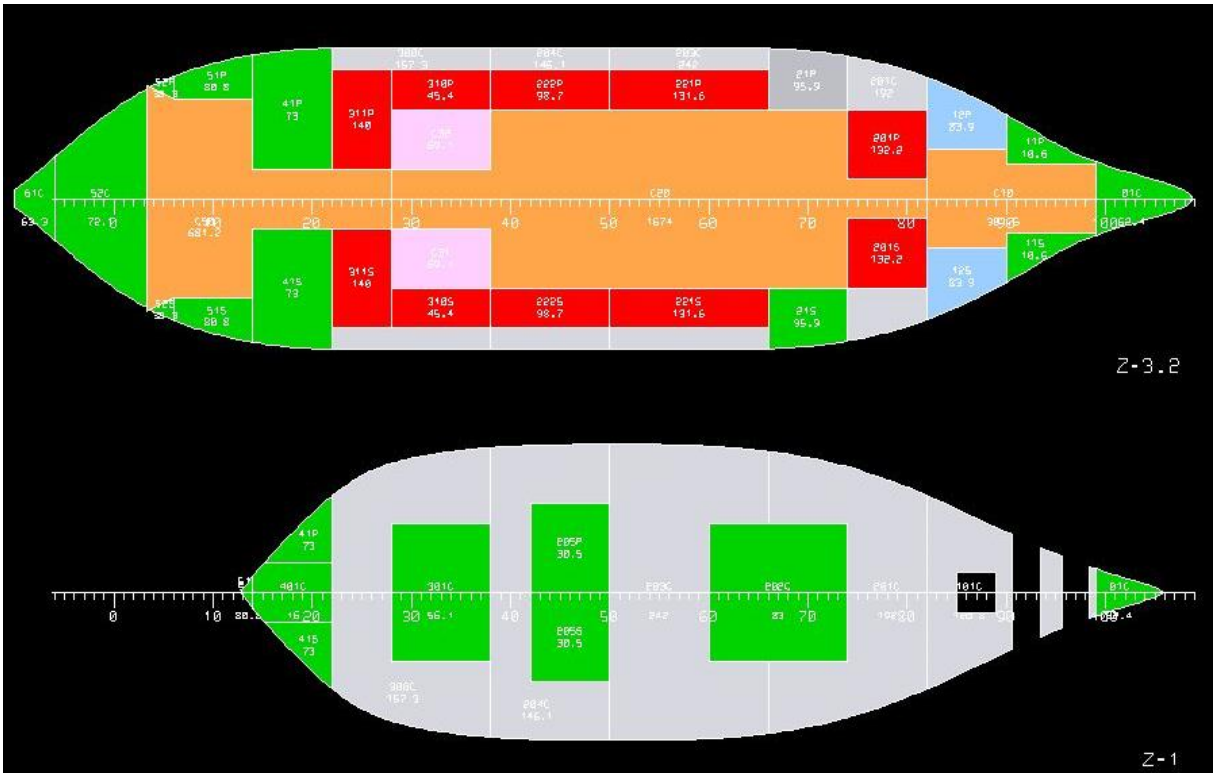

Colour code of compartment	Purpose description
Light grey	Void space
Dark grey	Sewage (Grey water) tanks
Green	Water ballast and roll-reduction tanks
Gold	Machinery spaces
Red	Fuel oil (MDO) tanks
Light blue	Fresh water tanks
Pink	Storage
Turquoise	Accommodation

Appendix D – The ship's buoyant hull created in NAPA

The buoyant hull of the ship, or 'DAMHULL' as it is named in the NAPA text files, is presented in the figure below.

STIAN
Napa Oy
USER SRS

2016-05-03
15:07
Page 11

GENERAL DATA

BUOYANT HULL

Name of buoyant hull: DAMHULL
Date of buoyant hull: 2016-05-03

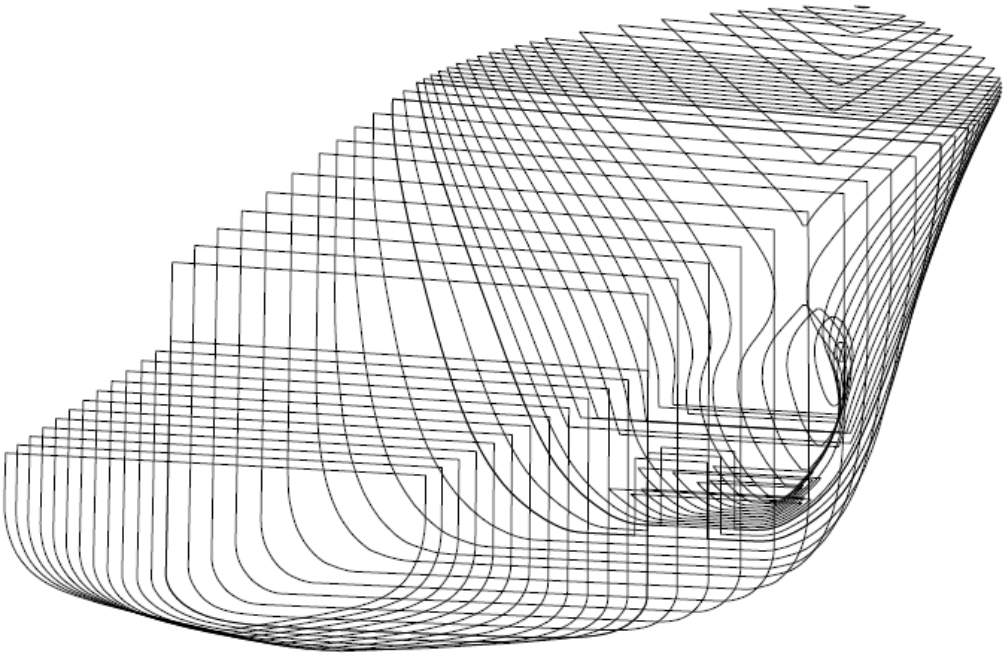

Description of DAMHULL:

ROOM DAMHULL
LIM <STABHULL

Appendix E – Simplification of GA in NAPA

The below figure, which is drawn in AutoCAD, illustrates how the arrangement of the ship is simplified in NAPA in order to save some valuable computation time; the above illustration represents of course the simplified arrangement.

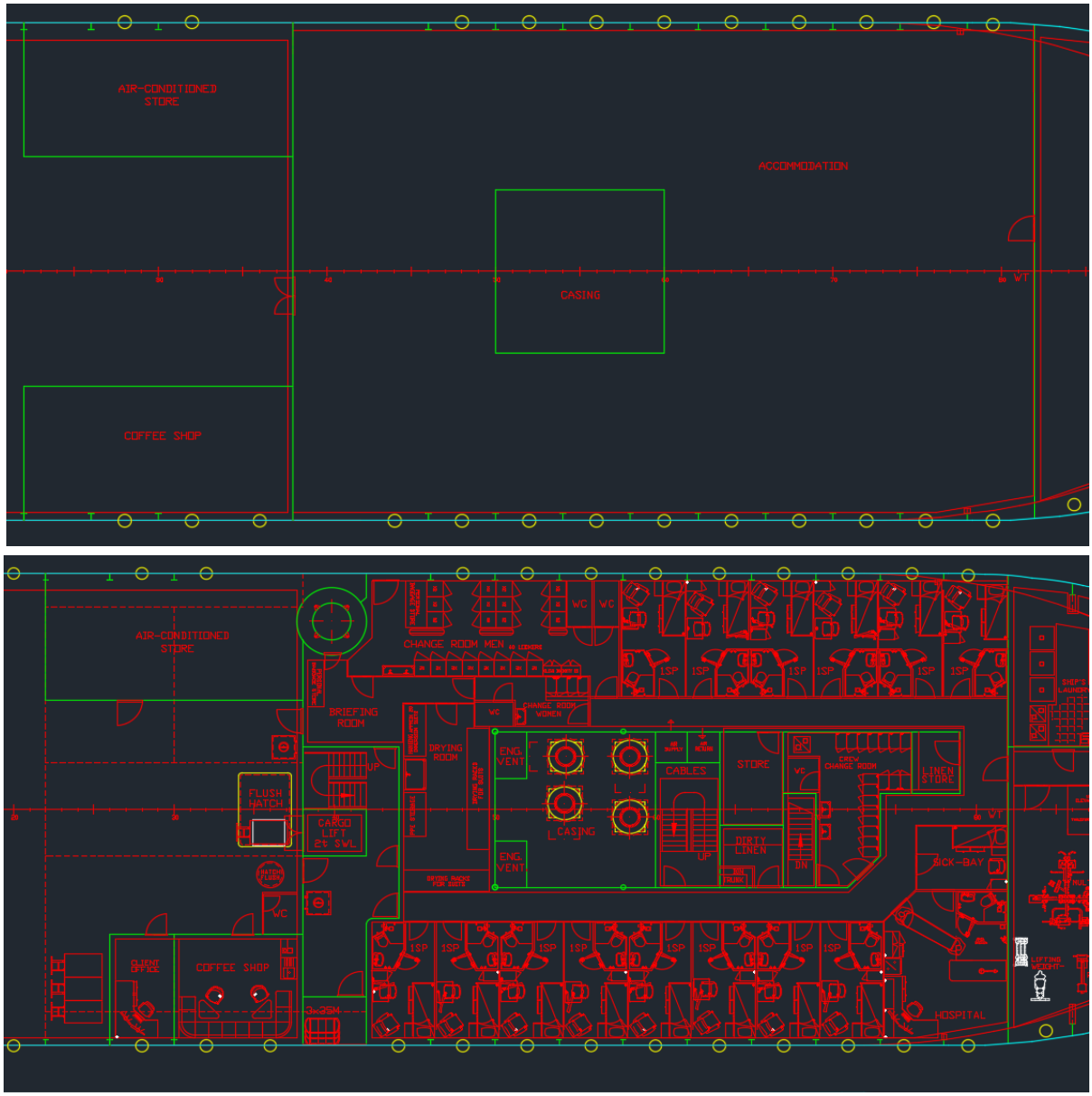

Appendix F – Reduction of curvatures in NAPA

The below figure illustrates how curvatures are replaced with straight lines in NAPA, as an attempt to save some valuable computation time. The drawing is made with AutoCAD.

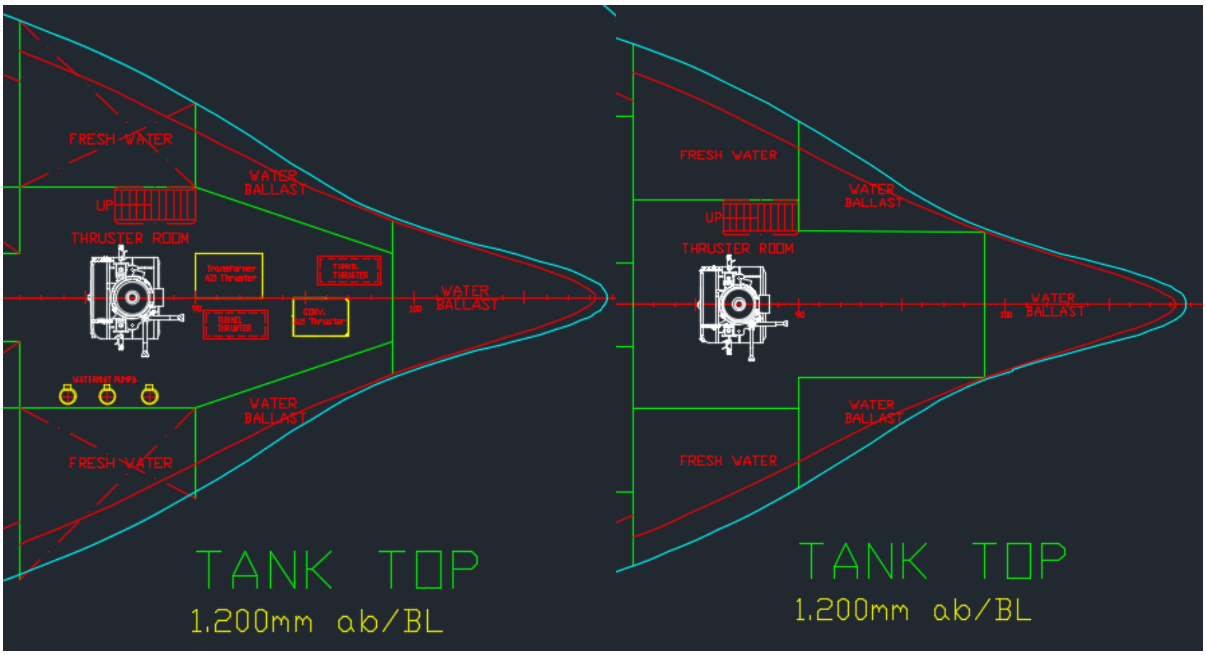

Appendix G – Permeability values in NAPA

The below table includes some key permeability values for the study in this master's thesis. The values are default in NAPA.

Permeability values for certain compartments in NAPA.

Compartment purpose	Permeability value
Void spaces	0.95
Water ballast tanks	0.95
Fuel oil (MDO) tanks	0.85
Sewage and fresh water tanks	0.95
Machinery spaces	0.85
Accommodation, storage, workshops etc.	0.95

Appendix H – Subdivision data output: Subdivision drawing

The below figure is the subdivision illustration, or the output, from the input in the subdivision table in NAPA. The input is presented in Appendix I. The subdivision drawing from NAPA thus illustrates the subdivision of damage zones of the ship, in longitudinal, transverse and vertical direction.

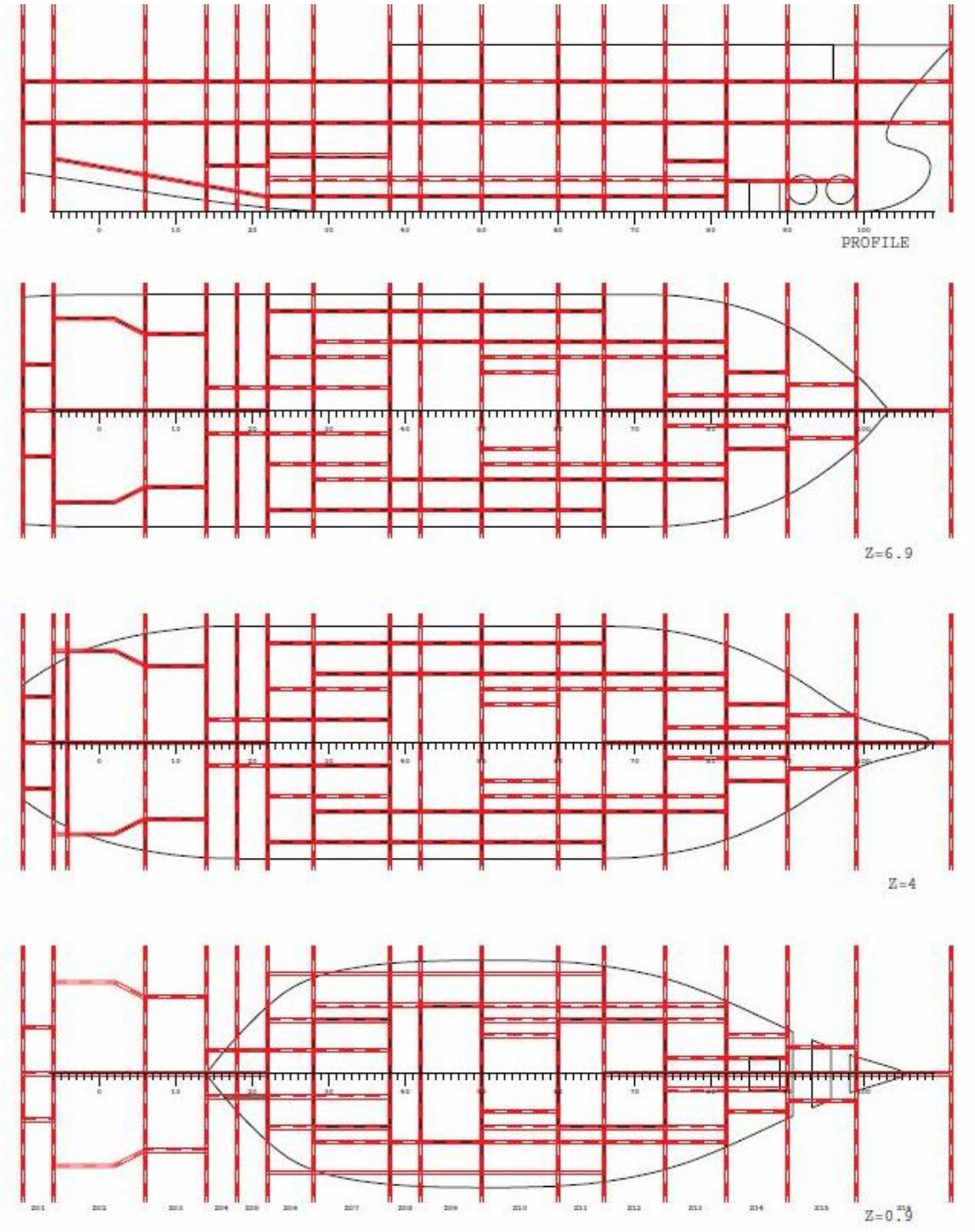

Subdivision of the ship used in the study, as illustrated in the NAPA results report.

Appendix I – Subdivision data input

As explained in Sub-section 3.5.4 and shown in the figure below, the subdivision is done in a table editor tool in NAPA and is mainly user input.

	ZONE	Aft Limit	Fwd Limit	PS Limit	SB Limit	Deck Lower	Deck Upper
1	Z01	-6	#-6	-3.6/0	3.6/0		1DK/ADK
2	Z02	#-6	#6	LBH4P/0	LBH4/0	TTOP	1DK/ADK
3	Z03	#6	#14	LBH4P/0	LBH4/0	TTOP	1DK/ADK
4	Z04	#14	#18	-1.8/0	1.8/0	TTOP/2DK	1DK/ADK
5	Z05	#18	#22	-1.8/0	1.8/0	TTOP/2DK	1DK/ADK
6	Z06	#22	#28	-7.8/-4.2/-1.8	7.8/4.2/1.8	TTOP/UDK/2DK	1DK/ADK
7	Z07	#28	#38	-7.8/-5.4/-4.2/-1.8	7.8/5.4/4.2/1.8	TTOP/UDK/2DK	1DK/ADK
8	Z08	#38	#42	-7.8/-5.4	7.8/5.4	TTOP/UDK	1DK/ADK
9	Z09	#42	#50	-7.8/-5.4	7.8/5.4	TTOP/UDK	1DK/ADK
10	Z10	#50	#60	-7.8/-5.4/-4.2/-3.0	7.8/5.4/4.2/3.0	TTOP/UDK	1DK/ADK
11	Z11	#60	#66	-7.8/-5.4/-4.2	7.8/5.4/4.2	TTOP/UDK	1DK/ADK
12	Z12	#66	#74	-5.4/-4.2/0	5.4/4.2/0	TTOP/UDK	1DK/ADK
13	Z13	#74	#82	-5.4/-4.2/-1.2/0	5.4/4.2/1.2/0	TTOP/2DK/UDK	1DK/ADK
14	Z14	#82	#90	LBH1P/-1.2/0	LBH1/1.2/0	TTOP	1DK/ADK
15	Z15	#90	#99	LBH1P/0	LBH1/0	TTOP	1DK/ADK
16	Z16	#99	DAMHULL	0	0		1DK/ADK

Subdivision table in NAPA.

'PS Limit' – port side boundaries and 'SB Limit' – starboard boundaries define the boundaries that goes in longitudinal direction and, thus, also the penetration depth b for the calculation of the p(x1,x2,b) factor. The distance b from the hull to a longitudinal boundary can be found in the 'BP' and 'BS' columns from the output subdivision table, which can be seen in Appendix J. NAPA calculates the b value according to SOLAS Resolution MSC.281(85) – Explanatory Notes. Examples of how this is done are shown in the figure below.

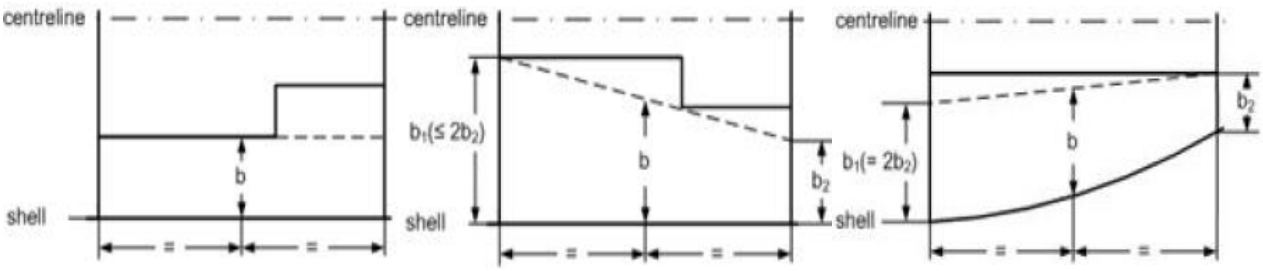

Calculation of the penetration depth b according to SOLAS.
The illustration is adapted from SOLAS Resolution MSC.281(85) (IMO, 2008c).

Furthermore, it is of high importance to get the horizontal subdivision correct in NAPA; the insertion of the deck as a horizontal boundary in the subdivision table depends on whether the deck height is higher than the lightest subdivision draught or whether it is lower than the deepest subdivision draught, or neither. In the first case, the deck should be listed in the 'Deck Upper' column as shown in, as shown in the first figure on the previous page. In the second case, it should be listed in the 'Deck Lower' column. In the third case, it should not be listed.

The below figure then exemplifies how the values that should be inserted in the columns 'Deck Lower' and 'Deck Upper' are obtained for zone 7 of the ship used in this study. A 'zone' in this context is normally referred to as a 'longitudinal zone' when discussing PDS calculations (NAPA, 2015). In other words, a zone is defined by transverse bulkheads. The abovementioned approach is the same for any zone.

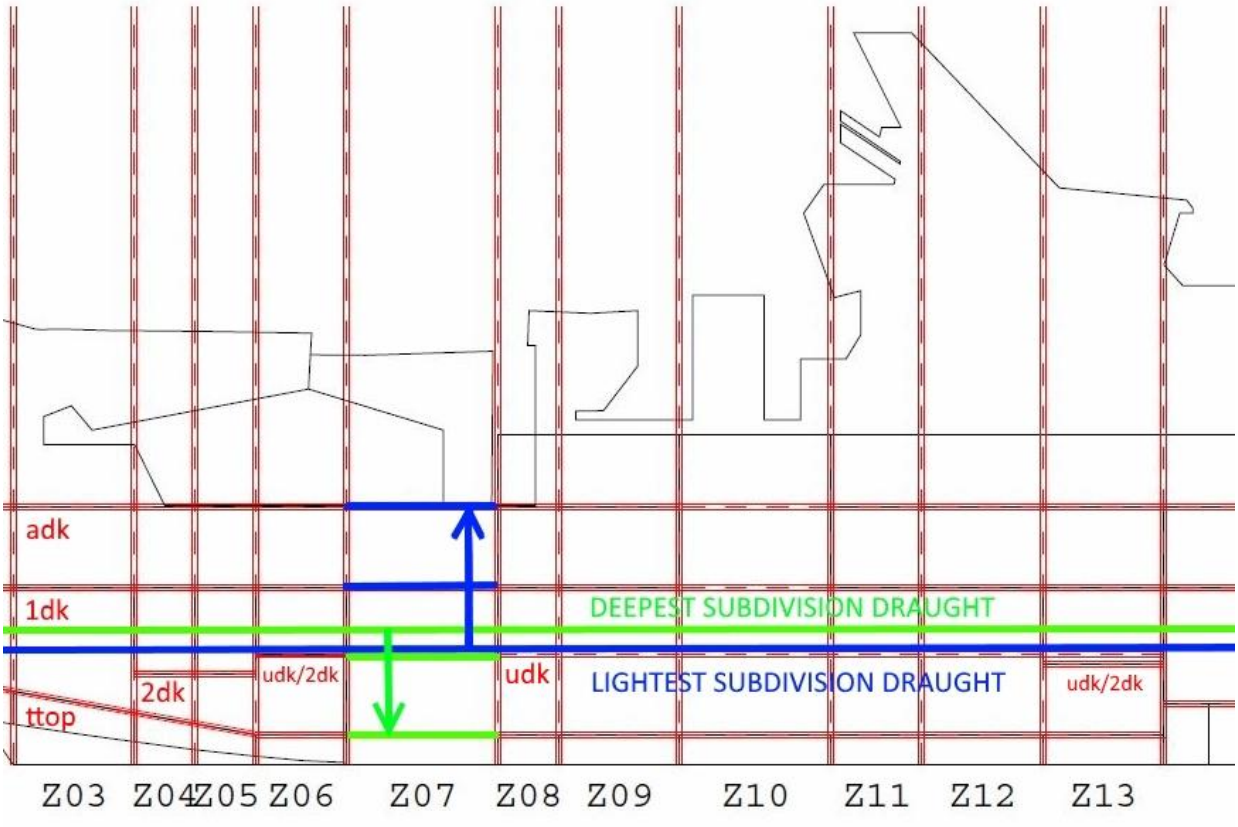

Decks as horizontal subdivision limits. The figure is inspired by the NAPA manuals, p. 5402 (NAPA, 2015).

Appendix J – Subdivision data output: Subdivision table

The figure, or table, below is the subdivision table that NAPA presents in the results report in the Probabilistic Manager.

STIAN 2016-05-02
Napa Oy 18:41
USER SRS Page 18

ZONE	X1 m	X2 m	BP	BS	HHSD
Z01	-6.0	-3.6	4.539/8.139	4.539/8.139	-
Z02	-3.6	3.6	1.62/8.82	1.62/8.82	4.187
Z03	3.6	8.4	3.1/9.1	3.1/9.1	2.906
Z04	8.4	10.8	7.3/9.1	7.3/9.1	2.053/3.6
Z05	10.8	13.2	7.3/9.1	7.3/9.1	1.624/3.6
Z06	13.2	16.8	1.3/4.9/7.3	1.3/4.9/7.3	1.2/4.4/4.6
Z07	16.8	22.8	1.3/3.7/4.9/7.3	1.3/3.7/4.9/7.3	1.2/4.4/4.6
Z08	22.8	25.2	1.3/3.7	1.3/3.7	1.2/4.6
Z09	25.2	30.0	1.3/3.7	1.3/3.7	1.2/4.6
Z10	30.0	36.0	1.3/3.7/4.9/6.1	1.3/3.7/4.9/6.1	1.2/4.6
Z11	36.0	39.6	1.3/3.7/4.9	1.3/3.7/4.9	1.2/4.6
Z12	39.6	44.4	3.693/4.893/9.093	3.693/4.893/9.093	1.2/4.6
Z13	44.4	49.2	3.205/4.405/7.405/8.605	3.205/4.405/7.405/8.605	1.2/4/4.6
Z14	49.2	54.0	4.158/5.958/7.158	4.158/5.958/7.158	2.4
Z15	54.0	59.4	0.189/3.339	0.189/3.339	2.4
Z16	59.4	66.9	0	0	-

ZONE	HHSU
Z01	7/10.2
Z02	7/10.2
Z03	7/10.2
Z04	7/10.2
Z05	7/10.2
Z06	4.6/7/10.2
Z07	4.6/7/10.2
Z08	4.6/7/10.2
Z09	4.6/7/10.2
Z10	4.6/7/10.2
Z11	4.6/7/10.2
Z12	4.6/7/10.2
Z13	4.6/7/10.2
Z14	7/10.2
Z15	7/10.2
Z16	7/10.2

Appendix K – R-index calculated in NAPA

The calculation of the R-index is the same for any arrangement configuration or for any GM values, i.e. it is the same for objective 1 and 2 in this study, since the relevant formula only is dependent on the subdivision length and the number of persons on board. The value for the R-index obtained in NAPA is highlighted with a yellow colour below.

STIAN 2016-05-03
Napa Oy 18:45
USER SRS Page 6

INDEX SUMMARY

TRIM 0

ATTAINED AND REQUIRED SUBDIVISION INDEX

Subdivision length	72.924 m
Breadth at the load line	18.208 m
Breadth at the bulkhead deck	18.201 m
Number of persons N1	0
Number of persons N2	60

Required subdivision index R = 0.54356

Attained subdivision index A = 0.59105

INIT	T m	GM m	A/R	A	A*WCOEF	WCOEF
DL	4.400	1.000	1.05	0.57227	0.11445	0.200
DP	4.940	1.100	1.07	0.57899	0.23160	0.400
DS	5.300	1.300	1.13	0.61250	0.24500	0.400

Appendix L – How SFAC diagrams develop with the draught

As the following three figures show, the survivability factor s_i is generally more critical for lower subdivision draughts in this study. This is probably a result of the GM values corresponding to the subdivision draughts: the KG value for d_L is higher than the KG values for d_P and d_S. As expected, a higher KG leads to a lower GM, which furthermore seems to have a negative effect on the A-index.

- SFAC diagram for the light service draught, with U-deck height 2.6 m:

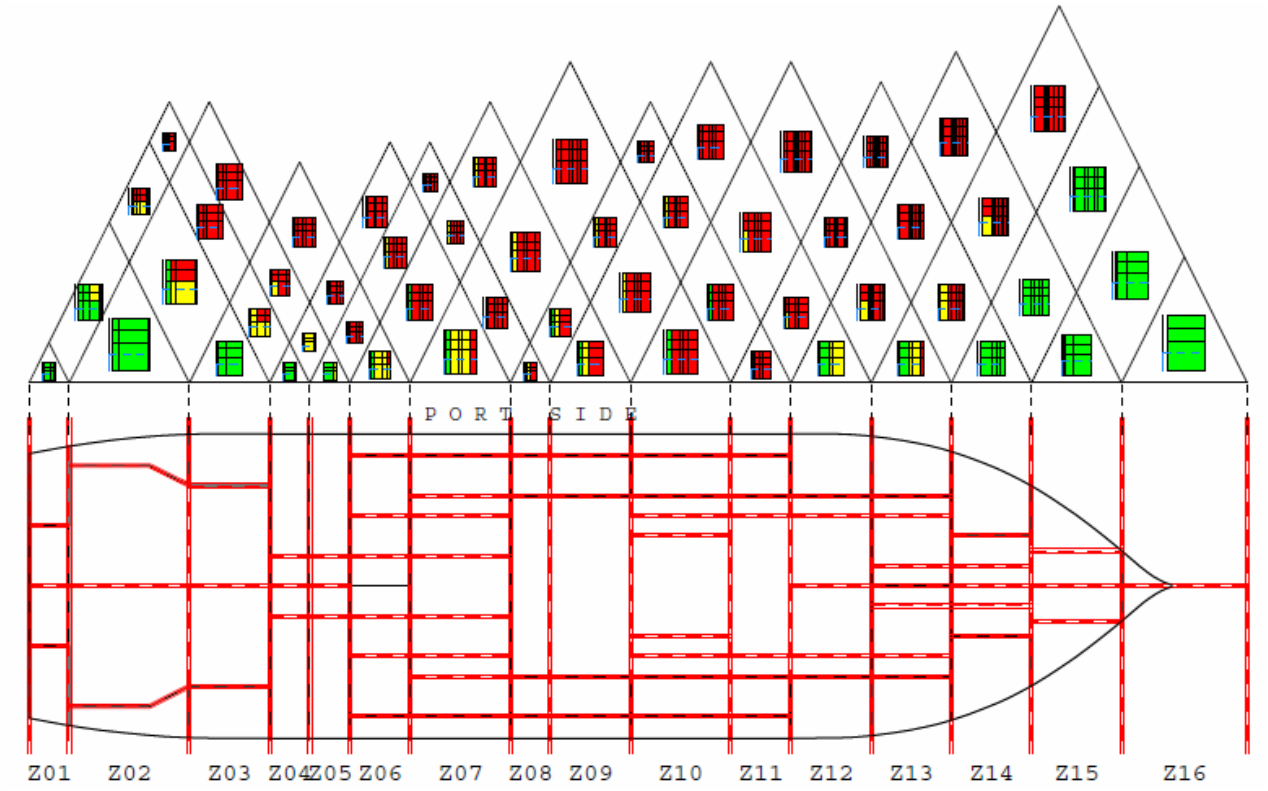

- SFAC diagram for the partial subdivision draught, with U-deck height 2.6 m:

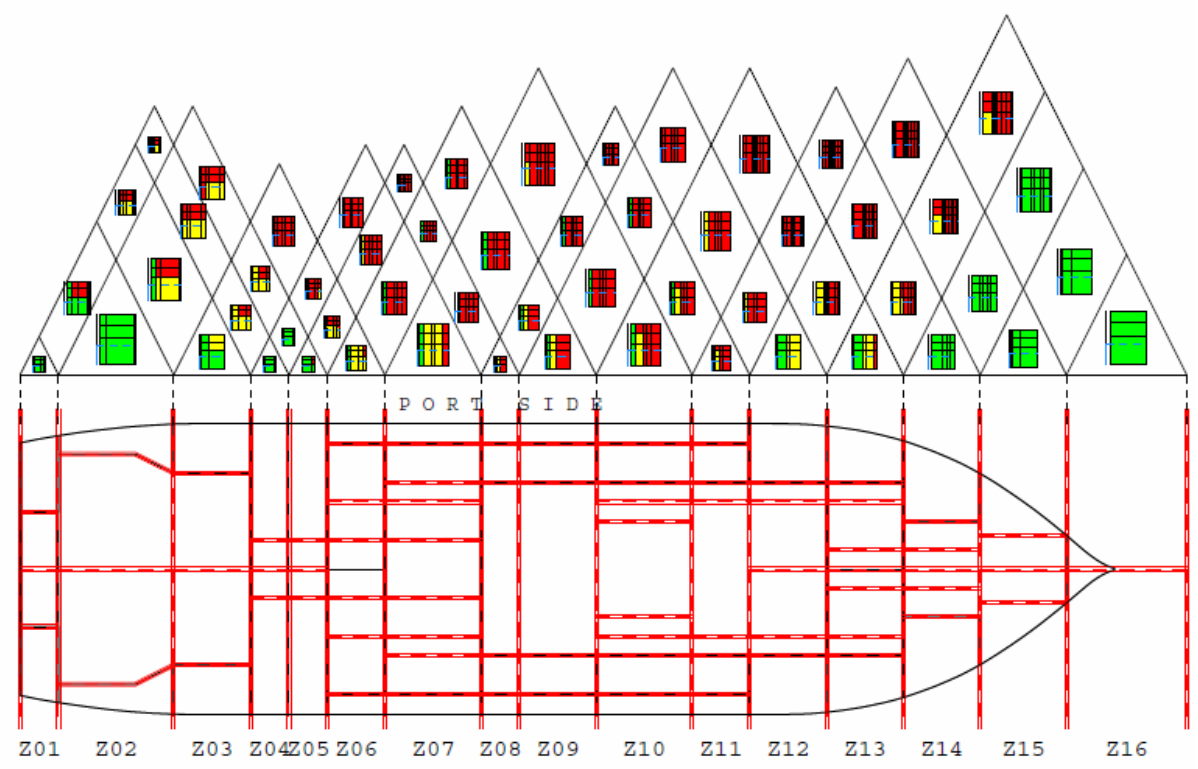

- SFAC diagram for the deepest subdivision draught, with U-deck height 2.6 m:

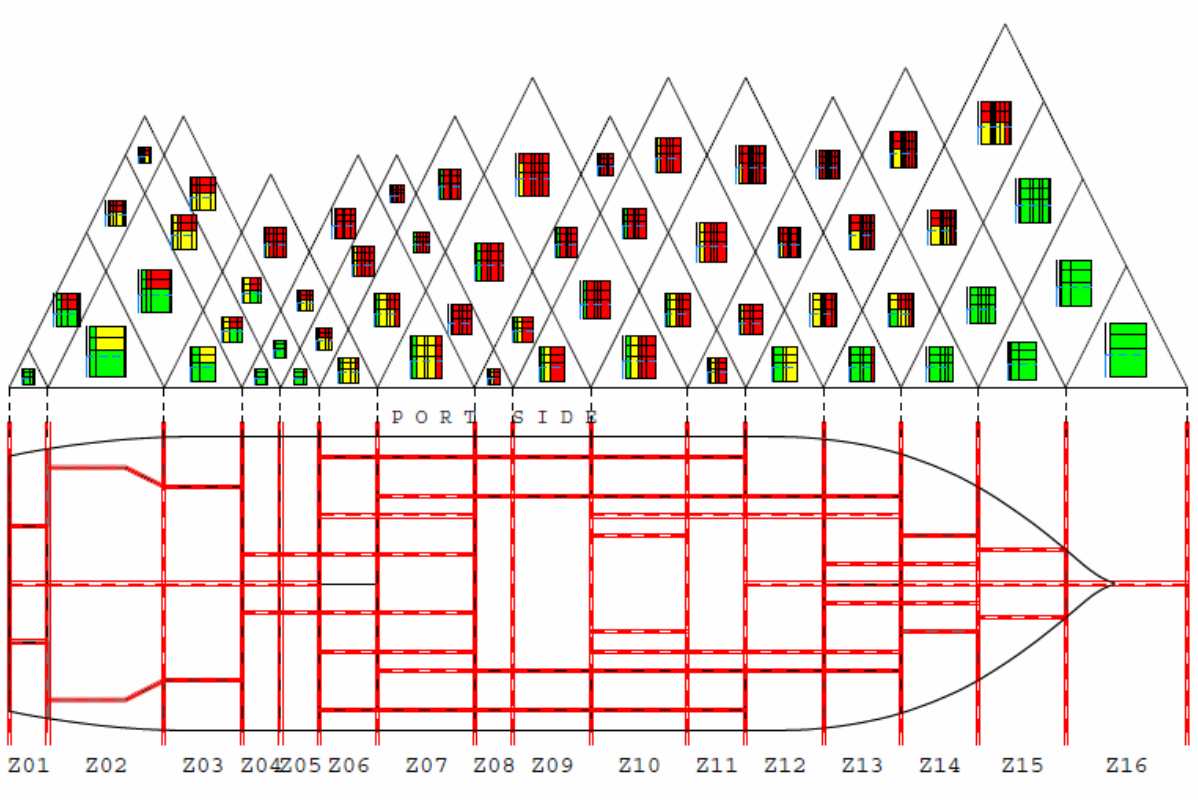

Appendix M – SFAC diagrams for the selected U-deck heights

The SFAC diagrams for the U-deck heights that were selected for discussion in Section 5.1, except for U-deck height 2.6 m, are presented in this appendix. All SFAC diagrams correspond to the light service draught, which was considered to be most critical with respect to the ship's survivability.

- SFAC diagram for U-deck height 3.6 m:

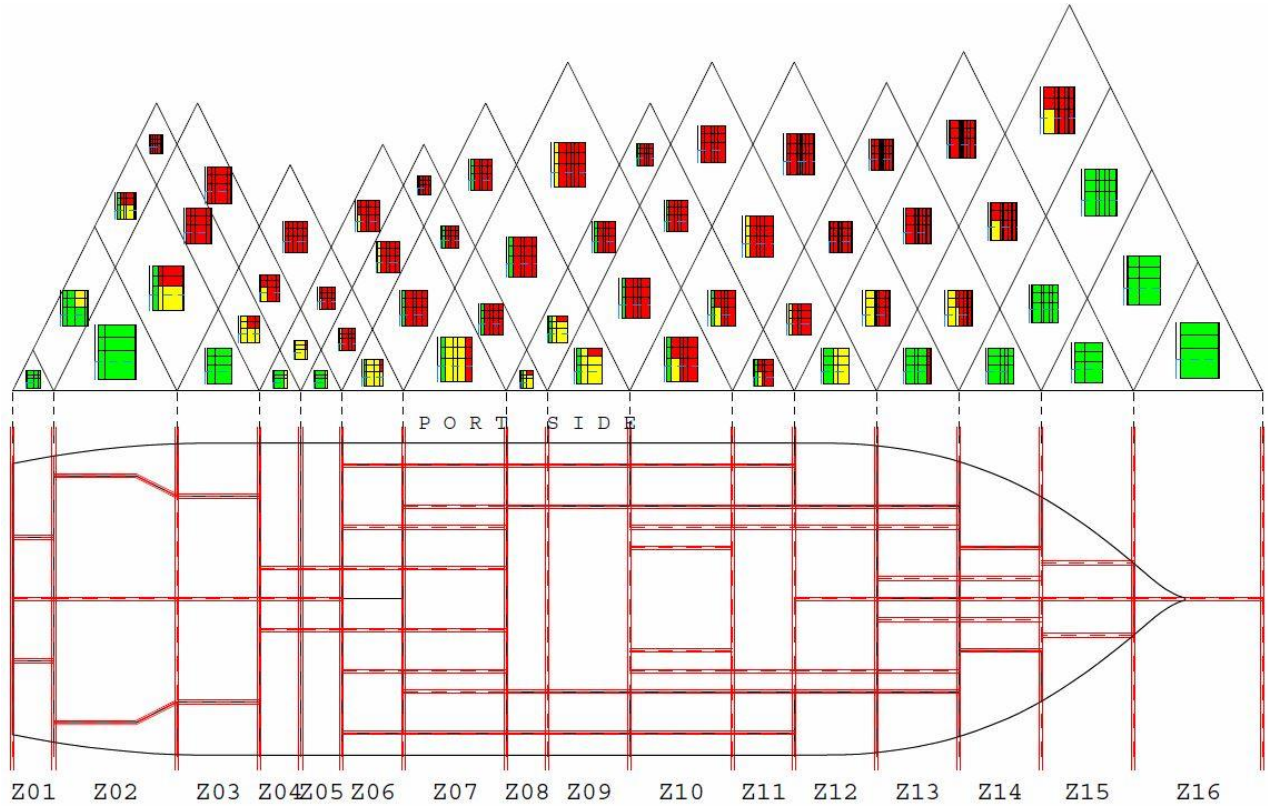

- SFAC diagram for U-deck height 4.6 m:

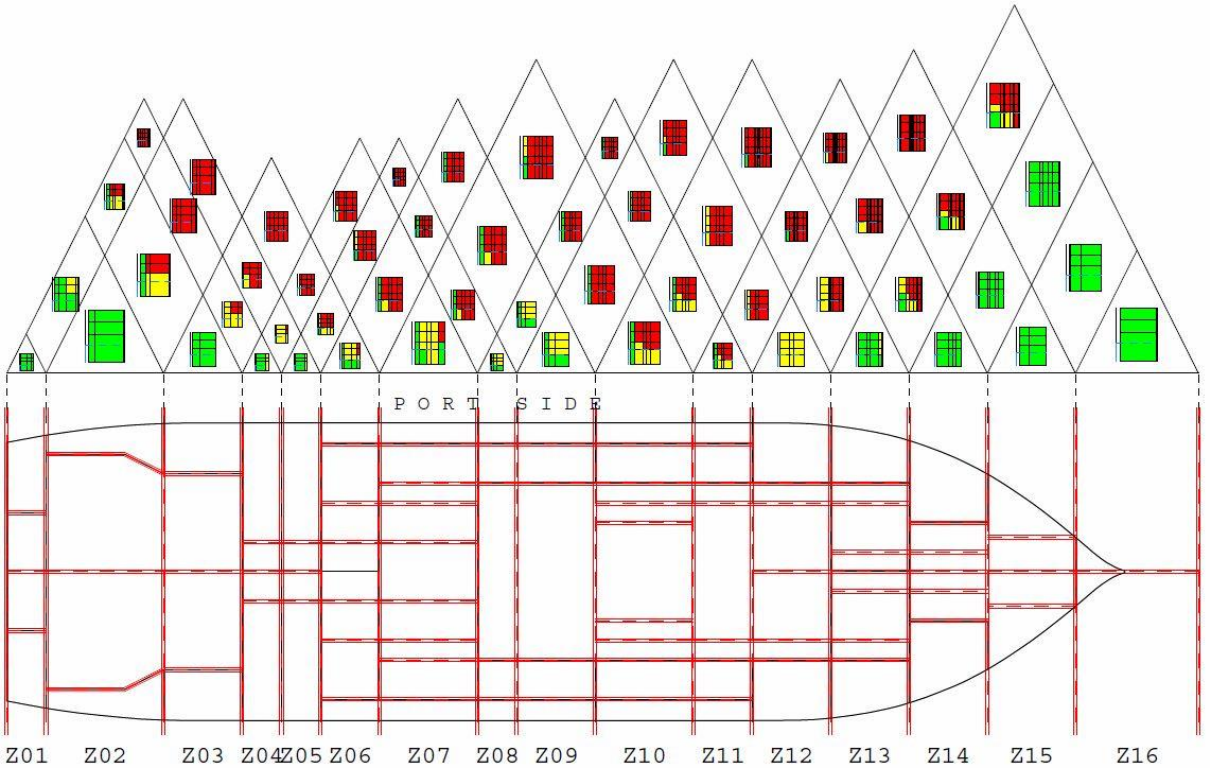

- SFAC diagram for U-deck height 5.6 m:

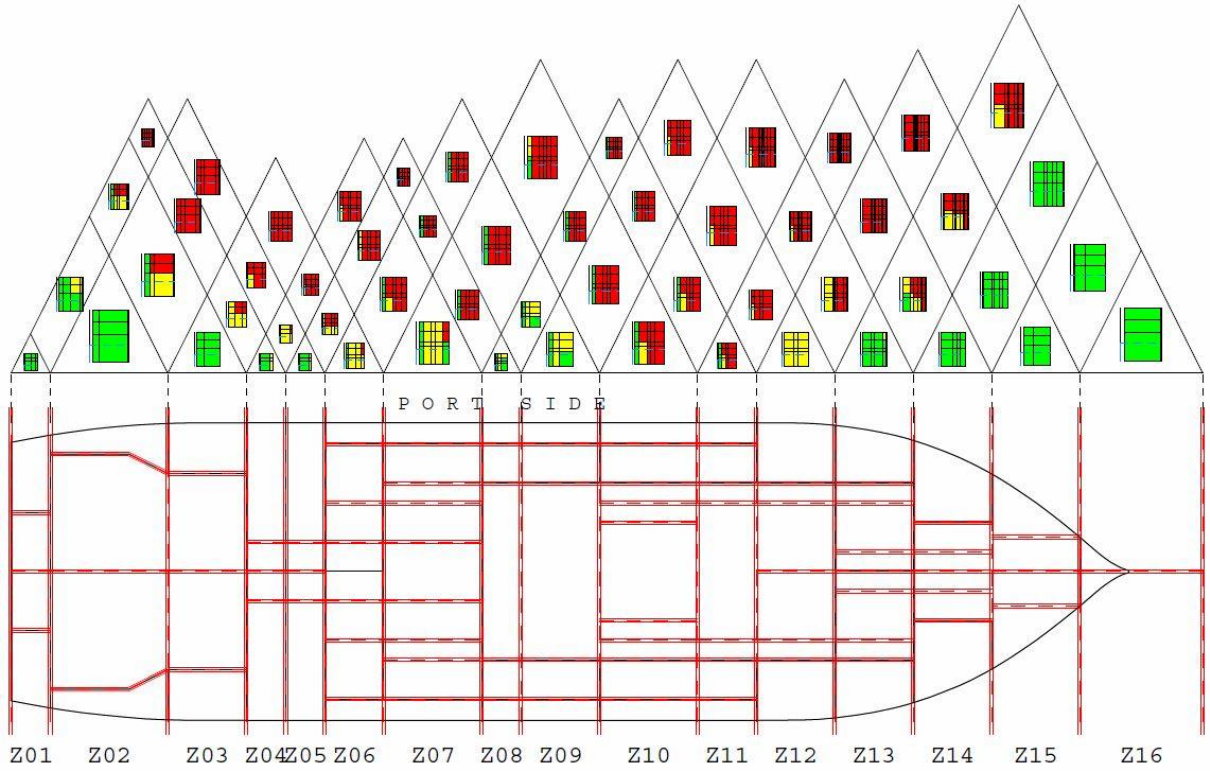

Appendix N – SFAC diagrams for zone 6-7 and zone 13

SFAC diagrams for zone 6, 7 and 13, from the calculations for objective 1 of the thesis, are presented in this appendix. This is done in order to investigate the development of the s_i-factor in the zones where both deck 2 and U-deck are present. The development is investigated for all of the selected U-deck heights, as can be seen below, for the light service draught (d_L). Deck 2 is not displayed in the SFAC diagrams below, because deck 2 is not placed above the waterline in any of the damage zones under investigation. However, a deck might have an effect on the s_i-factor even though it is placed below the waterline.

- U-deck height 5.6 m:

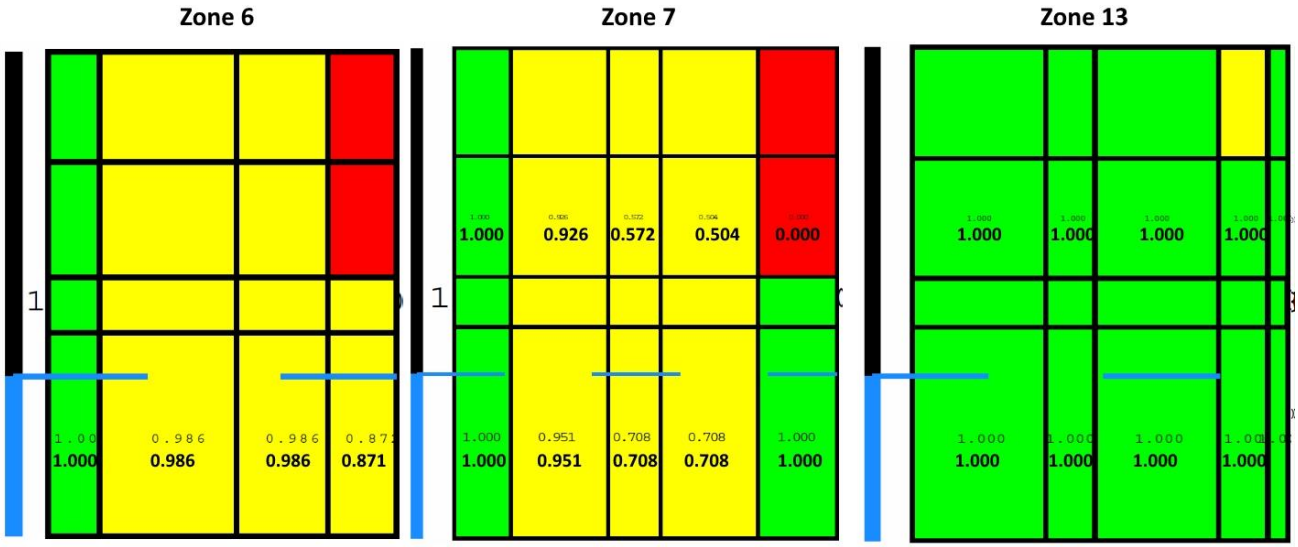

- U-deck height 4.6 m:

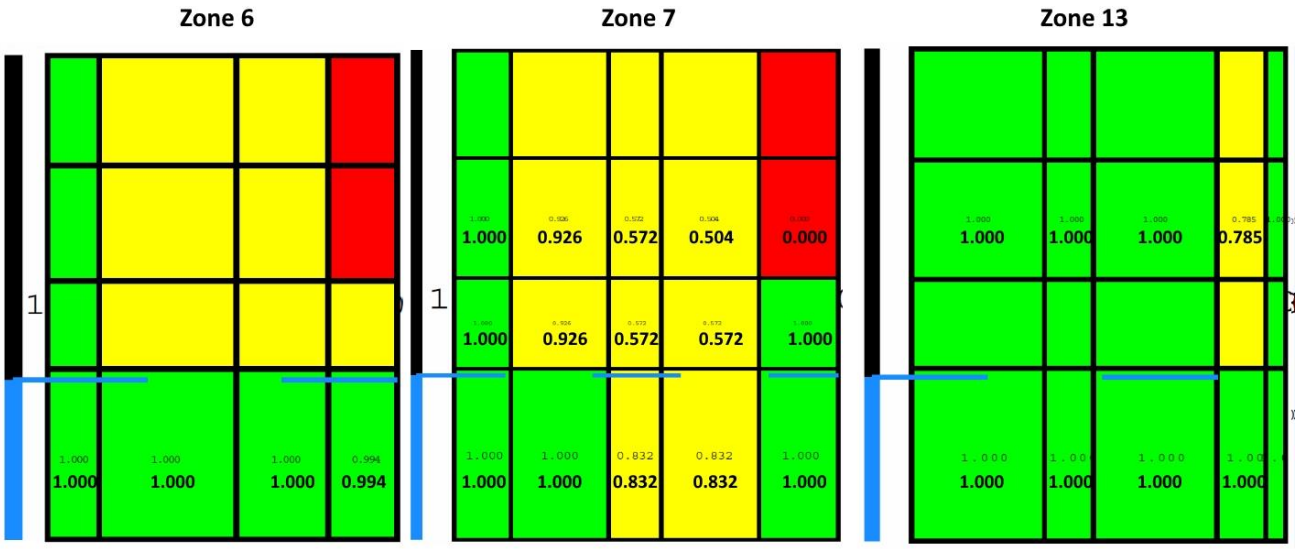

- U-deck height 3.6 m:

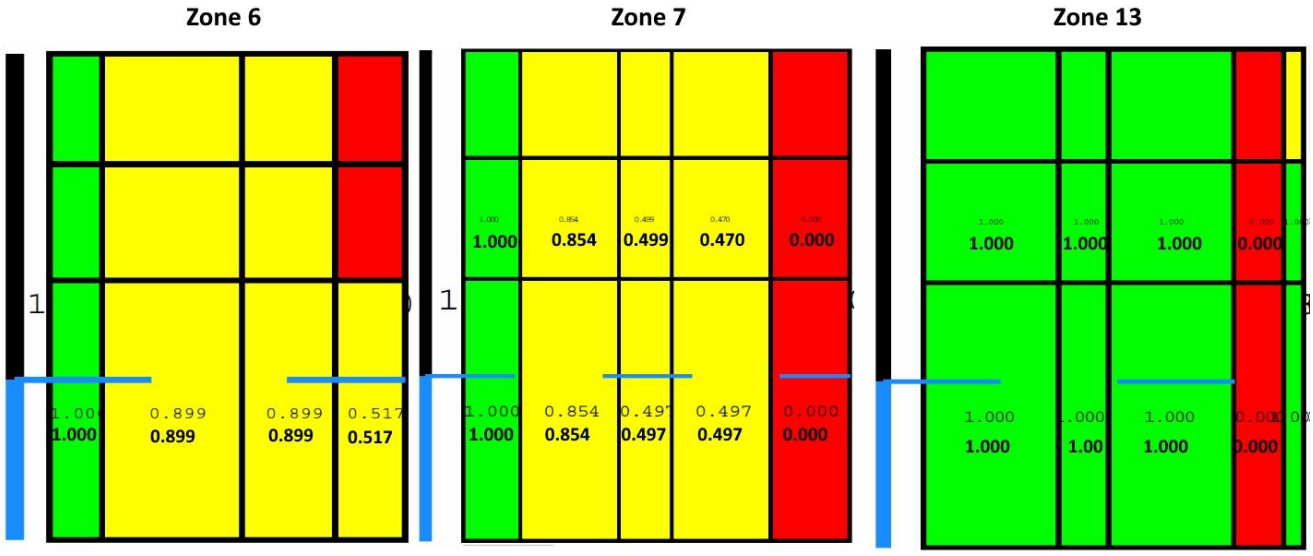

- U-deck height 2.6 m:

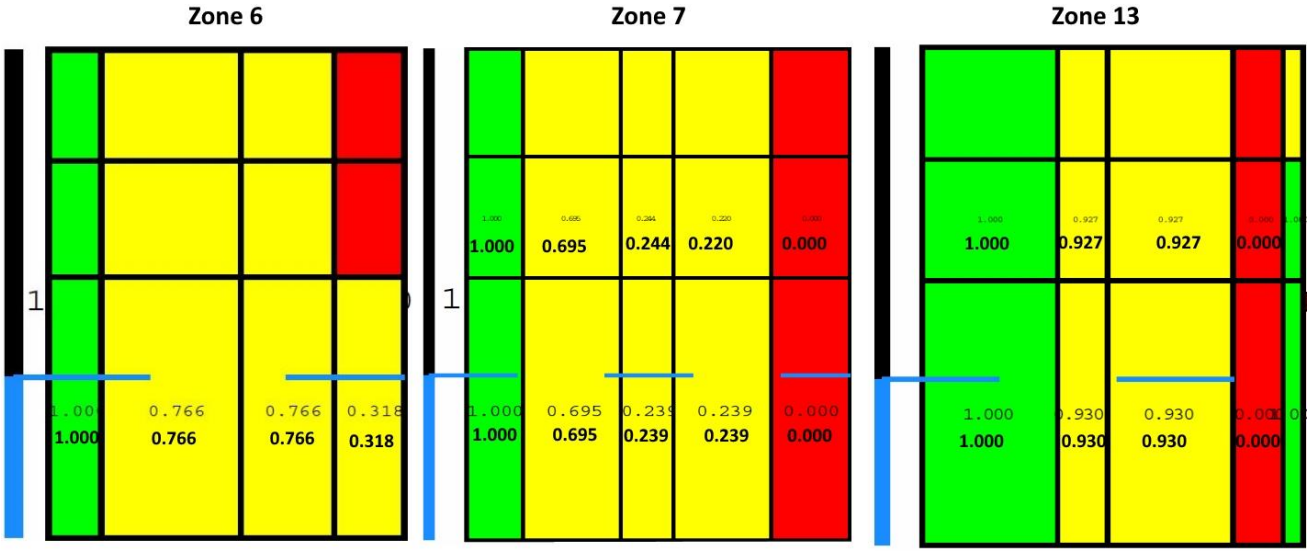

Appendix O – v_i-factor illustration for damaged wing tanks and U-tanks

The illustration below shows a scenario where both the wing ballast tank and U-tank is damaged. In Sub-section 5.1.3, Table 15, this damage scenario is referred to as 'damage case C'. The illustration furthermore displays how the H_m and H_{m-1} values should be taken for this damage case.

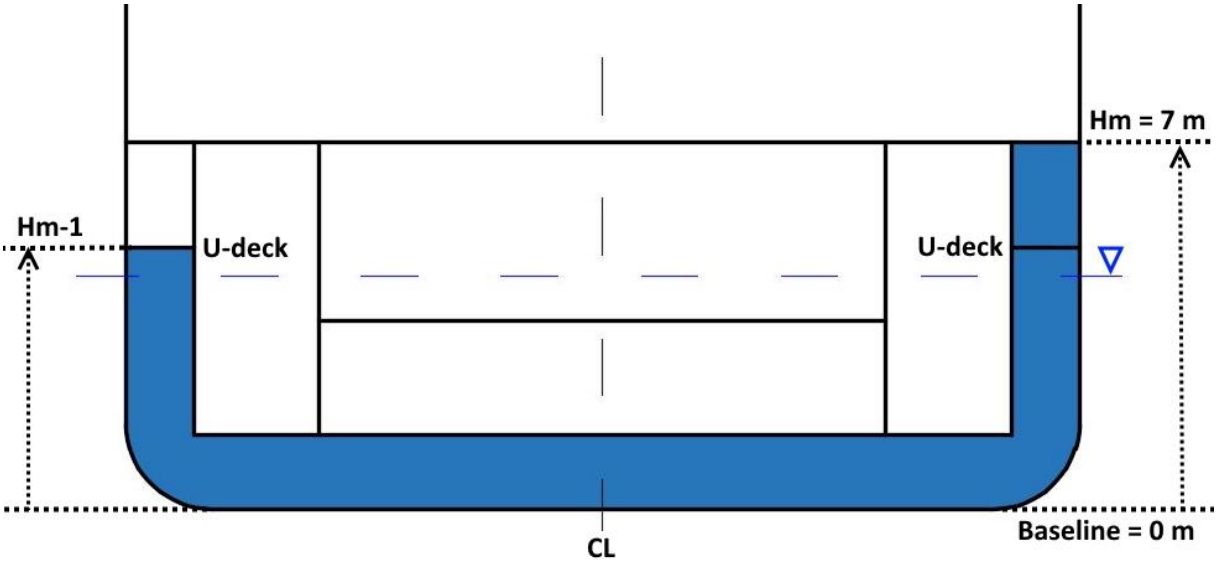

Appendix P – Calculation input and results for v_i-factor

The tables below contain values for H_m and H_{m-1} for the three damage cases A, B and C, for all of the selected U-deck heights in Chapter 5.1 of the master's thesis. These values are furthermore used to calculate the mean v_i-factor of the three damage cases for each U-deck height. There is one table for each of the three subdivision draughts, d_L, d_P and d_S, and the calculations to find mean v_i-factor values are thus repeated for all three subdivision draughts. The calculations were done in Microsoft Excel. All of the results are presented in this appendix, while only the mean values from each loading condition are presented in Sub-section 5.1.3.

- **Loading condition d_L = 4.4 m:**

Damage case	Damaged compartments	U-deck height 5.6 m		U-deck height 4.6 m		U-deck height 3.6 m		U-deck height 2.6 m	
		H_m [m]	H_{m-1} [m]	H_m [m]	H_{m-1} [m]	H_m [m]	H_{m-1} [m]	H_m [m]	H_{m-1} [m]
A	Wing ballast tank (See Figure 45 / Figure 46)	7	5.6	7	4.6	7	-	7	-
B	U-tank (See Figure 47)	5.6	-	4.6	-	-	-	-	-
C	Wing ballast tank + U-tank (See Appendix O)	7	5.6	7	4.6	-	-	-	-

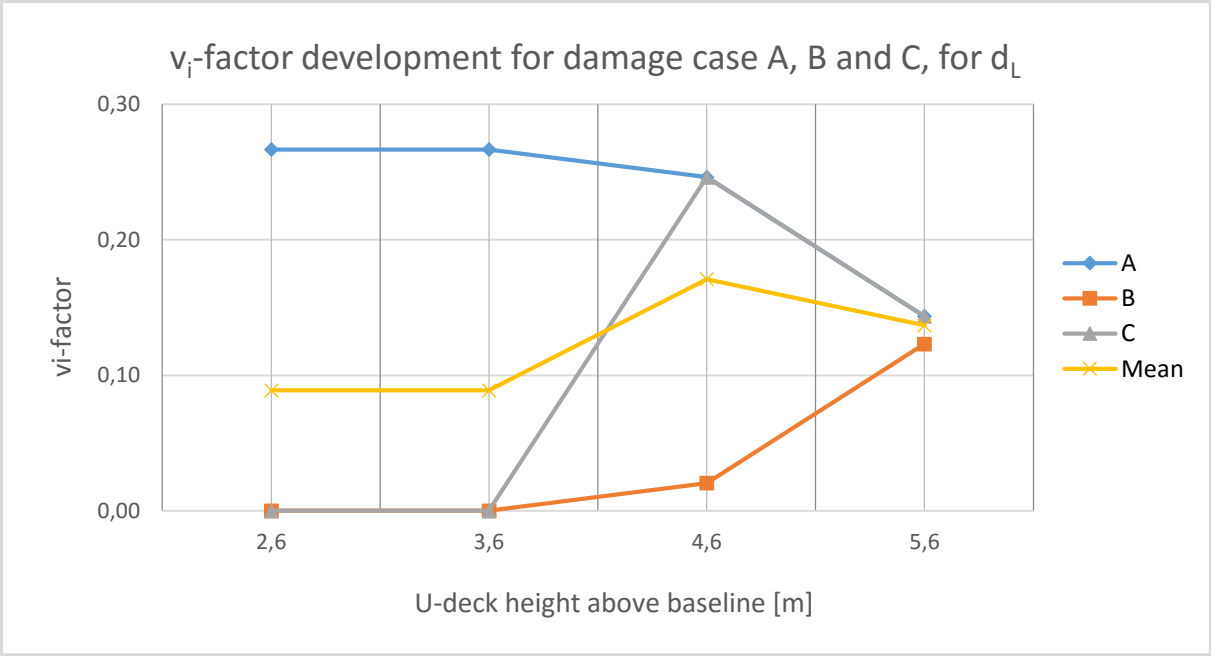

- **Loading condition d_P = 4.9 m:**

Damage case	Damaged compartments	U-deck height 5.6 m		U-deck height 4.6 m		U-deck height 3.6 m		U-deck height 2.6 m	
		H_m [m]	H_{m-1} [m]	H_m [m]	H_{m-1} [m]	H_m [m]	H_{m-1} [m]	H_m [m]	H_{m-1} [m]
A	Wing ballast tank (See Figure 45 / Figure 46)	7	5.6	7	-	7	-	7	-
B	U-tank (See Figure 47)	5.6	-	-	-	-	-	-	-
C	Wing ballast tank + U-tank (See Appendix O)	7	5.6	7	-	-	-	-	-

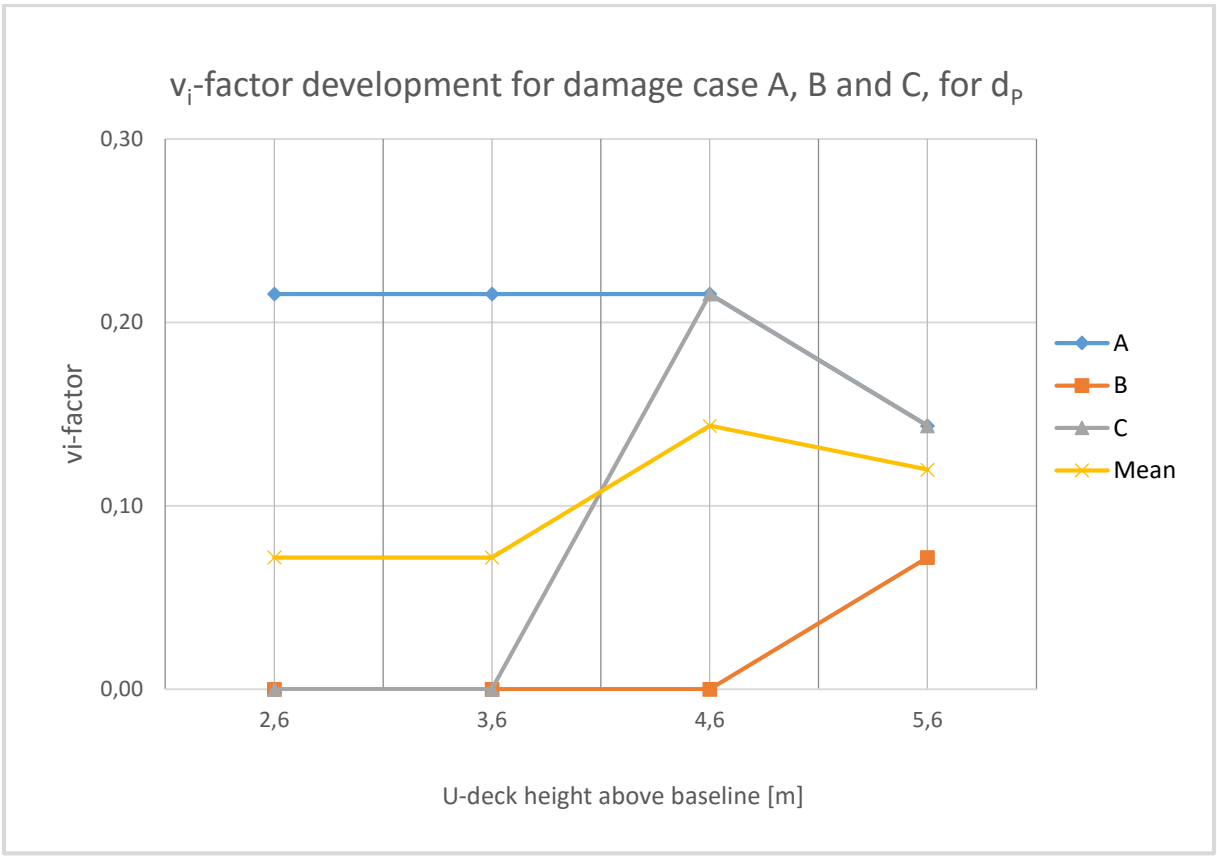
v_i-factor development for damage case A, B and C, for d_P
0,30
0,20
0,10
0,00
vi-factor
2,6
3,6
4,6
5,6
U-deck height above baseline [m]
A
B
C
Mean

- **Loading condition ds = 5.3 m:**

Damage case	Damaged compartments	U-deck height 5.6 m		U-deck height 4.6 m		U-deck height 3.6 m		U-deck height 2.6 m	
		H_m [m]	H_{m-1} [m]	H_m [m]	H_{m-1} [m]	H_m [m]	H_{m-1} [m]	H_m [m]	H_{m-1} [m]
A	Wing ballast tank (See Figure 45 / Figure 46)	7	5.6	7	-	7	-	7	-
B	U-tank (See Figure 47)	5.6	-	-	-	-	-	-	-
C	Wing ballast tank + U-tank (See Appendix O)	7	5.6	7	-	-	-	-	-

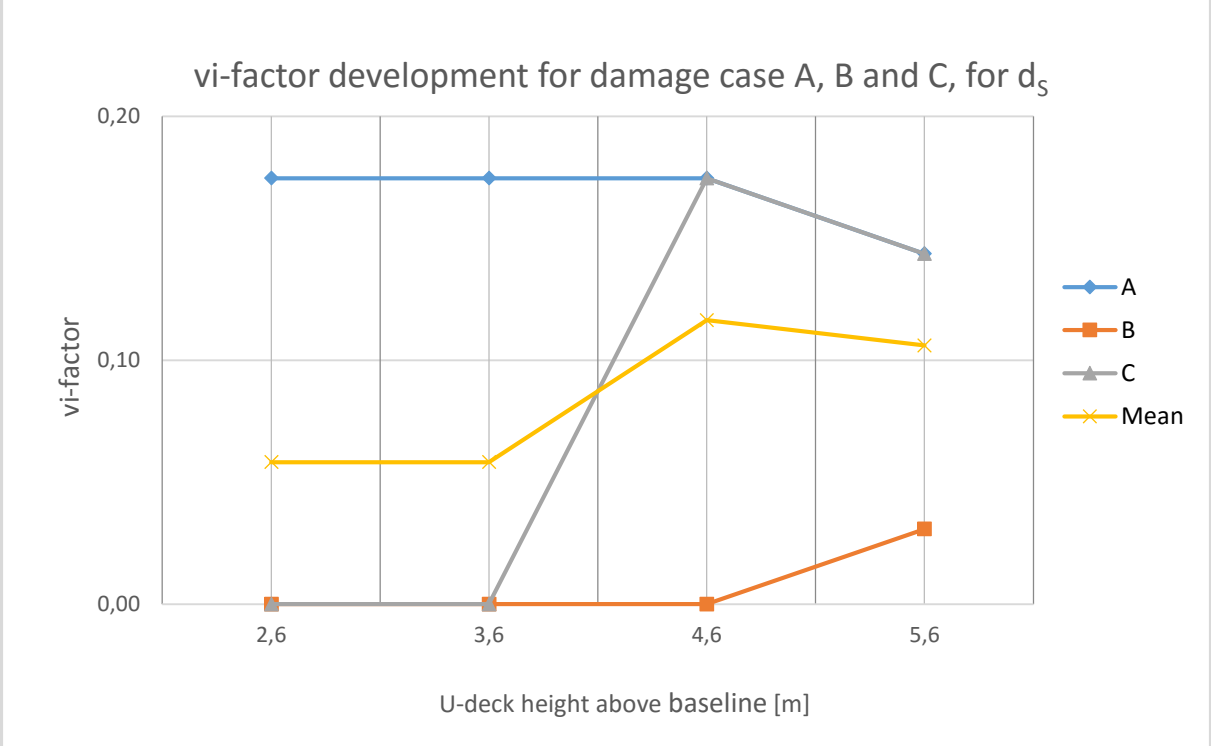

Appendix Q – SFAC diagrams for the selected GM values

The SFAC diagrams for the GM_S values that were selected for discussion in Section 0, are presented in this appendix. All SFAC diagrams correspond to the deepest subdivision draught, d_L, which was considered to be the most critical loading condition for objective 2 of the thesis.

- **SFAC diagram for GM_S = 0.9 m:**

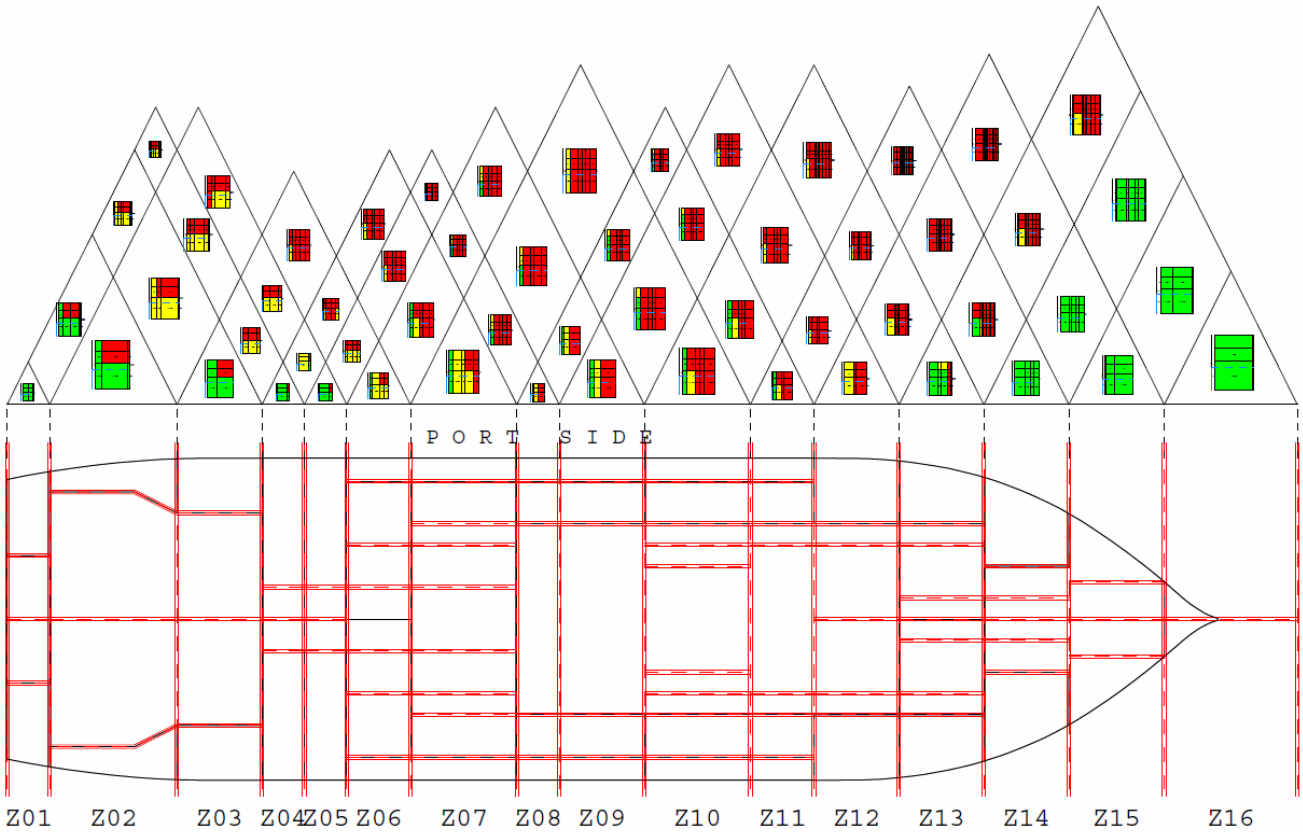

- **SFAC diagram for GMs = 1.3 m:**

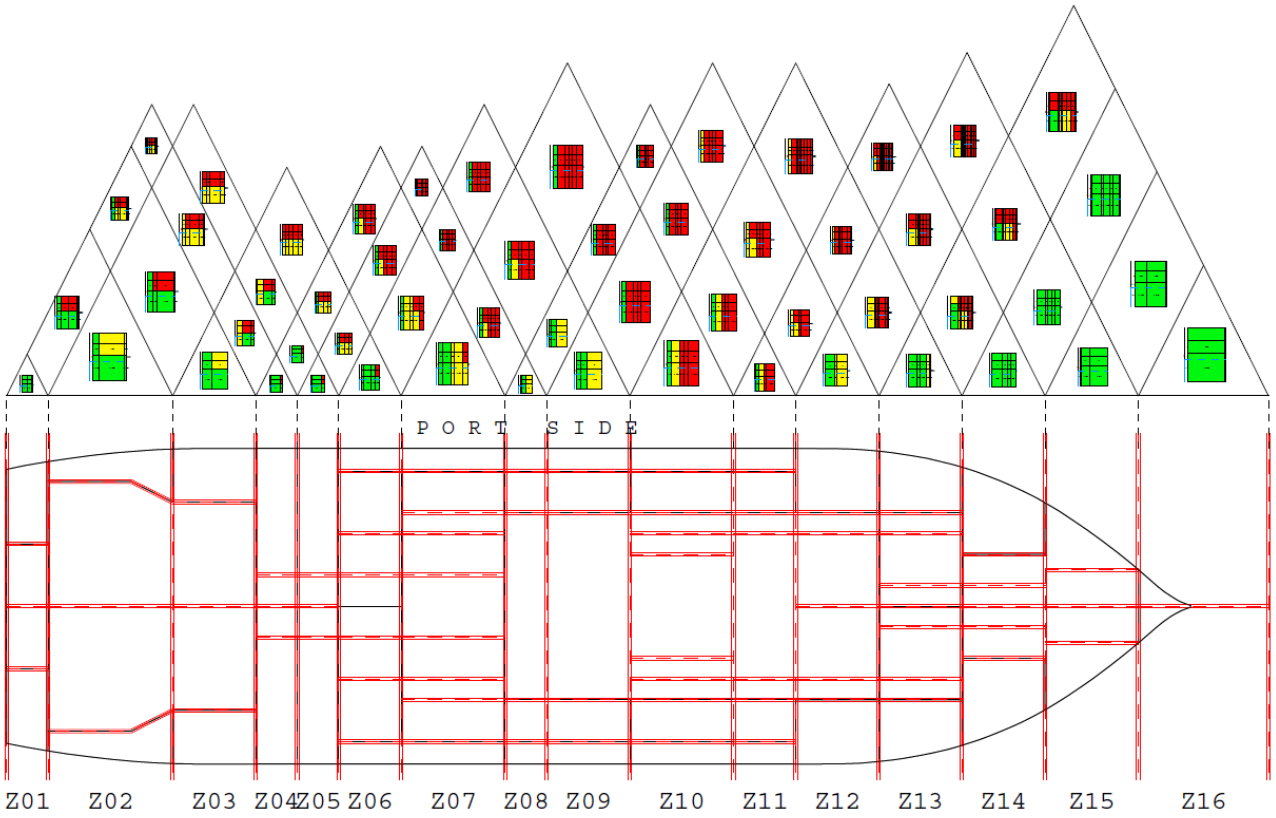

- **SFAC diagram for GMs = 1.9 m:**

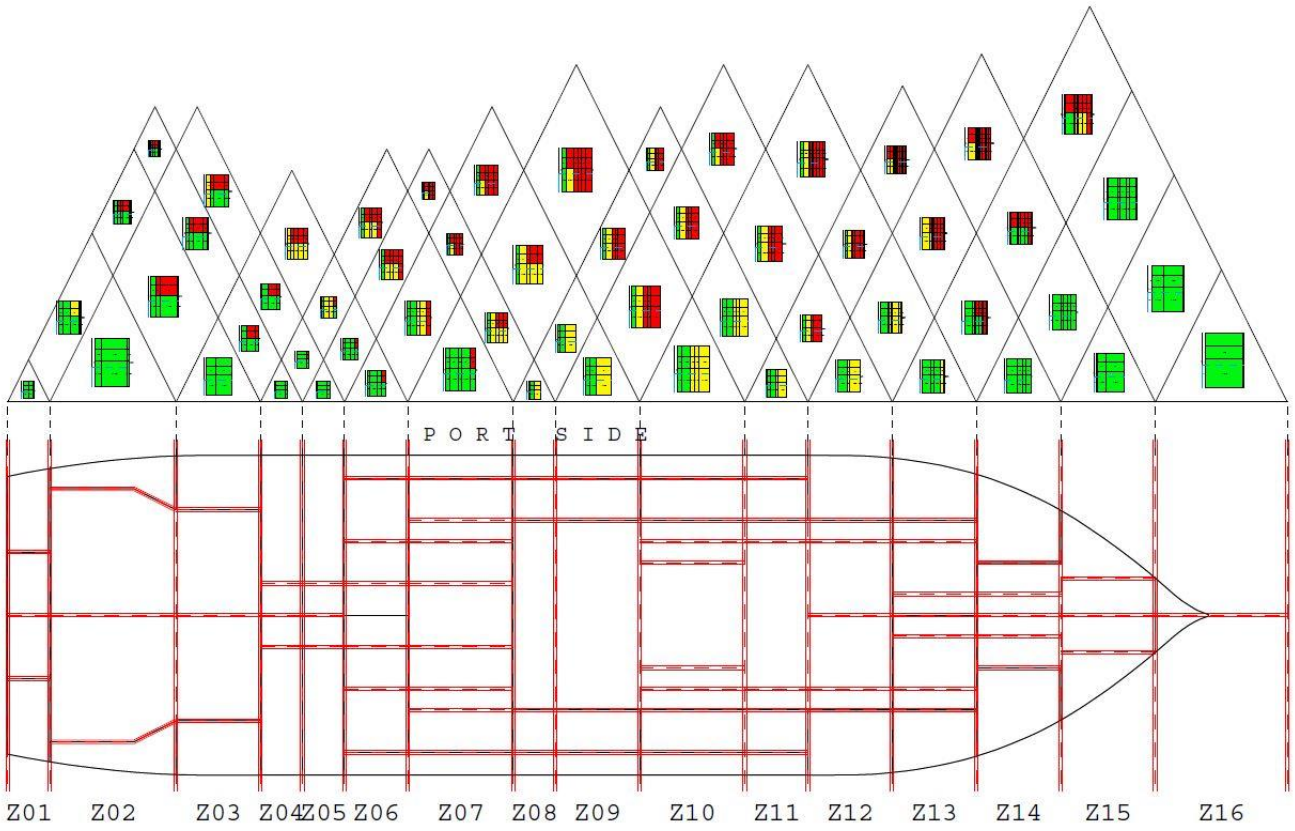

Appendix R – Damage drawings from NAPA for objective 2

Damage drawings created by NAPA, for the two selected damage cases under investigation in objective 2 of the thesis, are presented below:

- Damage drawing for the single-zone damage case in zone 2, for loading condition d_S:

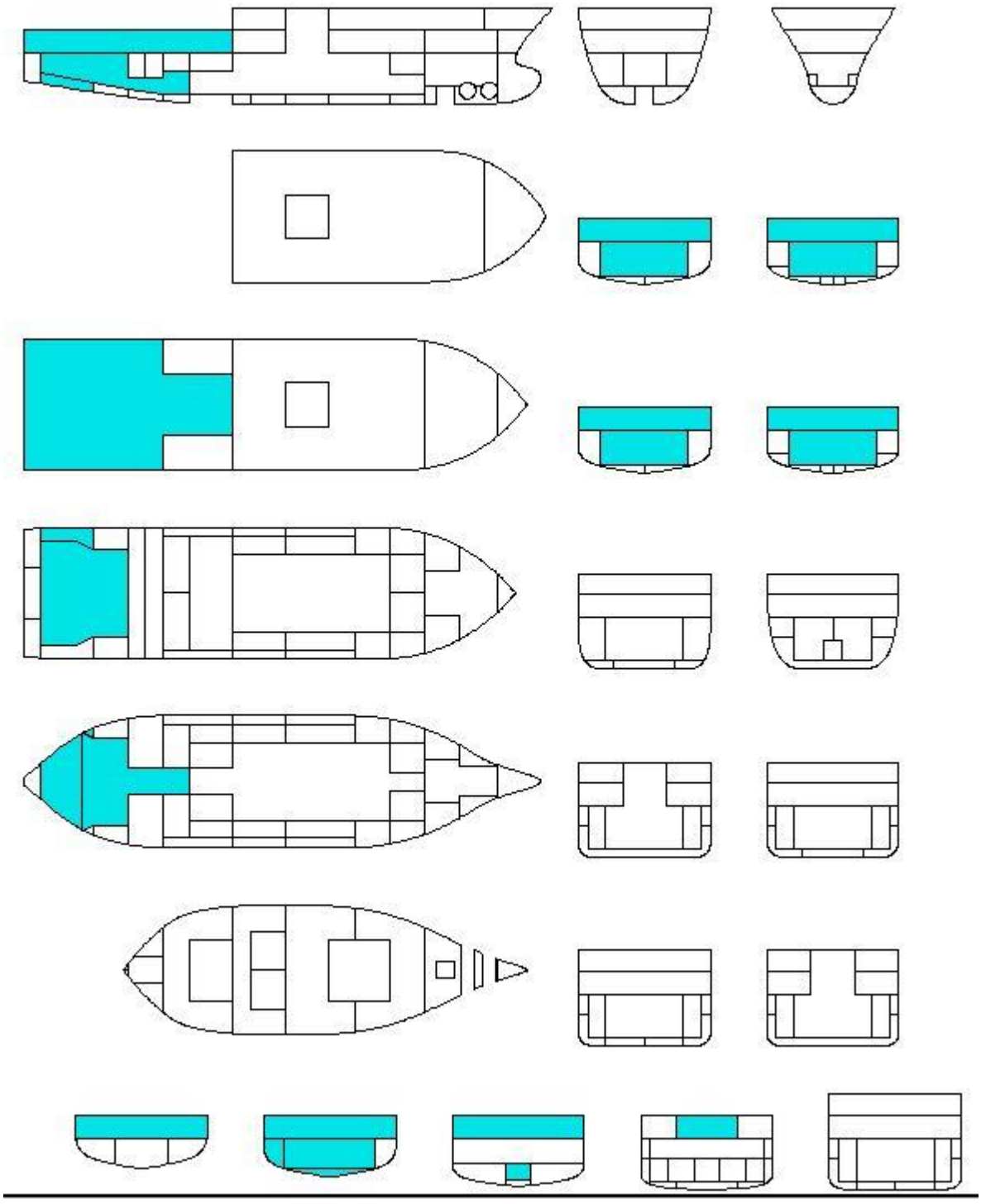

- Damage drawing for the two-zone damage case involving zone 10 and 11, for loading condition d_S:

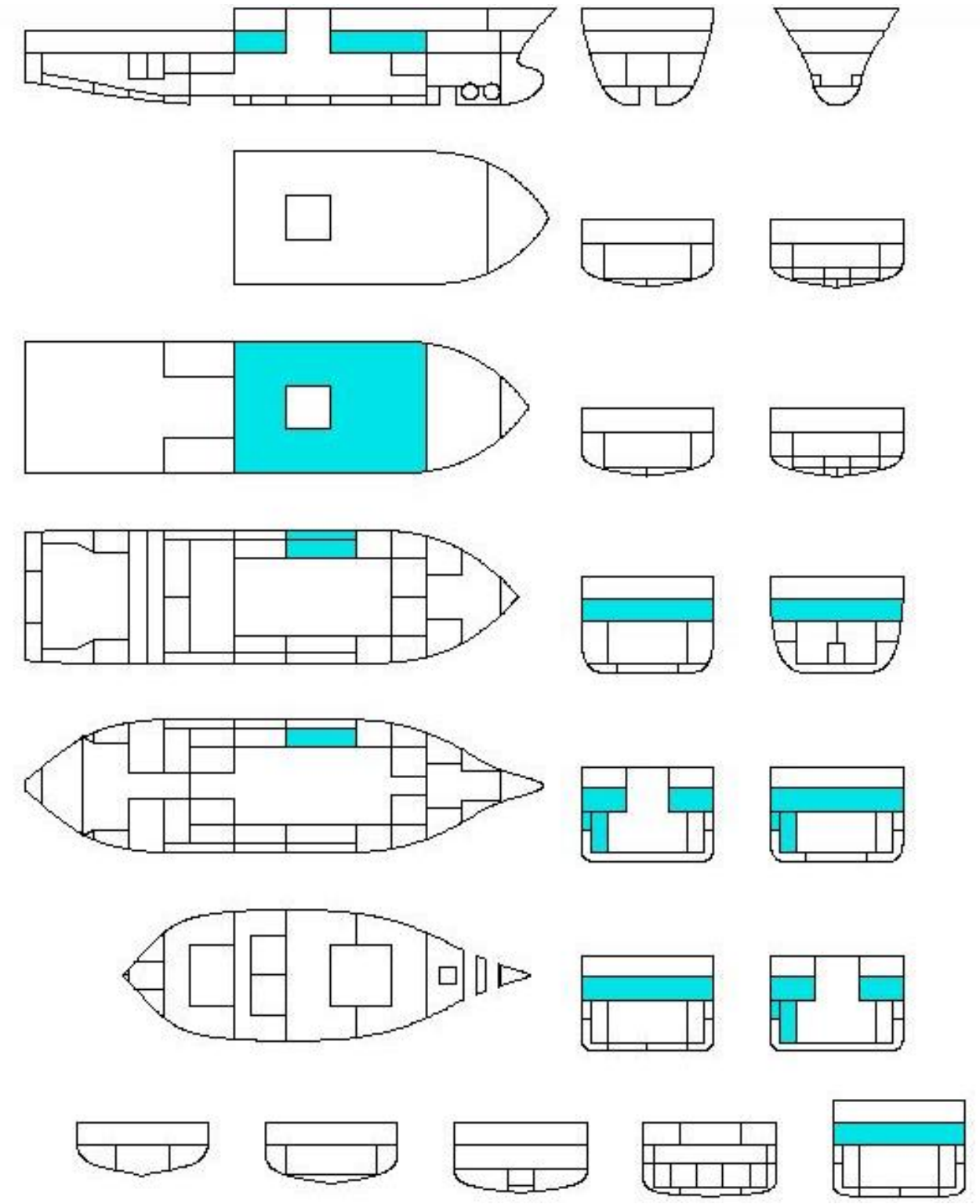

Appendix S – Damaged floating positions for objective 2

This appendix presents the equilibrium floating positions of the ship for the damage scenarios discussed in Section 5.2.

- Floating positions for the single-zone damage scenarios corresponding to the three selected GM_S values in zone 2:

- **GM_S = 0.9 m:**

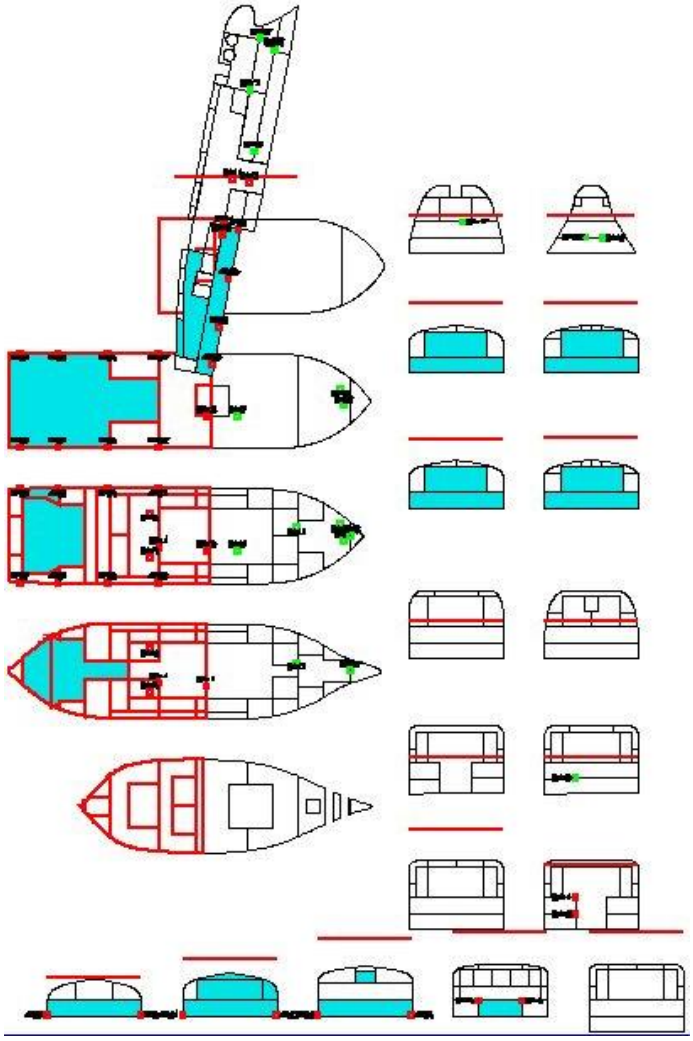

- **GMs = 1.3 m:**

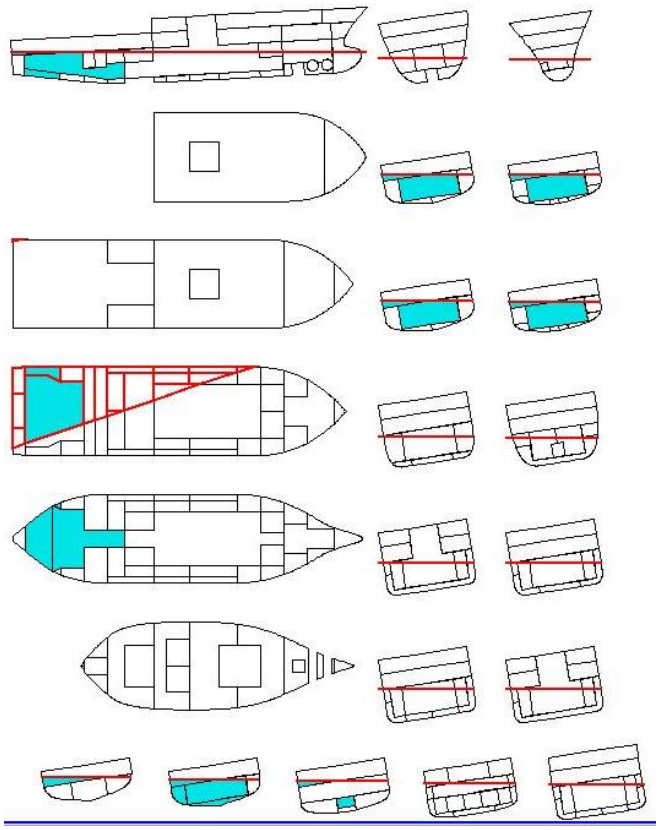

- **GMs = 1.9 m:**

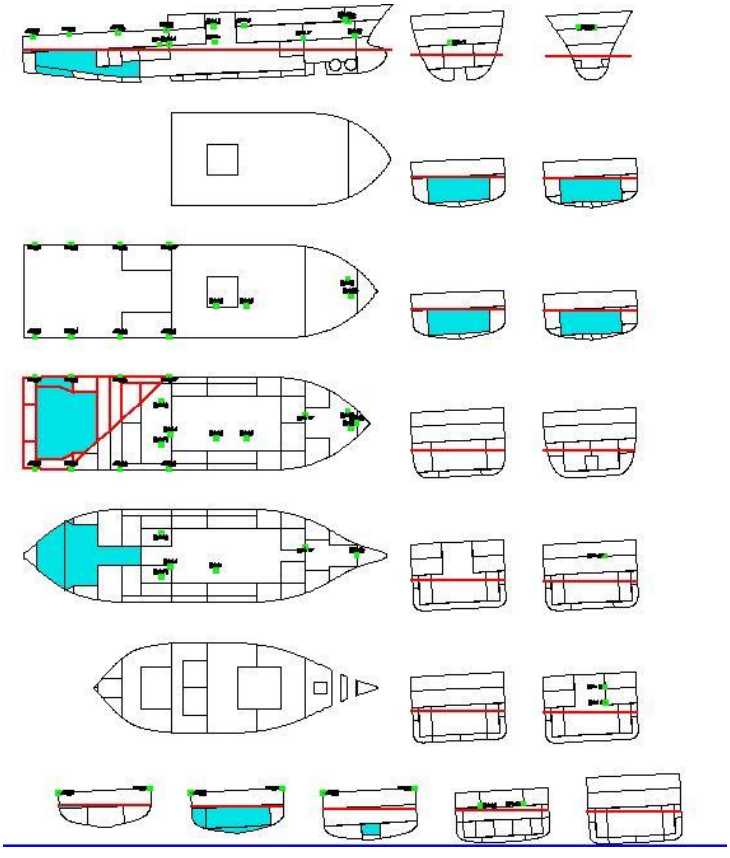

- Floating positions for the two-zone damage scenarios corresponding to the three selected GM_S values in zone 10 and 11:

- **GM_S = 0.9 m:**

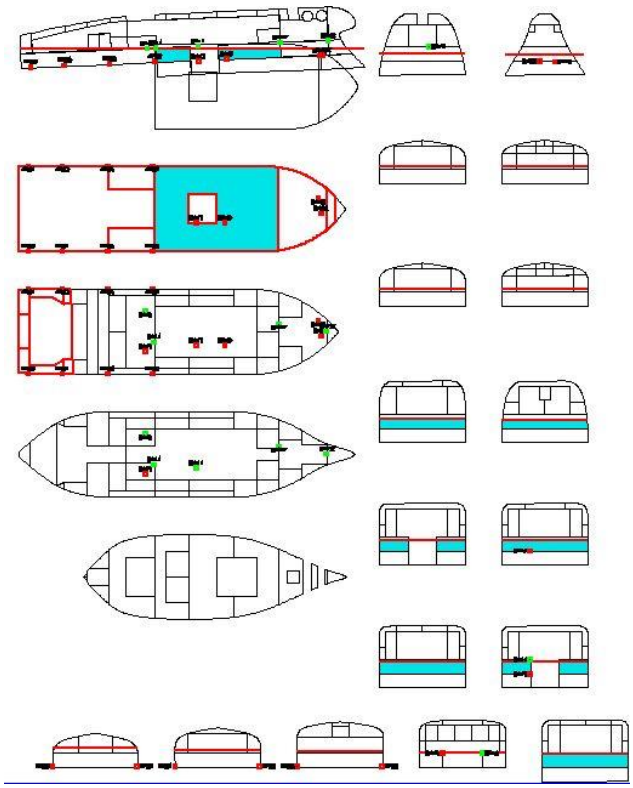

- **GM_S = 1.3 m:**

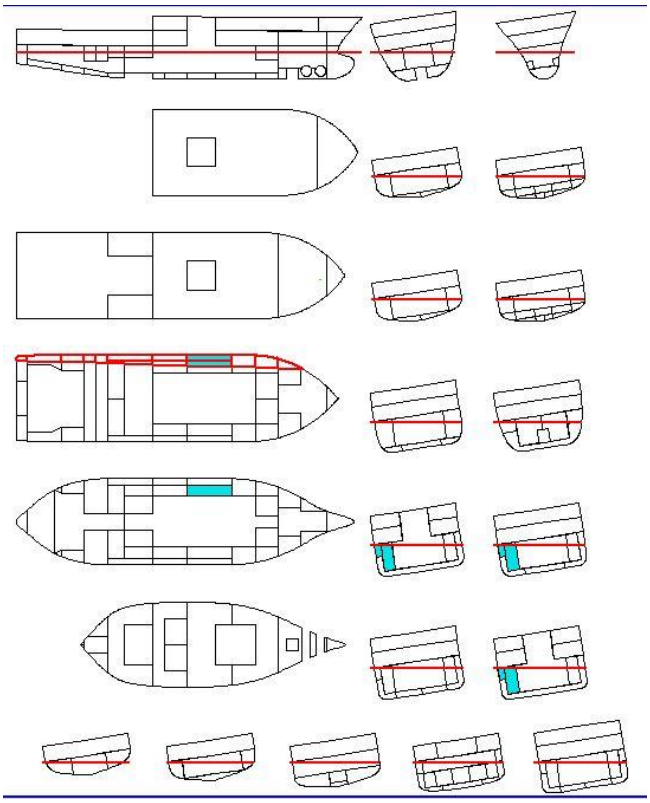

- **GMs = 1.9 m:**

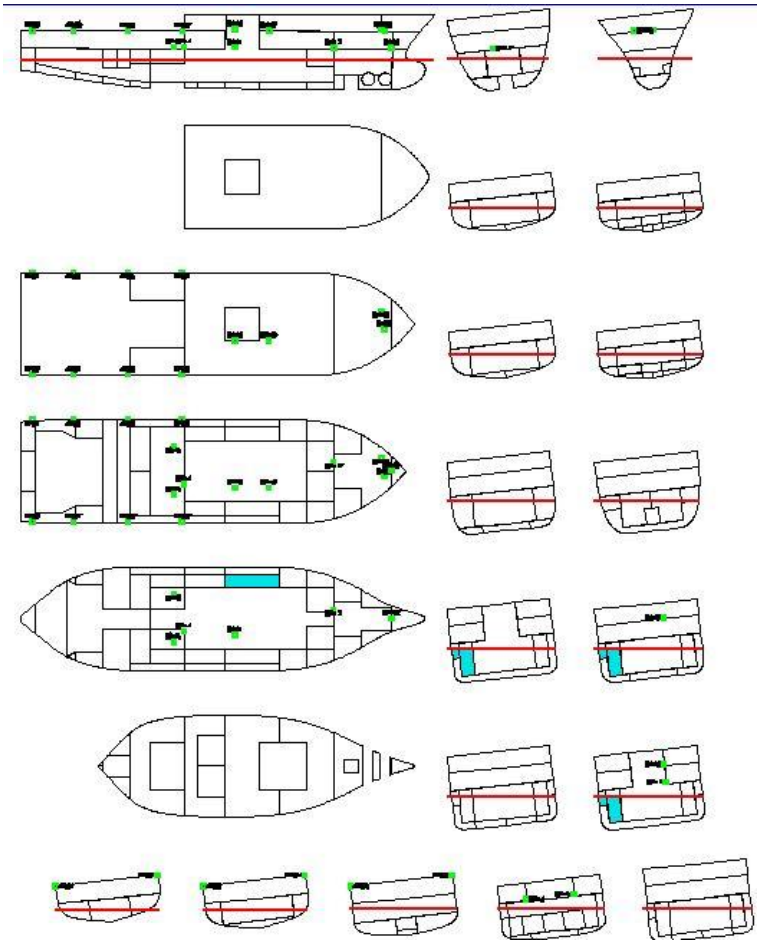

-